University of Adelaide

Department of Geology and Geophysics

Interpretation of Airborne Geophysical Data Over the Petermann Ranges Area, Southwestern Northern Territory

Andrew M. Lewis B.Sc. (Hons)

March, 1989

A thesis submitted to the University of Adelaide in fulfilment of the requirements for the degree of Master of Science.

Contents

List of Figures

List of Tables

Statement

This thesis contains no material which has been accepted for the award of any other degree or diploma in any university and, to the best of my knowledge, no material previously published or written by another person, except where due reference is made in the text.

I consent to the thesis being made available for photocopying and loan where applicable if accepted for the award of the degree.

Andrew M. Lewis

March, 1989

Acknowledgements

There are many people who should be thanked for their helpful contributions throughout this project. Professor David Boyd supervised the work from start to finish and made many useful comments and suggestions, particularly at difficult stages. Dr. Peter Brooker is thanked for his guidance and help over the time I have known him. Dr. John Paine and Mr. Andy Mitchell are gratefully acknowledged for access to their excellent software programs on the computer. I would also like to thank my colleagues, Shanti Rajagopalan, Robert O'Dowd and Zhiqun Shi for their discussion and help on many occasions, especially on computer related matters, and for permission to use many of their programs.

Other people from the department that should be thanked are Dr. Pat James, Dr. Robin Oliver and Dr. Ding Puquan for some helpful discussion. Mr. John Willoughby is also thanked, as is Rick Barrett for his photographic skills.

Numerous people from outside the Department of Geology and Geophysics were also involved, these include Mr. A.J. Hosking, formerly of the Northern Territory Department of Mines and Energy, who kindly arranged access to the geophysical survey data. Mr. Bruce Simons and Dr. Ted Findhammer of the N.T.D.M.E. are thanked for their helpful discussion and some very useful maps. Dr. Tom Whiting gave useful advice on aspects of the data processing and interpretation.

Mr. Jim Reid of the Bureau of Mineral Resources was extremely helpful and made a trip to Canberra very enjoyable. Dr. D.J. Forman of the B.M.R. is thanked for his useful comments and interest, as is Mr. Bob Major of the South Australian Department of Mines and Energy.

Finally I would like to thank my family who were supportive and encouraging throughout.

Abstract

Semidetailed airborne magnetic and radiometric data from the Petermann Ranges have been processed and a geological interpretation carried out. The Petermann study area lies within an aboriginal reserve and covers the Precambrian crystalline basement of the northern Musgrave Block and the southwest margin of the Amadeus Basin and associated infolded sediments and metasediments. Geological detail is severely limited by extensive sand and alluvial cover, and airborne geophysics is the only practical method for mapping the solid geology over much of the area.

The geophysical data have been reprocessed and presented as greyscale digital pixel maps. Interpretation of these maps using a textural interpretation scheme has delineated two major magnetic domains. Each Domain consists of smaller textural zones based on magnetic characteristics such as amplitude, frequency and linearity of anomalies which reflect lithological variations. The magnetic data is consistent with the regional scale fold nappe structure which dominates the north of the study area and much of the southwestern margin of the Amadeus Basin. The interpreted Northern Magnetic Domain includes the sediments of the Amadeus Basin, the Petermann nappe as well as original gneissic and granitic basement rocks. Large scale east–west basement shearing has been delineated within the basement of the Northern Domain. A two stage model for the emplacement of the Pottoyu Granite Complex of the Musgrave Block is proposed, with components both pre and post basement shearing, and a further deep seated granitic intrusion is interpreted as the major source of the Cobb Gravity Depression within the study area.

The Southern Magnetic Domain correlates with the high grade granulite gneisses of the Musgrave Block and has been subdivided into two lithomagnetic units which reflect large scale basement structure. The boundary between the Northern and Southern Domains is interpreted as the geophysical response of the Woodroffe Thrust, a major crustal dislocation in Central Australia. Current geological information only provides an approximate position for the Thrust whereas the geophysical data has been used to trace the feature more accurately than previously possible in the study area. The extension of the Mann Fault Zone from South Australia into the Northern Territory is confirmed and local to semiregional scale faulting and folding is defined in both Domains.

This research has shown that by detailed reprocessing and interpretation the geophysical data can be a useful aid to geological mapping in areas where access is limited and geological control is sparse. The results of this project provide the starting point for detailed geological mapping in sections of the aboriginal land in central Australia.

Chapter 1

Study Objectives and Location

1.1 Introduction

A large section of central Australia has been geologically mapped on a regional scale though much of the area, including the Petermann Ranges study area, is deficient in more detailed geological information. This thesis represents the results of an interpretation of airborne geophysical data from the Petermann Ranges and is an attempt to improve upon the currently available geological information from the area. The interpretation of airborne geophysics is one of the few tools available to improve the detail of geological knowledge from inaccessible or difficult terrains such as the study area.

This chapter sets out the objectives and main problems addressed in the interpretation. The methods required to solve the problems are introduced and a description of the location and environment of the study area is presented.

1.2 Aims

The ultimate goal of any aeromagnetic/radiometric survey is to gain more information about the geology of an area. The type of information extracted from the geophysical data depends very much upon the specifications of the survey, and can range from broad scale information such as the extent and regional structure of a large sedimentary basin, to local knowledge such as the structural details of individual magnetic horizons or magnetic ore bodies. Between these two extremes lies the semidetailed airborne survey used to aid geological mapping of significantly sized areas (several thousand square kilometres).

Before the aims of this project can be adequately defined the limitations of the methods used must be realized. A major limiting factor is the size of the study area. The regional geological setting of the area surrounding the study location is on a very large scale, and the study area itself only covers a relatively small section of that structure, hence it is not possible to use the geophysical data to develop theories on regional structure. However it is possible to use the data to determine whether the presently accepted structural models are applicable in the light of the

new information in the geophysical data.

The other major restriction arises from the geophysical data itself. The inherent ambiguity of potential field data has been well documented, but there are also limitations on resolution of anomalies. These are due to the flight line spacing and flight altitudes which can cause small magnetic sources between flight lines to be missed and individual anomalies produced by closely spaced bodies can appear as a single magnetic feature. It should also be noted that the magnetic method only responds to rocks which contain magnetic minerals. A further limitation to be considered is the quality of the auxiliary information such as the detail of the geological mapping, and other ground control.

With these limitations in mind, the aims of this thesis work are primarily to use the semidetailed airborne magnetic and radiometric data, and other available information from the Petermann Ranges area:

- to improve the understanding of the geology of the area,
- to investigate the usefulness of the geophysical data in an area where geological control is lacking and ground access is limited.

1.3 Location Specific Problems

The Petermann Ranges area, like much of central Australia, is very remote. The nearest built up area is at the Ayers Rock Yulara tourist resort, some 100 kilometres to the east. There is one unsurfaced road passing through the area travelling between Ayers Rock, the Olgas and the Giles Meteorological station across the Western Australian border. The isolation of the locality means that collecting geological information is made difficult due to poor access. This problem is compounded because the majority of the area is blanketed by a Tertiary and Recent cover of unconsolidated conglomerate, sand and alluvium which obscures most of the more geologically significant rock types. The task of ground geological mapping has been further complicated recently because the whole area lies within an aboriginal reserve. This means that permission is required from the traditional land owners before any work can be done in the area; such permission is not always easy to obtain.

Hence it is apparent that a vast area of central Australia is largely unmappable by either ground, airphoto or satellite remote sensing methods because of the reasons mentioned above. The only practical way these problems can be overcome is by applying airborne geophysical methods which are able to cover significant areas quickly and, more importantly, can provide useful geological information from sand covered areas which lack outcrop.

1.4 Overview of Procedures

The geological understanding of a complex area only develops after many years and much work. The Broken Hill area, for example, has been studied for nearly a century and not until the last few decades when it was the focus of concentrated study, applying both geological and geophysical methods, was a better understanding of the area developed (Isles, 1983). Much of the Precambrian in central Australia requires a similar concerted effort, the use of airborne geophysics being particularly useful in contributing to solving the geological problems.

The work in this project can be subdivided into two categories. The first task was the (re)processing of the geophysical data and its display as greyscaled digital pixel maps. Digital images are a form of display more conducive to certain aspects of detailed interpretation than the traditional contour map presentation. Prior to this work the majority of the geophysical data covering the area was only available in standard contour map form.

The second part of the work was the geological interpretation of the geophysical data using all the available forms of the data, contour maps, processed images, flight line profiles and other information from the area, including geological reports and maps, aerial photography and previous geophysical and geochemical work.

Geological interpretation methods of aeromagnetic and radiometric data have been well established over many years and well represented in the literature (Boyd, 1967; Whiting, 1983; Pitkin, 1968; Potts, 1976) and are discussed in more detail in later chapters. The processing and display of the data as greyscale images means that these methods have to be adapted to be compatible both with the nature of the data and the location of the study, which is characterized by a lack of geological control. It has been found that the "Textural Interpretation" scheme proposed by Tucker and D'Addario (1986, 1986a, 1987) is suitable to both the available data and the aims of the interpretation. Textural interpretation is discussed in further detail in Chapter 3.

1.5 The Study Area

The Petermann Ranges study area lies in the far southwestern corner of the Northern Territory (see Figure 1.1). The area covers the southwestern margin of the Amadeus Basin, which is an east–west trending Adelaidean and younger sedimentary basin, and to the south the area lies over the crystalline basement of the Musgrave Block.

The study area spans two 1:250 000 map sheets, *PETERMANN RANGES* and *BLOODS RANGE* and includes six 1:100 000 map sheet areas (see Figure 1.2 for the sheet names and locations). In order to distinguish between the different scale map sheet names and place names a standard system of writing 1:100 000 sheet names in *emphasized* text and 1:250 000 sheet names in upper case, *EMPHASIZED* text will be adopted throughout this thesis.

Physiographically the area lies approximately 650 metres above sea level and is typically

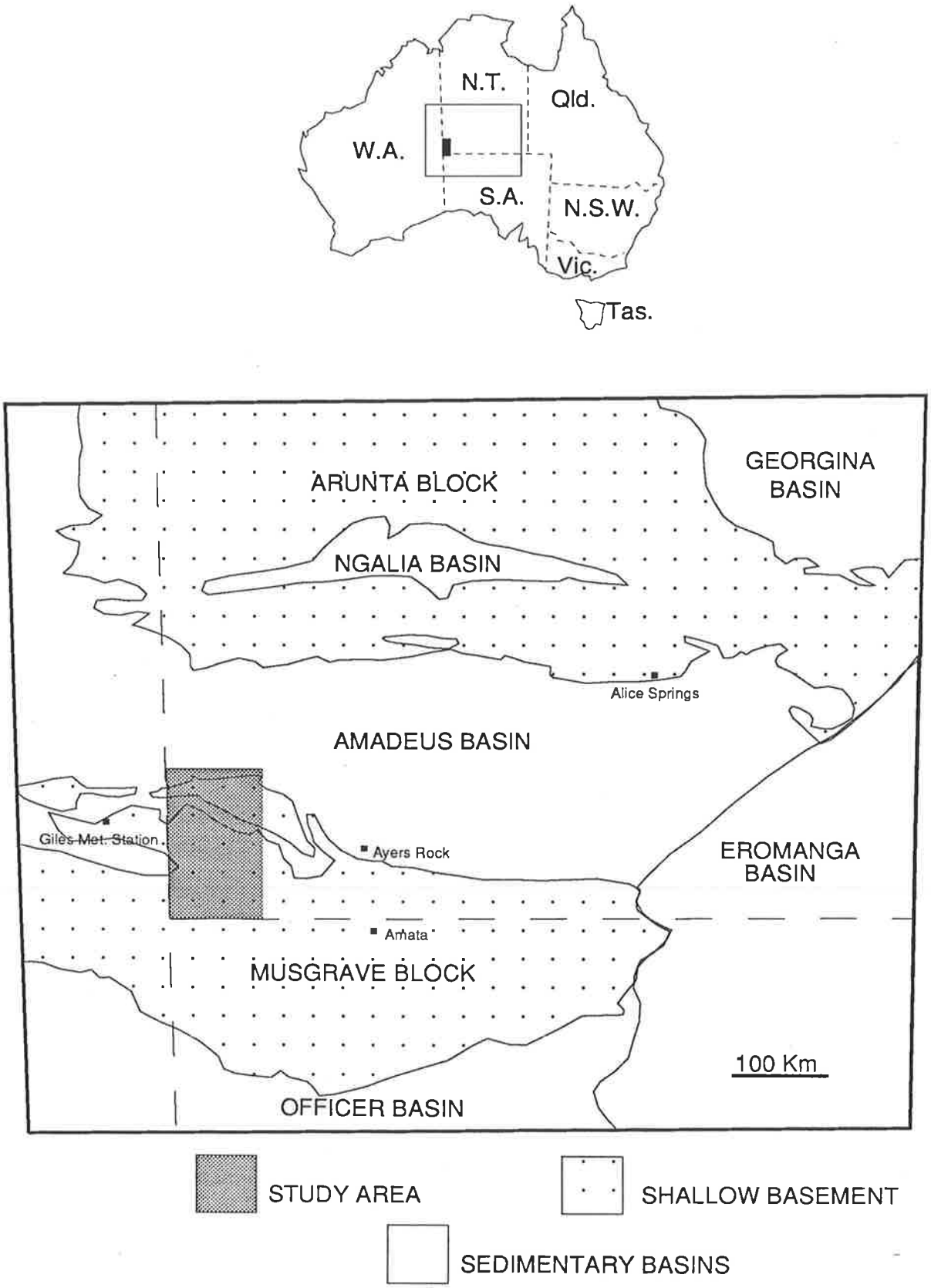

Figure 1.1: Study Area Location

sandy plains and longitudinal sand dunes up to twelve metres high, particularly in the far north of the area. The prominent ranges in the north, the Bloods Range and Petermann Ranges, stand up to four hundred metres above the surrounding plain and consist mainly of resistant quartzite. The Mann Ranges in the far south of the area make up the rugged outcrops of high grade metamorphic and granitic lithologies extending southerly and easterly across the South Australian border.

No economic mineral deposits have been found in the area, although traces of copper, silver and gold have been reported (Forman, 1972). Low grade nickeliferous ochre has been detected in drillholes in exploration extending from the nickel deposits south of the South Australian border (Miller and Rowan, 1968).

In any magnetic study an important parameter is the direction and strength of the geomagnetic field which controls, at least in part, the size and shape of the local magnetic anomalies produces by subsurface magnetic bodies. The Earth's magnetic field in the Petermann study area has an average value of 55000 nanoteslas (nT) with an inclination of $-58°$ and a declination of 3°. This is assumed to be a constant over the study area. The nearest first order magnetic stations are at Giles, across the Western Australian border, Ayers Rock and Alice Springs, both east of the study area (Finlayson, 1973).

1.6 Previous Work

Geological

There have been numerous geological expeditions into the Petermann Ranges area since the first European exploration by Ernest Giles in 1872, many of which have been described by Ellis (1937). Between the time of Ellis's expedition (in 1936) and the 1960's the most notable work reported from the area was a brief expedition made to the country around the Petermann Ranges by a Sydney company, Centralian Holdings, in 1951 with G.F. Joklik from the Bureau of Mineral Resources (hereafter referred to as the B.M.R.) as head geologist of the party (Joklik, 1952). Since that time there have been two major periods of ground activity in the area, both concentrated on the northern area of outcrop. The first was by the B.M.R. when the study area was mapped in the early 1960's as part of the regional geological mapping of a large section of the central Australian region.

The second major period of activity was in the mid to late 1960's when Planet Mining Company conducted a helicopter and fixed wing geological reconnaissance of the northern section of the survey area (Wilson, 1966) in a search for base metals. This was in conjunction with a reinterpretation of the available aerial photography (Jorgenson, 1966) and a geochemical survey (Kenneth McMahon and Partners, 1968). This effort was initiated after the occurrence of possible gossanous cappings were reported on some of the metasediments in the area.

Since that time little published geological work has been done in the area.

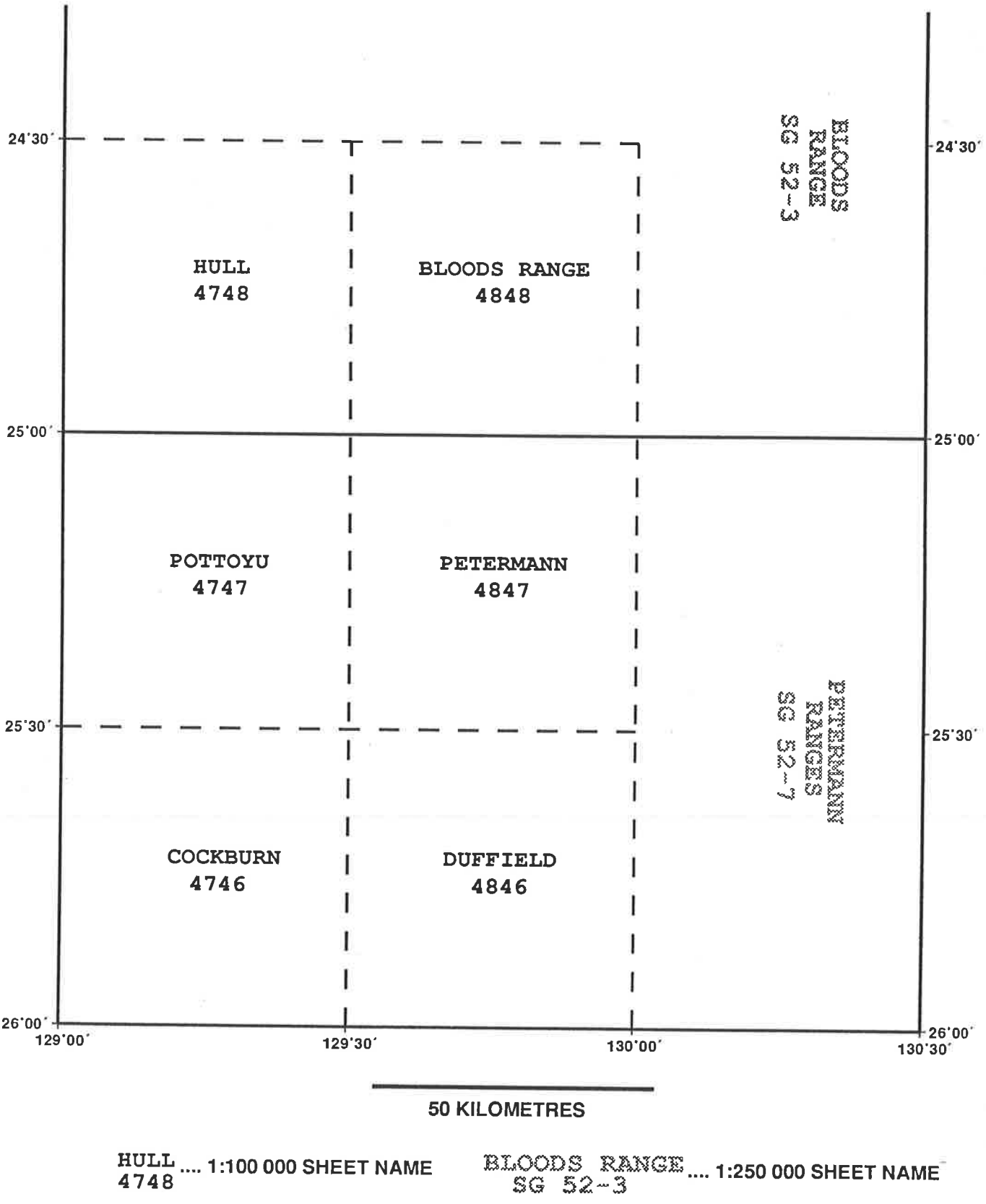

Figure 1.2: Map Sheet Locations

Geophysical

One of the earliest observations on the magnetic properties of the rocks in the vicinity of the study area was made by Wilson (1946):

> "The magnetic variation is very erratic, even on the same hill I have noted a difference of up to 5 and 6 degrees between readings (*of a compass*) taken sitting down and standing up, although in exactly the same place."

This was an early indication of the highly magnetic nature of the basement rocks in the area and implied the possible usefulness of the magnetic method as a mapping tool long before any systematic geophysical surveys had been done in the area.

The area was first crossed by a single aerial magnetic traverse line flown by the B.M.R. between Alice Springs and the Giles Meteorological station in October 1961 (Goodeve, 1961). A regional helicopter gravity survey conducted by the B.M.R. in 1962 of the Amadeus and south Canning Basins included the study area. Station elevations in the survey were established using microbarometers and the station density was approximately one station per eleven kilometre (seven mile) grid cell (Lonsdale and Flavelle, 1968).

The gravity survey was followed by a major regional aeromagnetic and radiometric survey covering the Amadeus Basin and surrounding basement rocks in 1965 (Young and Shelley, 1977) which covered the entire study area. A similar survey done over the South Australian section of the Musgrave Block, the Mann-Woodroffe survey, included approximately fifteen minutes of latitude in the study area immediately north of the South Australian border (Shelley and Downie, 1971). Both these aeromagnetic surveys had flight line spacings of at least 3.2 kilometres.

Planet Mining Company conducted an airborne magnetic survey over parts of the north of the study area in conjunction with their other work which has been mentioned above (Woyzbun, 1968).

The study area has been included in two aerial photographic surveys flown by the Division of National Mapping. The first was flown in 1957 at an altitude of 7700 metres (25000 feet) and the second in 1984 at 7620 metres. Both were in black and white, and the former was collated into uncontrolled photomosaics at an approximate scale of 1:63 360.

The geophysical data being used in this work, the **Petermann Survey**, was collected for the Northern Territory Department of Mines and Energy (N.T.D.M.E.) in 1985 by Austirex International (see Appendix B for full survey specifications). The survey represents the first new geophysical data to have been collected in the area for nearly twenty years.

The six 1:100 000 map sheet areas flown represent the first step in the Petermann/Musgrave Block Project of the Northern Territory Geological Survey (N.T.G.S.). This project includes the collection of semidetailed airborne magnetic and radiometric data, the occupation of new gravity stations and the geological remapping of areas of the far south of the Northern Territory.

The location of the Petermann Survey, and its spatial relationship to the previously mentioned aeromagnetic surveys, is shown on Figure 1.3.

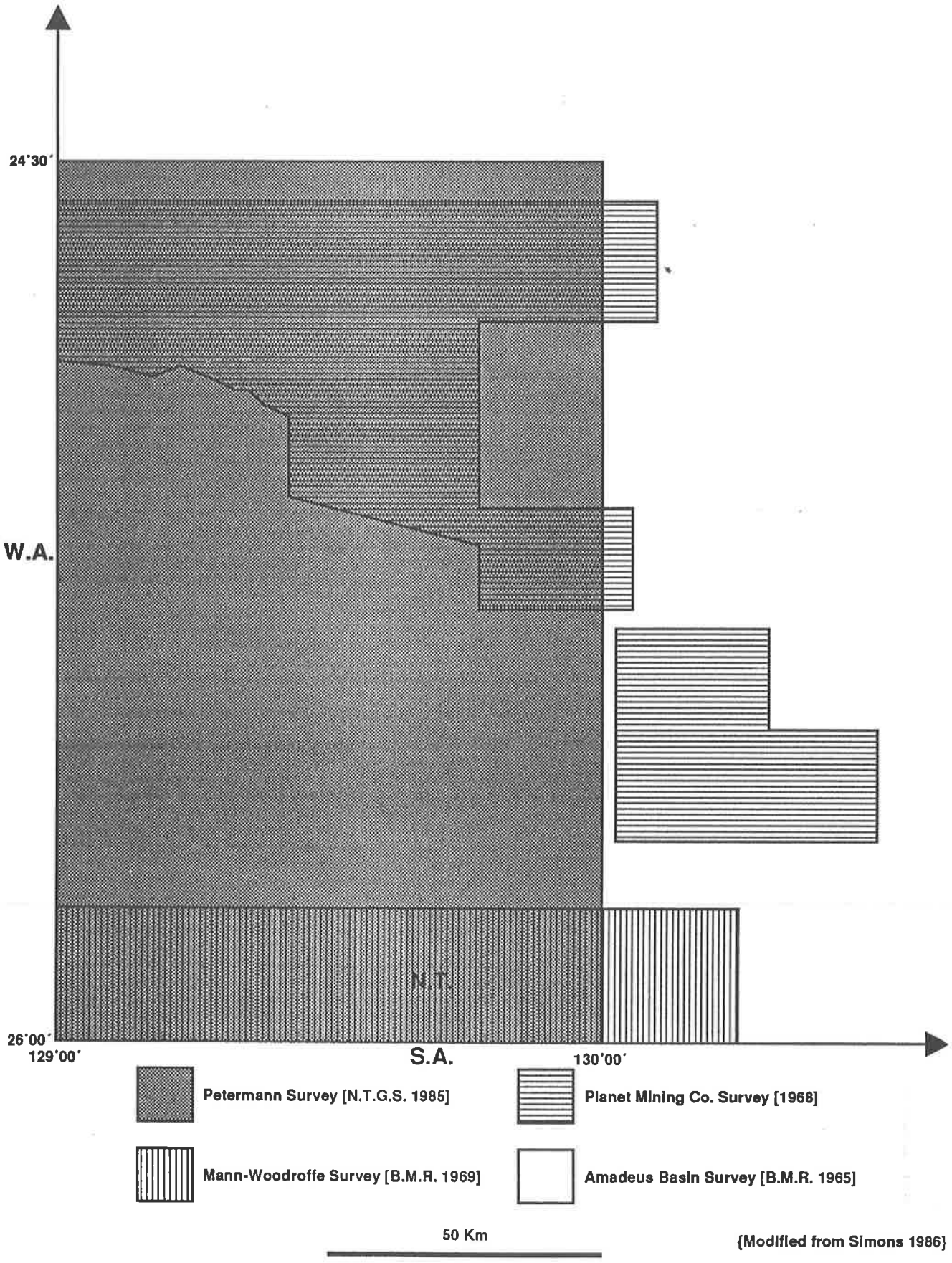

Figure 1.3: Aeromagnetic Surveys, Southwestern Northern Territory

1.7 Historical Note

No work on this part of central Australia would be complete without at least a brief mention of the legend of Lasseter's Reef, a fabulously rich gold bearing quartzite reef. The first alleged sighting of the reef was by Lewis Harold Bell Lasseter in 1897. The discovery took place while Lasseter was travelling alone in the general vicinity of the Petermann Ranges. Unfortunately Lasseter was lost at the time of the alleged discovery, or soon afterwards, and hence could not place an accurate location on the position of the reef. The reef was alleged to have been rediscovered, again by Lasseter, some three years later. On this occasion he did take accurate bearings on the location but upon returning from the sight found that his watch was running over an hour slow, thus making his calculated position considerably in error.

Numerous efforts were made to relocate the reef, by Lasseter and others, between the time of its first discovery and the early 1930's. In 1929 or 1930 a company was formed in Sydney, the Central Australian Exploration Company, which organized and equipped a party to search for the reef, with Lasseter himself as guide. Evidence from Lasseter's diaries (Stokes, 1986) indicates that Lasseter again located the reef while travelling alone in Western Australia, but soon after the rediscovery his camel bolted and he was forced to spend several weeks in a cave on the Hull River in *Pottoyu* waiting for help. That cave is now known as Lasseter's Cave. After about a month of waiting with little food or water no assistance had arrived, so Lasseter attempted to walk to Ayers Rock for help. Severely weakened by the weeks of deprivation at the cave, he died in January 1931 on Irving Creek (*Petermann*) after having travelled some 50 kilometres to the east.

Several attempts have been made since Lasseter's death to relocate the gold reef. The most recent was in 1987 with the backing of the Australian Army (Adelaide *Advertiser*, 19 June 1987). None of these later expeditions have been successful and this study has not identified any particularly likely positions for the location of the elusive bonanza.

Chapter 2

Regional Geology

2.1 Introduction

The interpretation of geophysical data requires a good knowledge of the geological setting. A more complete and detailed geological understanding will mean that more can be extracted from the geophysics, with subtle geophysical features taking on significant geological meaning which may otherwise have been overlooked. This chapter includes a description of the geology in and around the study area, and the geological theories currently held about the area. The contents of this chapter forms an important basis for the rest of this thesis.

Most of the geological work has been done by officers of the B.M.R. (Joklik, 1952; Forman and Hancock, 1964; Forman, 1966; Forman, 1966a; Forman, 1972; Forman and Shaw, 1973; Cook, 1972). That work concentrated on the outcropping sediments, metasediments and basement material of the southwest margin of the Amadeus Basin, which covers the northern half of the study area.

The geological details in the south of the area are sparse, due to lack of significant outcrops, and detailed descriptions of the geology are not available. For this reason it is necessary to turn to literature dealing with areas immediately adjacent to the study area, both in Western Australia and South Australia, and extrapolate the results, where applicable, into Northern Territory. (Wilson, 1946; Wilson, 1947; Mirams, 1964; Miller and Rowan, 1968; Goode, 1970; Moore, 1970; Collerson et al., 1972; Daniels, 1972; Daniels, 1974; Bell, 1974; Thomson, 1975).

2.2 Tectonic Setting

The study area covers two very different geological settings (see Figure 1.1 in Chapter 1). The upper Proterozoic to mid Palaeozoic Amadeus Basin in the north and the Precambrian Musgrave Block in the south.

The Amadeus Basin is an east–west trending intracratonic basin stretching some 800 kilometres. The basin is unusual in that it contains areas of very complex deformation, particularly along its northern and southern margins, the nature of which are not common in an intracratonic

setting. Lambeck (1983, 1984) notes the symmetry of the Amadeus and Officer basins about the Musgrave Block, and his computer modeling of the evolution of the central Australian basins and basement blocks, using an origin within the Musgrave Block, indicates that a compressional regime formed the series of basins (Officer, Amadeus, Ngalia) and arches (Musgrave and Arunta Blocks) in the area. Lambeck's modeling also indicates that the Musgrave Block has been uplifted by at least 17 kilometres, with the boundary between the Musgrave Block and the Amadeus Basin being a major thrust, possibly covered by a smaller secondary basin.

The Musgrave Block is a major Precambrian crystalline basement feature extending 750 kilometres east–west and 270 kilometres north–south. Several authors have postulated that the Musgrave Block and the Arunta Block (to the north of the Amadeus Basin) are infact connected beneath the basin:

> "The Musgrave Block has many similarities to the Arunta Inlier and it is quite likely that they link up beneath the Amadeus Basin to form an intracontinental mobile belt between the North Australian and Gawler Cratons."

(Plumb et al., in Hunter, 1981)

Daniels (1974) came to a similar conclusion. However a different, and more recent view on the subject is held by Shaw et al., (1984):

> "The Musgrave Inlier appears to be part of a separate mobile belt, initially unrelated to the Arunta Inlier."

It is evident from these contrasting opinions that this question is still open to debate. The Arunta Block has been the focus of intensive study over recent years (Ding and James, 1985; Whiting, 1987; James and Ding, 1988; Shaw et al., 1984) and more detailed work on the Musgrave Block is required to resolve this problem.

2.3 Stratigraphy

The stratigraphy of the study area can be broadly divided into three main categories (Forman and Shaw, 1973; Wells et al., 1970). The oldest of these categories, known as the *Older Basement*, is predominately high metamorphic grade gneissic lithologies intruded by several phases of igneous activity. In the study area this group makes up the shallow basement rocks of the Mann Ranges in the south and the gneisses in the centre of the area. Younger than this group is the so called *Younger Basement*, a series of Precambrian metamorphosed sediments and volcanic rocks which have been intruded by granites. The third and youngest category, referred to as "the Adelaidean sedimentary rocks" by Forman and Shaw (1973) are the sediments of the Amadeus Basin and are referred to in this work as the *Amadeus Basin Sequence*. This group has been extended from that of Forman and Shaw to include some of the Palaeozoic sediments that also crop out in the study area. The stratigraphy is set out in more detail in Table 2.1 and each of the three main categories are discussed in the following sections.

AGE	UNIT	LITHOLOGY	THICKNESS (max.metres)	CORRELATIVES
Quaternary	sand,alluvium travertine	dunes,sand plains	–	–
Tertiary	conglomerate	pebble,cobble,boulder conglomerate,sandstone	6	–
Ordovician	sandstone	very fine sandstone, some marine fossils	20	Stairway Sandstone
Cambrian	Mt. Currie Conglomerate	conglomerate,sandstone	–	Ayers Rock Arkose
Proterozoic	Winnall Beds	siltstone,sandstone	1500	Pertatataka Formation
	Inindia Beds	siltstone,sandstone,	2100	Areyonga Formation
	Pinyinna Beds	chert crystalline dolomite limestone,siltstone, schistose carbonate	300	Bitter Springs Formation
	Dean Quartzite	slate quartzite,conglomeratic quartzite,kyanite-muscovite-quartz schist	1200	Heavitree Quartzite
Undifferentiated Precambrian	Mannanana Porphyry	porphyroblastic schist amphibolite schist	1000	–
	Porphyry	quartz-feldspar porphyry	–	–
	Bloods Range Beds	sandstone,siltstone, shale,tuff,agglomerate basalt	1000	Dixon Range Beds
	Mt. Harris Basalt	amygdaloidal basalt, tuff,agglomerate, quartzite	1000	–
	Pottoyu Granite Complex	coarse porphyritic granite, fine-med-coarse granite, gneiss	–	–
Precambrian	Olia Gneiss	amphibolite facies gneiss, schist	–	–
	Musgrave-Mann Metamorphics	granulite facies gneiss intruded by acid,basic igneous rocks	–	–

Table 2.1: Stratigraphic Succession in the Project Area

Compiled from Forman and Hancock, 1964; Forman, 1966; Forman, 1972 Jorgenson, 1966; Wells et al., 1966; Preiss and Forbes, 1981; Shergold et al., 1985

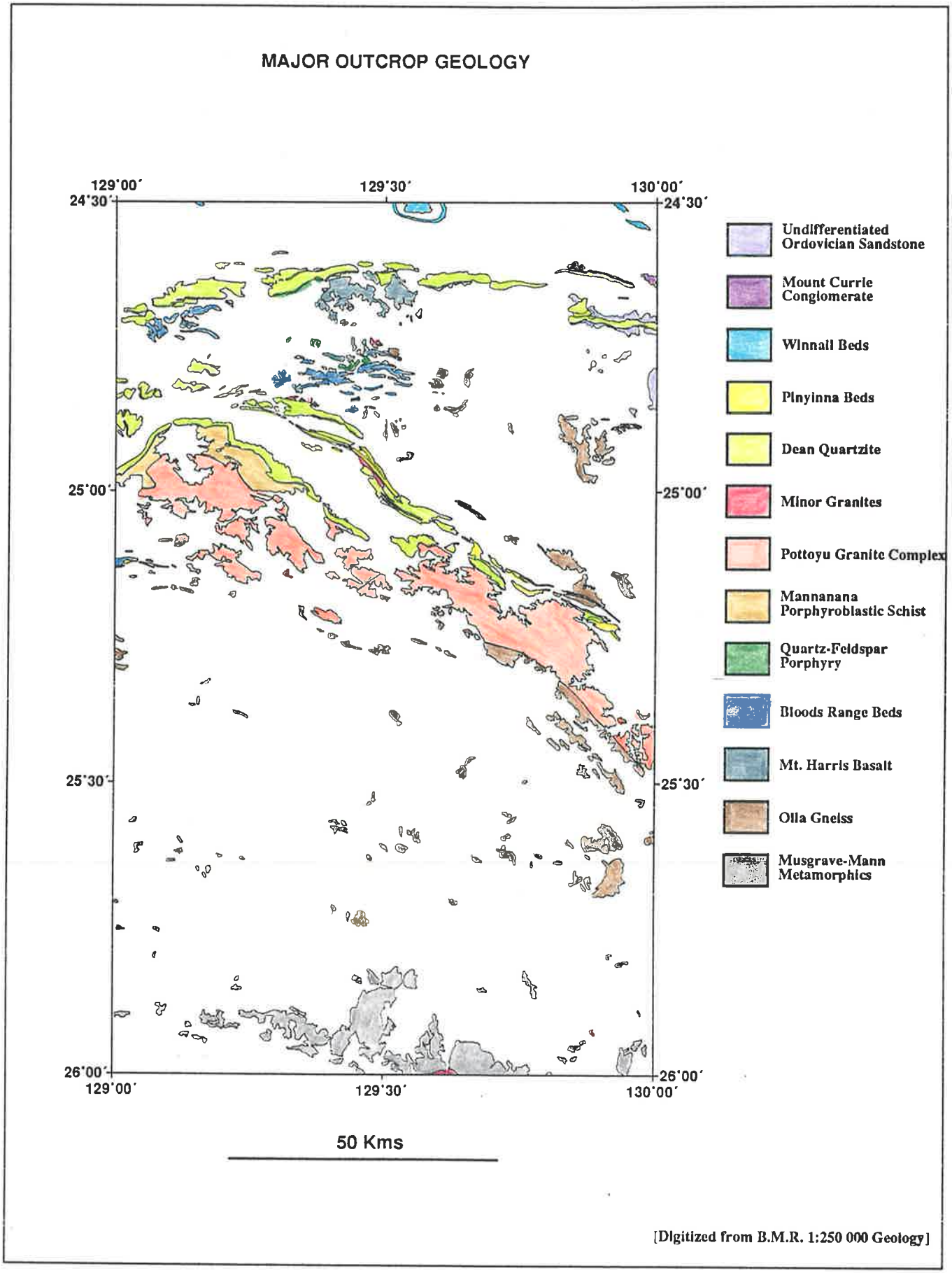

Figure 2.1: Major Outcrop Geology

2.3.1 Older Basement

The Older Basement material is primarily the high grade metamorphic rocks of the Musgrave Block. According to Thomson (1975) the Precambrian of the Musgrave Block can be tentatively subdivided into three major units, the two oldest units are of direct concern here (the Older Precambrian Basement Rocks and the Younger Precambrian Basement Rocks) with the Adelaidean Cover Rocks of Thomson's unit three referring to the Dean Quartzite and younger sediments which are discussed below.

The highest metamorphic grade basement material is the Musgrave-Mann Metamorphics which outcrop in the far south of the study area, making up the high ground of the Mann Ranges. In general the Musgrave-Mann Metamorphics are well layered granulites and gneisses, with transitional granulite–amphibolite facies material also, which can be subdivided into quartzofeldspathic, mafic, intermediate, ultramafic and pelitic components (Collerson et al., 1972). Quartzites and compositional layering in the granulites indicate that the protolith was perhaps a sedimentary succession with silty, sandy and carbonaceous components (Thomson, 1975).

Arriens and Lambert (1969) give the time of metamorphism of granulites from the Musgrave Ranges as 1350 ± 120 (my) using Rb-Sr measurements. More recently Gray (1978) reports consistent ages of 1550 my on granulites from the northern region of the Tomkinson Ranges in South Australia. Maboko et al. (1987) have dated the granulite facies in South Australia at 1175–1200 my. According to Forman and Shaw (1973) there is evidence for at least two metamorphic events in the Musgrave-Mann Metamorphics outcropping in southern *PETERMANN RANGES*. The second of these metamorphisms (about 1400 my) being a high pressure event possibly related to thrusting.

The Musgrave-Mann Metamorphics have been intruded by several phases of igneous activity. The Kulgeran granites, which include the Permano and Illbillie Adamellites (Smith, 1979) have been dated at between 1100 to 1140 my, and have been noted by Smith to be highly magnetic, having the highest magnetic susceptibilities of rock types that had been sampled from the area at the time (0.628 S.I. units). Consequently the Kulgeran Granites are often associated with high amplitude, circular magnetic anomalies (Smith, op. cit.).

A second phase of intrusion produced the basic and ultrabasic Giles Complex. The Giles Complex intrusions outcrop as a number of individual sheets and plugs in an east–west trending belt stretching 350 kilometres from well into Western Australia to Mt. Woodroffe in South Australia. The intrusions are mainly anorthosite, norite, gabbro and pyroxenites with prominent mineralogical layering. The intrusive bodies of the Giles Complex are associated with the large scale faults (Hinckley, Mann, Woodroffe Thrust) which trend east–west across the northern Musgrave Block (Thomson, 1966), although their emplacement preceded the development of the faults (Goode, 1970).

The Claude Hills pyroxenite intrusion, which is the only Giles Complex intrusion that has been mapped in the study area, lies within the Central Zone of Nesbitt et al. (1972) together

with the better exposed intrusions of Ewarara, Kalka, Mt. Davies and Gosse Pile. Although detailed work has been done on some of these better exposed bodies (Goode, 1970; Moore, 1970) little appears to have been done on Claude Hills.

Remanent magnetic measurements on several of the Giles Complex bodies (Facer, 1971) indicate that they have an average remanent magnetization direction with an inclination of $+62°$ and a declination of 343°, which is opposed to the present day Earth's field (inclination $-58°$ and declination 3°). No samples were taken from the Claude Hills intrusion in Facers' study, although some samples came from the Ewarara, Kalka and Mt. Davies intrusions, which are south of the study area by some 25 kilometres.

Also falling into the category of Older Basement is the Olia Gneiss, which crops out in southern *BLOODS RANGE* and northern and central *PETERMANN RANGES*. The major occurrence of the gneiss within the study area is in the Pottoyu Hills on central *PETERMANN RANGES*. The rock type varies from coarse porphyroblastic to fine grained gneiss with a strongly jointed and folded texture. The bands of coarse porphyroblastic and fine grained gneiss vary from several hundred feet to a few feet in thickness (Forman and Hancock, 1964). The Olia Gneiss has been classified in the amphibolite metamorphic facies by Forman and Hancock (1964). Amphibolite grade gneisses of the Musgrave Block in South Australia have been dated at 1525-1575 my (U-Pb age) by Maboko et al. (1987). The different ages recorded on the granulites and amphibolites indicate that these two rock types have undergone considerably different pressure-temperature histories.

Isoclinal folding within the gneiss of the Pottoyu Hills trends northwest and anhedral quartz grains in that area exhibit strain effects which suggest that they have undergone shearing and recrystallization (Forman and Hancock, 1964).

On the southern flank of the Pottoyu Hills the gneiss is fine and even grained, well foliated and lineated and contains isoclinal folding along northwest to southeast axes. The Olia Gneiss in *BLOODS RANGE* is medium grained, pink to greenish grey and is strongly foliated and lineated with the gneissosity dipping to the north.

The gneiss grades into the overlying lithologies (Mt. Harris Basalt, Bloods Range Beds and Dean Quartzite) and is believed to have formed, at least in part, by metamorphism of the units underlying the Dean Quartzite. Some of the Olia Gneiss may be original gneissic basement, particularly in the south of the study area (Forman, 1966).

2.3.2 Younger Basement

The younger basement is made up of the Mt. Harris Basalt, Bloods Range Beds and various metamorphosed equivalents of these units, including the Mannanana Porphyroblastic Schists, and a quartz-feldspar porphyry. The Mt. Harris Basalt, at the base of this younger basement sequence, is a thick series of amygdaloidal basalt, green schist, tuff and agglomerate which outcrops in the northern section of the study area (see Figure 2.1). The base of the Mt. Harris

Basalt is marked by a cross bedded quartzite overlain by basalt which is mainly epidotized, amygdaloidal and massive, typical of quiet lava outpourings with an absence of any explosive volcanism (Kenneth McMahon and Partners, 1968).

Apparently conformably overlying the Mt. Harris Basalt are the Bloods Range Beds, which are a series of sandstone, quartzite, sericite feldspar schist, porphyry, slate and interbedded basic extrusive rocks (Forman and Hancock, 1964). The unit outcrops in northern *BLOODS RANGE* and also on the western edge of *PETERMANN RANGES* and is correlated with the Dixon Range Beds, mapped in the neighbouring *RAWLINSON* sheet area in Western Australia.

The Bloods Range Beds have been subdivided into three units by Kenneth McMahon and Partners (1968):

1. Arenaceous sediments at the base,
2. volcanic sediments and basic flows,
3. lutites and calcic sediments with graphite rich equivalents.

Forman (1966) notes that some of the basaltic material mapped as Mt. Harris Basalt may belong to the Bloods Range Beds.

The Mannanana Porphyroblastic Schist, which is mapped on southwestern *BLOODS RANGE* as an arcuate belt of outcrop, is noted as having an iron rich ground mass (Forman and Hancock, 1964). The Mannanana Schist is thought by several investigators (Forman and Hancock, 1964; Jorgenson, 1966) to be derived from the Bloods Range Beds and Mt. Harris Basalt. This conclusion is based on the similarity in stratigraphic position of the Mannanana Schist and metavolcanic units beneath the Dean Quartzite, and the presence of schistose porphyry and tuff within the Bloods Range Beds.

The mapped Mannanana Porphyroblastic Schist on *BLOODS RANGE* is discontinued at the southern boundary of that sheet. Immediately adjacent rocks on *PETERMANN RANGES* are mapped as Pottoyu Granite Complex. Forman and Hancock (op. cit.) do note that the schist is gradational with gneiss and granite.

Other porphyroblastic rock types occur associated with the Mt. Harris Basalt and Bloods Range Beds, most notably a quartz-feldspar porphyry which forms a lenticular outcrop ten kilometres (6 miles) long and three kilometres (2 miles) wide trending east–west across the boundary between *Hull* and *Bloods Range*. This lithology is closely associated with the Mt. Harris Basalt and stratigraphically placed near the top of that unit according to Wilson (1966).

2.3.3 Amadeus Basin Sequence

The Adelaidean and younger sediments and metasediments which outcrop in the study area are grouped together in the Amadeus Basin Sequence. At the base of this sequence is the Dean Quartzite. This quartzite is the major resistant outcrop forming the Dean and Bloods Ranges. The Dean Quartzite is a medium to coarse grained moderately sorted, moderately rounded white

and brown quartzite and sandstone with thin bedding, laminae and cross laminae (Forman and Hancock, 1964). The unit lies unconformably upon the Mt. Harris Basalt and Bloods Range Beds, with a thin basal conglomerate in some places which contains fragments of amygdaloidal basalt. In many places the quartzite has been metamorphosed to sericitic quartzite which is often schistose.

The Dean Quartzite is a prominent and important marker horizon all along the southwestern margin of the Amadeus Basin and is correlated with the Heavitree Quartzite which occurs further north in the basin.

Conformably overlying the Dean Quartzite are the Pinyinna Beds, which are a sequence of crystalline dolomite limestones and siltstones containing a few poor stromatolites (Forman, 1966). The Pinyinna Beds have undergone recrystallization and metamorphism. Outcrop is generally poor mainly due to the rapid weathering of the soft calcareous rocks that make up the unit. The Pinyinna Beds have been subdivided into five units by Kenneth McMahon and Partners (1968):

1. Quartz sericite schists, schistose slate,
2. hematite-goethite schist,
3. black graphitic slate, phyllite schist,
4. grey green siltstone,
5. yellow grey limestone.

The basal quartz sericite schist unit, which is in contact with the Dean Quartzite is in agreement with the metamorphosed basal unit of Forman and Hancock (1964) as a grey schistose slate, phyllite and fine grained quartz sericite schist, however the unit is not further subdivided by those workers.

The Pinyinna Beds, together with the underlying Bloods Range Beds and Mt. Harris Basalt, were the subject of an exploration effort after iron rich cappings were found which were thought to be gossanous (Wilson, 1966). These cappings occur in the hematite-goethite schist (unit 2) of the Pinyinna Beds. Geochemical surveys (Kenneth McMahon and Partners, 1968) suggested that the beds contain no significant base metal concentrations.

The Pinyinna Beds are correlated with the Bitter Springs Limestone which outcrops north of the study area and extensively along the northern margin of the basin.

Conformably above the Pinyinna Beds lie the Inindia Beds, a yellow brown siltstone, white sandstone and chert with thin interbeds of dolomite. There is no outcrop of this unit in the study area, although it is prominent north of the area in Souths Range. The Inindia Beds are likely to underlie the recent sand and alluvium in the far north of the study area. The northern correlative of the Inindia Beds is the Areyonga Formation. (Wells et al., 1966).

The Winnall Beds, which are possibly unconformably above the Inindia Beds (Forman and Hancock, 1964) outcrop in the far north of the study area in several small basinlike structures

at Mt. Cowle and west of the Hull River (on *Hull*). Both these circular features are tentatively mapped as Winnall Beds. Ranford et al. (1965) divided the Winnall Beds into four units alternating between siltstone and sandstone with siltstone and silty sandstone being the basal unit. The more resistant sandstone units form most of the strike ridges of Winnall Beds outcrop that occur north and east of the study area (Wells et al., 1966). Within the study area the sandstone units are white medium grained and medium to coarse grained with common purple marls and cross laminations. The sandstone units have been broken into flags and blocks (Forman, 1966). The silt units are yellow brown and red brown, laminated and micaceous.

The Mt. Currie Conglomerate unconformably overlies the Winnall Beds in the Pinyinna Range (northeast *Bloods Range*). The upper portions of the Mt. Currie Conglomerate form the well known inselbergs at Mt. Olga, eighty kilometres to the east of the area. The Conglomerate is described by Forman and Hancock (1964) as a sequence of pebble, cobble and boulder conglomerates which were probably deposited at the same time as the arkose at Ayers Rock as a lithological variant of that unit.

A fifteen to twenty metre thickness of undifferentiated Ordovician Sandstone outcrops in the northeastern corner of the study area. The unit is an essentially flat lying fossiliferous white and grey very fine sandstone. It is an outlier of the shallow marine Stairway Sandstone (Cook, 1972). The sandstone in the study area is probably part of the wide spread upper unit of the Stairway Sandstone which is a white very fine grained sandstone. The middle unit of the Stairway Sandstone is noted for the occurrence of phosphorite (Cook, 1972).

Tertiary pebble, cobble and boulder conglomerates are common on the flanks of the quartzite topographic highs, but most of the area is covered by Quaternary sands and alluvium. Ten to twelve metre high northwest trending longitudinal sand dunes dominate the far north and much of the area to the south is flatter sand plains with occasional dunes (Forman, 1966; Forman, 1972).

2.3.4 Granites

The Pottoyu Granite Complex forms a large area of outcrop in northern *PETERMANN RANGES* and into southern *BLOODS RANGE*. The main mass of the granite has been described by Forman and Hancock (1964) as a coarsely porphyritic biotite-quartz-feldspar rapakivi granite with up to 50 % interlayered gneiss, schist, amphibolite and quartzite. The granite is in contact with Bloods Range Beds, Olia Gneiss, Mannanana Porphyry and Dean Quartzite. The contact with the Dean Quartzite is generally gradational (transitional) but in places is reported as being clearly intrusive. Outcrop near the Hull River on *PETERMANN RANGES* includes at least three types of intrusive granites from which relative ages can be determined (Forman, 1972). Rubidium-Strontium whole rock dating on granite specimens from Mt. McCulloch (eastern central *Petermann*) and Katamala Cone, east of the study area, give an age of emplacement as 1190 my and 1150 my respectively and a 600 my age on biotite and microcline from the

specimens is interpreted by Forman (1972) as the time of the last metamorphism of the granite complex. Thompson (1975) includes the Pottoyu Granite Complex in the Kulgeran Granites of the Musgrave Block.

A prominent and well developed northwest foliation is visible in the Granite Complex in the Pottoyu Hills from air photographs. This foliation is less well developed in the granite around the Hull River in southwestern *BLOODS RANGE* and northwestern *PETERMANN RANGES.*

The northern edge of the Granite Complex (*Hull, Pottoyu*) has a border phase of pink medium grained granite and medium grained porphyritic granite (Forman and Hancock, 1964). The width of this border phase is not reported in the literature.

Further north in *BLOODS RANGE* there are several smaller sheets and bosses of granite referred to by Jorgenson (1966) as undifferentiated or minor granites. These show gradational contacts with the Mt. Harris Basalt, Bloods Range Beds and Dean Quartzite and, in general, are very coarse porphyritic granites. The northern most granite outcropping near the eastern edge of *Hull* (13 kilometres southwest of Mt. Harris) is described as intrusive into the Mt. Harris Basalt (Forman and Hancock, 1964). Jorgenson (1966) believes that these outcrops and the Pottoyu Granite Complex are possibly lateral equivalents.

2.4 Geological Structure

There are several interpretations of the regional geological structure in the southwestern margin of the Amadeus Basin, all of which concentrate on the region in the north of the study area. Two structural theories will be discussed here. The first, proposed by Forman, is the most widely accepted and published. The second is the result of a reinterpretation of air photographs and other information by Jorgenson (1966) and a fixed wing and helicopter reconnaissance carried out by Wilson (1966) in the north and to the east of the study area.

2.4.1 Forman's Interpretation

Forman suggests that there is a uniform structural style for over 320 kilometers (200 miles) along the southwest margin of the Amadeus Basin. The distribution of the Dean Quartzite throughout the area of the southern margin of the basin was important in formulating and defining this theory, since the unit is a unique and prominent marker horizon.

According to this interpretation the regional structure is dominated by a recumbent fold which is over 320 kilometres long and 50 kilometres or more wide. The folding took place at the end of the Precambrian during a compressional deformation called the Petermann Ranges Orogeny 600 my ago. The orogeny has been attributed to the rising isotherms that led to continental break up of Australia and Antarctica about 570 my ago (Veevers et al., 1982).

The regional structure is illustrated on the block diagram, Figure 2.2, from Forman and Hancock (1964). The diagram includes the area approximately covered by the *Hull* and *Bloods*

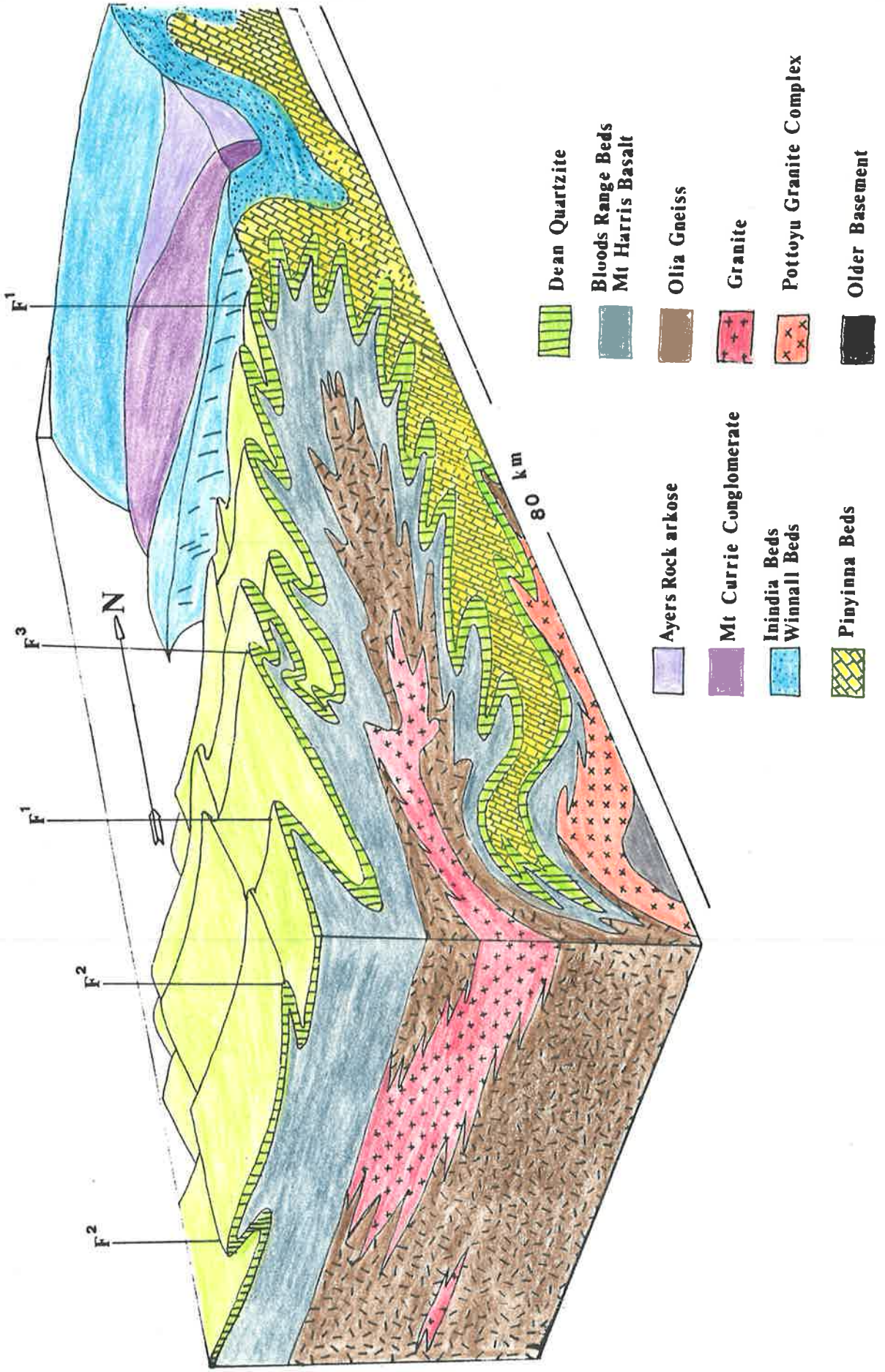

Figure 2.2: Regional Structure, Southwestern Margin Amadeus Basin (from Forman and Hancock, 1964)

Range sheets. There are three generations of folding in the area. The oldest folds, F^1, are isoclinal recumbent folds which trend east–west along the main trend of the ranges. These early folds are clearly refolded by second generation F^2 folds which are also isoclinal and recumbent with their axial planes trending in a north–south direction. A further generation of F^3 folds is present in the Mannanana and Curdie Ranges of southwest *BLOODS RANGE* and are a series of tight east southeasterly trending folds with overturned axes dipping to the south.

The regional recumbent fold involves the Olia Gneiss, Mt. Harris Basalt, Bloods Range Beds, Dean Quartzite and Pinyinna Beds. The overlying sediments (Winnall Beds and Inindia Beds) are believed to have been squeezed northwards out of the recumbent fold on a décollement surface within the mobile evaporitic Pinyinna Beds. Décollement surfaces within the Bitter Springs Formation have been reported by Froelich and Krieg (1969) on the basis of limited seismic control in the north of the Amadeus Basin where there are similar but smaller scale fold nappe structures. The Winnall and Inindia Beds exhibit only gentle folding developed by the much later mid-upper Devonian Alice Springs Orogeny, which was centred on the northern margin of the Amadeus Basin and the Arunta Block.

The Mt. Currie Conglomerate and Ayers Rock Arkose formed as a molasse type clastic wedge off the newly formed Petermann Mountain Range along the northern front of the recumbent fold early in the Cambrian.

Structural details from the south of the study area are scarce. One of the major structural features in the area is the Woodroffe Thrust. The Thrust has been mapped in South Australia as a gently southerly dipping to near horizontal zone of protomylonites, ultramylonites and pseudotachylite which varies in thickness from between 10 and 100 metres (Collerson et al., 1972; Bell, 1974). The southern granulite facies Musgrave-Mann Metamorphics were thrust northwards over the amphibolite facies Olia Gneiss along the Woodroffe Thrust with of the order of 25 kilometres of northerly movement (Major, pers. comm.). Forman (1972) postulated that the Thrust was active during the Petermann Ranges Orogeny (600 my) and recent dating of muscovite from a minor shear zone related to the Woodroffe Thrust in South Australia (Maboko et al., 1987) yielded an age of 540 my as the latest movement of the thrust.

2.4.2 Jorgenson and Wilson's Interpretation

An alternative interpretation of the structure of a smaller area in the north of the study area (Prospecting authorities 1435 and 1546) has been suggested by Jorgenson (1966) and Wilson (1966). These workers were aware of Forman's interpretation but could see no reason to involve the regional recumbent fold and consequent large scale décollement in the Pinyinna Beds.

The basis of this alternative interpretation is a series of large individual isoclinal anticlinal folds which are separated by the root zones of tightly folded isoclinal synclines, with their axes overturned to the south, so that the northern limbs of the anticlines and the southern limbs of the synclines are overturned. The synclinal root zones make up the prominent quartzite ranges

in the area (Dean, Bloods, Pinyinna, McNichol, Piultarana, Curdie).

The cause of this style of deformation is seen by Jorgenson (op. cit.) to be due to pressure from the north, possibly applied by very deep seated plutonic granite and porphyritic rocks which have moved outwards and upwards from the position of the present Amadeus Basin into the Precambrian rock sequence during the Petermann Ranges Orogeny.

2.5 Discussion

The task of making valid hypotheses on the regional structure of this part of central Australia requires careful study of the geology of a very large area. Jorgenson (1966) and Wilson (1966) were restricted to a small section of the area, just as the area covered in this thesis work, although substantial, is only a portion of the size required to get a truly regional picture.

Forman's interpretation is based on much first hand experience over a very large area and has, in general, been accepted by other workers who have looked at the area (Froelich and Krieg, 1969; Daniels, 1972; Lambeck, 1984; Korsch and Linsday, 1989). Since the aims of this thesis work, as defined in Chapter 1, are to produce a detailed geological interpretation of the study area, the interpretation needs to be set within a regional structural framework. The geophysical data is consistent with the recumbent fold model (see Chapter 5) and thus the framework which will be adopted for the northern section of the study is the regional recumbent fold hypothesis proposed by Forman.

Chapter 3

Image Interpretation

3.1 Introduction

The interpretation of airborne magnetic and radiometric data requires the data itself to be in a form that is both meaningful and easily understood. Traditionally the main formats of data presentation have been contour maps, stacked profiles and individual flight line profiles. Recently the use of digital imaging for remotely sensed data has become more common, first with satellite images and then with geophysical data sets. Digital images are more versatile than contour maps and their use means that the major step of computer contouring, during which numerous problems can arise, is avoided. The presentation of the geophysical data as digital images has been applied extensively in this work using a system developed in the Department of Geology and Geophysics by S. Rajagopalan (see Appendix A). Prior to this work the majority of the data covering the study area was available only as contour maps and computer tapes. The differences between a contour map presentation and a digital image are best illustrated with an example. Figure 3.1 shows the *Duffield* sheet at a scale of 1:500 000 both as a contour map and a greyscale digital image, and highlights the much finer detail visible in the image, particularly at this small scale.

This chapter describes the methods used for the interpretation of the magnetic images, and presents the qualitative interpretation framework of the study area.

3.2 Interpretation Method

A common and generally accepted method of interpreting airborne magnetic (and radiometric) data is to subdivide the study area into a number of smaller subareas, with common geophysical (geological) characteristics. This method has been well documented in general terms and case histories (Boyd, 1967; Emerson, 1973; Isles, 1983; Ukaigwe, 1985; Whiting, 1987). Most of the interpretation schemes based on this method differ in significant details from one another, and there does not appear to be any standardized method or nomenclature for this type of qualitative

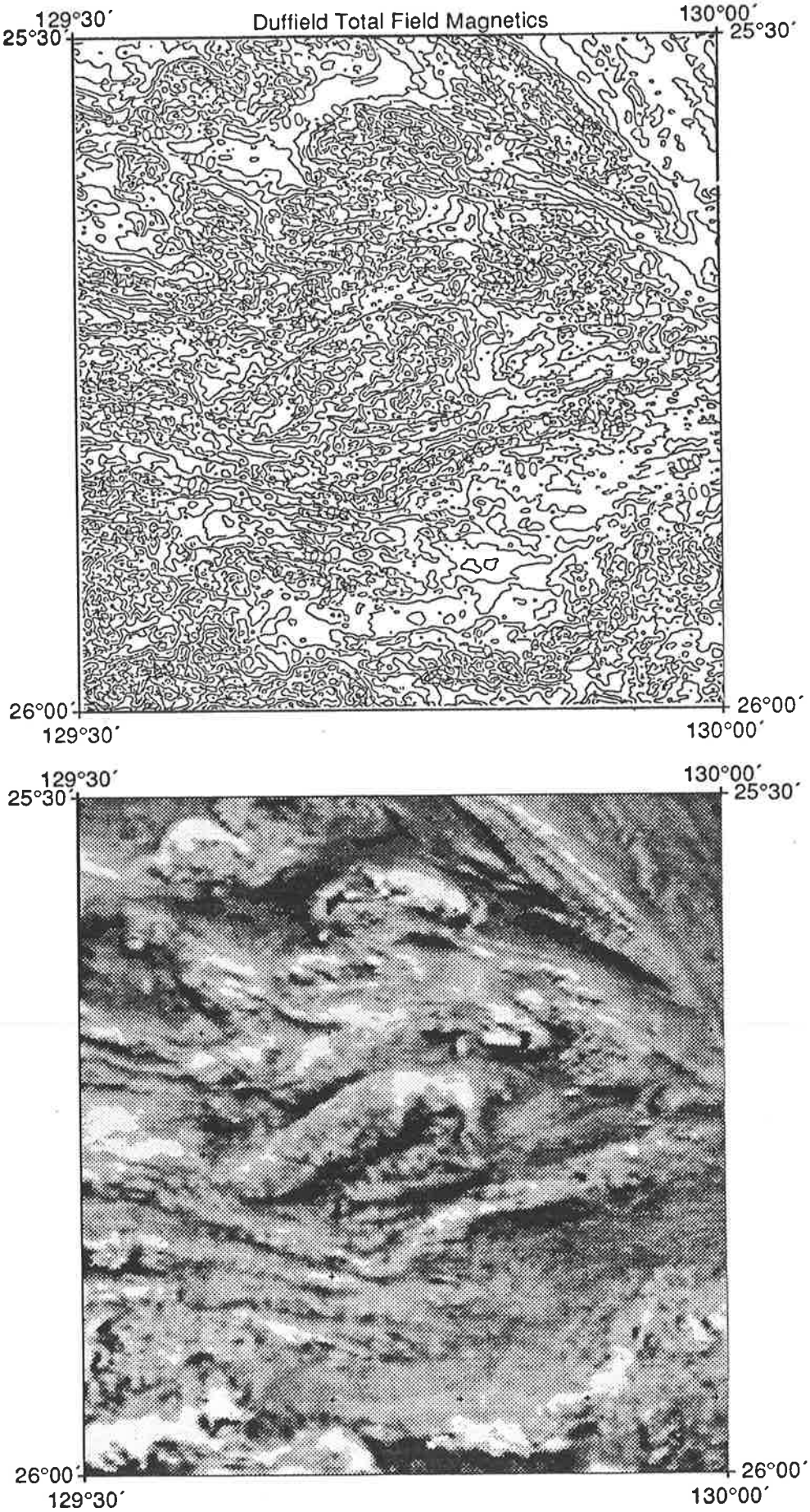

Figure 3.1: Comparison of Contour Map and Digital Image, *Duffield*

interpretation. Whiting (1987), in his study of the aeromagnetics over the Arunta Block N.T. divided the area into a number of provinces, whereas Emerson (1973) subdivided the magnetics of the eastern Yilgarn Block W.A. into a number of magnetic zones. Both Isles (1983) and Ukaigwe (1985) in their work on the Broken Hill Block subdivided the area into zones and Isles went a step further and broke his zones into smaller domains.

The division of an area into smaller subareas of consistent internal magnetic characteristics is generally achieved by comparing components of the overall magnetic data, such as anomaly amplitudes, frequency, shape, linearity and elongation direction, all of which add up to produce a distinct magnetic pattern or texture. The component parts of the anomalous magnetic field depend upon the disposition of the underlying lithologies, their magnetization, depth, strike and geological structure, thus subareas can be used to make inference on the causative geology.

The approach which has been used in this work is to give each of the commonly used terms to describe magnetic subareas (province, zone and domain) a hierarchical relationship related to scale or areal extent. The term province is used to describe the largest areas, which can be vast expanses of magnetically similar areas, such as the magnetic response of the Musgrave Block, or the Amadeus Basin as a whole. Thus the delineation of provinces requires small scale regional aeromagnetic maps such as the B.M.R. 1:1 000 000 series. Each province is then subdivided into domains, perhaps relating to major lithostratigraphic groupings. Domains can then be further broken down into smaller zones which pick out related magnetic lithologies (lithomagnetic units) or groups of several rock types which produce similar magnetic responses.

3.2.1 Textural Schemes

Most qualitative interpretation schemes are based on data presented as contour maps and if the data are in an alternative form then the interpretation schemes need to be adapted to that different form of presentation.

When using greyscale images for aeromagnetic interpretation a slightly different approach needs to be made where magnetic subdivisions are based on areas of similar image texture, where the overall texture is a result of the components of the anomalous magnetic field as discussed above. This "textural interpretation" approach based on greyscale digital images was proposed by Tucker and D'Addario (1986, 1986a, 1987) and has been successfully applied by those workers on several 1:1 000 000 scale total magnetic field greyscale images.

The interpretation scheme of Tucker et al. (1987) divides the greyscale image into a number of textural domains. Each domain contains several areas of differing textural characteristics (e.g. smooth, mottled, granular). This style of interpretation has been adopted in this thesis with some minor alterations which will be described below. An effort has been made to remain compatible with the original scheme.

As discussed in Appendix A the directionally filtered total field magnetic image gives the data the illusion of surface texture, and it was found that a textural interpretation was best

done based on this image, although considerable input came from all the other forms of the data. This is one of the major differences between the scheme applied here and that of Tucker et al. (op. cit.) which is based on unfiltered total field magnetic images. Another significant difference between this work and Tucker's scheme is the map scale. The latter is based on maps of a 1:1 000 000 scale with domains commonly of the order of the size of a 1:250 000 map sheet. The Petermann study area is the same size as a 1:250 000 map sheet and as such, more emphasis is placed on the textural components (here termed zones) which go to make up the larger domains than in the work of Tucker et al. (op. cit.). The working map scales used were 1:250 000 and 1:100 000. The 1:1 000 000 images presented in this thesis are at the smaller scale for convenience of display only.

3.3 Magnetic Textures

Textures of magnetic greyscale images are primarily dependent upon the magnetization and disposition of the rocks over which the data is flown (as discussed above) and, as such, textural zones will always tend to be relative, depending on whether the area under study is one where the lithologies are strongly magnetized or only weakly magnetic. A definition of the characteristics of each textural zone used in the qualitative interpretation is a prerequisite before conclusions are made about those zones. The zone definitions are best achieved by presenting a typical example of each zone from the data set. The majority of examples in Figure 3.2 are from the total magnetic field which has been directionally filtered to enhance east–west trending features. A discussion of each of the textural zones, with a description of their characteristics, is set out below in an order of increasing relative magnetic activity.

Smooth

A smooth texture (S) is perhaps the most intuitively obvious and is simply areas of flat or slowly varying smooth magnetic field which are devoid of high frequency anomalies. The typical smooth texture on Figure 3.2 comes from the *Hull* sheet. Anomalies within the smooth textural zone are low frequency, slowly varying and of variable amplitude.

Such zones are associated with significant thicknesses of nonmagnetic material, generally sediments or metamorphosed sedimentary rocks with a very low magnetic susceptibility, such as sandstones, quartzites and some nonmagnetic schists and carbonate rocks. The smooth texture as defined and used here is the same as that used by Tucker et al. (1986, 1987).

Granular

A granular texture (G) represents areas in which there is a higher magnetic activity than in smooth textured areas. The example in Figure 3.2 is taken from the southwestern section of *Hull*. The magnetic anomalies within the zone are of small amplitude (0–50 nT), caused by near

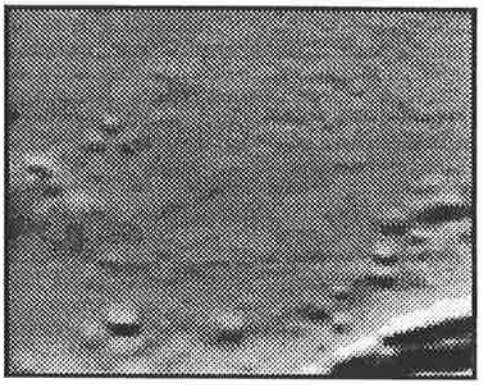

SMOOTH

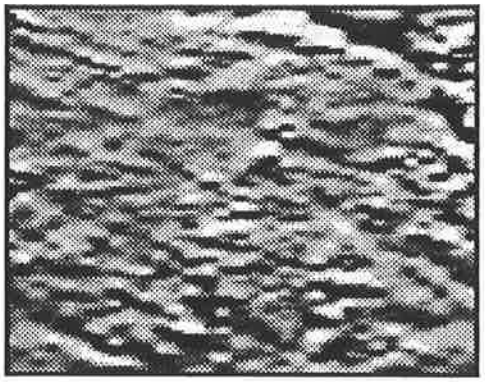

GRANULAR

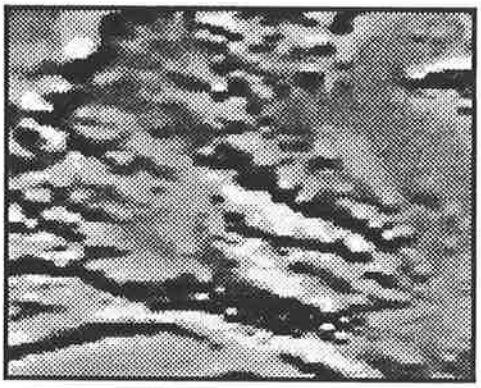

MOTTLED

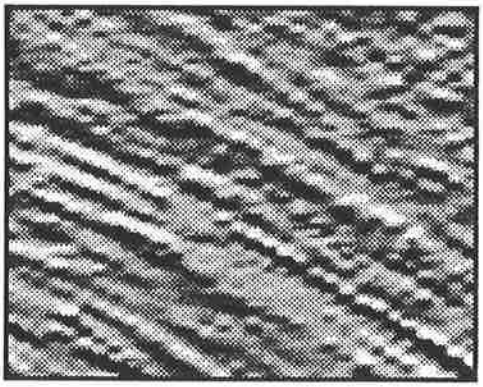

LINEAR

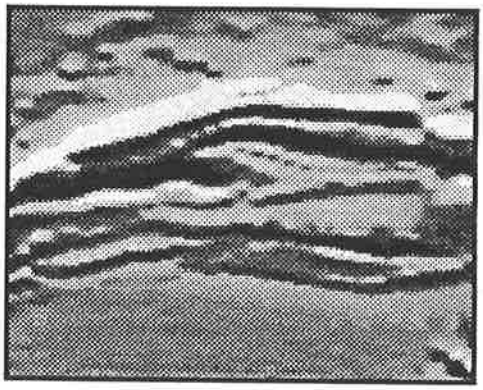

BROAD LINEAR

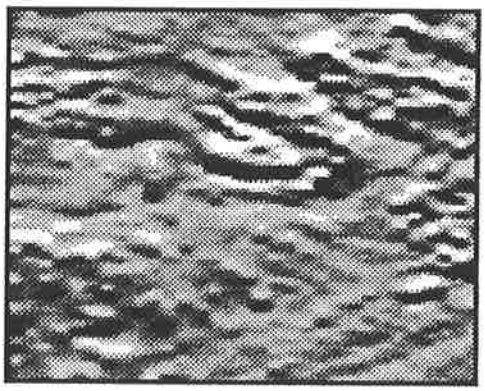

MURICATE

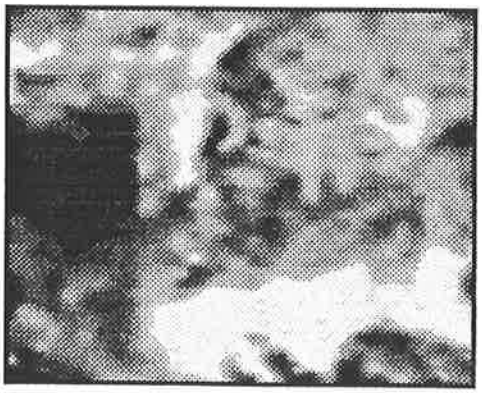

CIRCULAR/ELLIPTICAL

Figure 3.2: Typical Magnetic Textural Zones

surface sources. The anomalies are generally single flight line features with little continuation across flight lines, resulting in zones with very few linear anomalies. Granular zones in the study area are generally associated with near surface granitic rocks of low magnetic susceptibility.

Mottled

The mottled texture (**Mo**) is more magnetically active than the granular. The anomalies within mottled zones are of higher amplitude than those associated with granular zones, typically 40–150 nT. Linear anomalies are more prevalent although they tend to be only a few kilometres long. A typical mottled zone taken from *Hull* is shown in Figure 3.2. Rock types associated with mottled zones are those of moderately magnetic lithologies such as magnetic granites, porphyries, and metamorphosed material, volcanics and quartzofeldspathic basement rocks.

Linear

As the name suggests the linear textural zone (**L**) is characterized by long elongate anomalies, closely spaced and generally parallel to each other. The anomalies are high frequencies and moderate amplitude (50–150 nT) and correlate strongly across flight lines. The examples of the linear zone in Figure 3.2 comes from the central section of *Petermann*. Source rocks for this type of texture are near surface with moderate to high magnetic susceptibilities, and a strong linear fabric such as foliated gneisses or other metamorphically or structurally layered magnetic rocks.

Broad Linear

Broad linear zones (**BL**) are those which contain anomalies with a strong linearity similar to the linear zones but are of a lower frequency and higher amplitude. The type example for this texture comes from the northern section of *Hull*. Anomaly amplitudes can be up to 500 nT. Source material for the zone are strongly magnetized units, possibly magnetite rich sedimentary horizons or strongly magnetized layered metamorphic rocks buried beneath a nonmagnetic cover up to 400 metres thick.

Muricate

The muricate texture (**Mu**) is the high relief magnetic response of strongly magnetized near surface metamorphic basement rocks. It is characterized by large amplitude (up to 1100 nT) and high frequency complex magnetic anomalies made up of closely spaced shallow magnetic sources, often highly deformed by faulting and folding.

Circular/Elliptical Features

A common feature in aeromagnetic maps is the occurrence of circular or elliptical areas with magnetic characteristics which contrast with those of their surrounding areas. The circular features can be either more magnetically active than the neighbouring material or less active. They are not extensive enough to be classed as a textural zone in themselves but are a common and distinctive feature in several of the zone types discussed above, especially those of higher magnetic activity.

The shape of the zones suggests an igneous intrusive origin and the variable magnetic nature is dependent upon the lithology, nonmagnetic granites producing the low relief features and basic magnetite rich intrusions causing the more highly magnetic features.

There are numerous circular/elliptical features of various types and sizes in the southern half of the study area which manifest themselves most effectively in the unfiltered magnetic images. The examples shown in Figure 3.2 are of the unfiltered total magnetic field data from southern *Cockburn/Duffield* , and highlight a prominent circular magnetic low and part of a more subtle circular area of increased magnetic activity.

3.4 Magnetic Subdivisions of the Petermann Area

On the basis of the magnetic textures described above, the study area has been divided into a number of magnetic textural zones and two larger magnetic domains, the Northern Domain and the Southern Domain. These subdivisions form the framework of the geological interpretation of the area. The subdivisions are based only on the magnetic data and do not take the geological distribution into account and in this respect the divisions represent a geologically unbiased interpretation of the data. Not all the magnetic boundaries are sharp or definite and alternative interpretations would be possible, although only minor changes are likely from the interpretation presented here.

Each textural zone has been given an alphanumeric identification code (e.g. **NS1**, see Figure 3.3). The first letter in the code refers to the magnetic domain, **N** is the Northern Domain, **S** is the Southern Domain. This is followed by a one or two letter code describing the magnetic textures as listed above. The final number is a repeat code, if required, to identify zones within the same domain and with the same texture, but a different location. Such identification codes have been written in bold face type throughout this thesis. The locations of the interpreted zones are presented in Figure 3.3 and are referred to frequently in later chapters.

The Northern Domain is made up of a number of clearly defined textural zones. Most correlate closely with the known geology of the Amadeus Basin sediments and adjacent metasediments, metavolcanics and basement rocks. In contrast, the Southern Domain is a zone of higher magnetic activity and complex magnetic patterns, reflecting the near surface, high grade rocks of the Musgrave-Mann Metamorphics which have a complex multiple deformation history. All

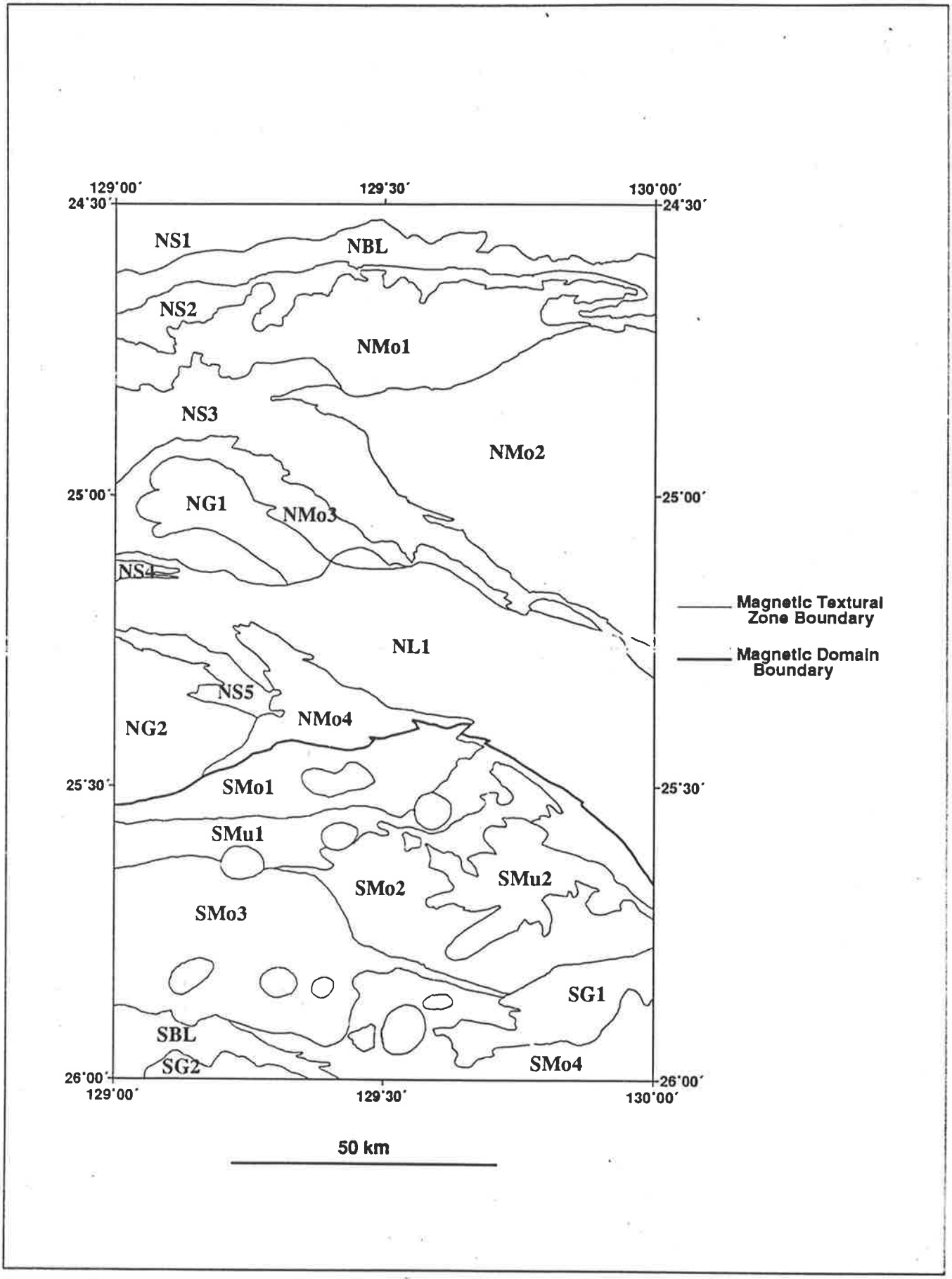

Figure 3.3: Interpreted Magnetic Zones and Domains

DIRECTIONALLY FILTERED TOTAL FIELD MAGNETICS

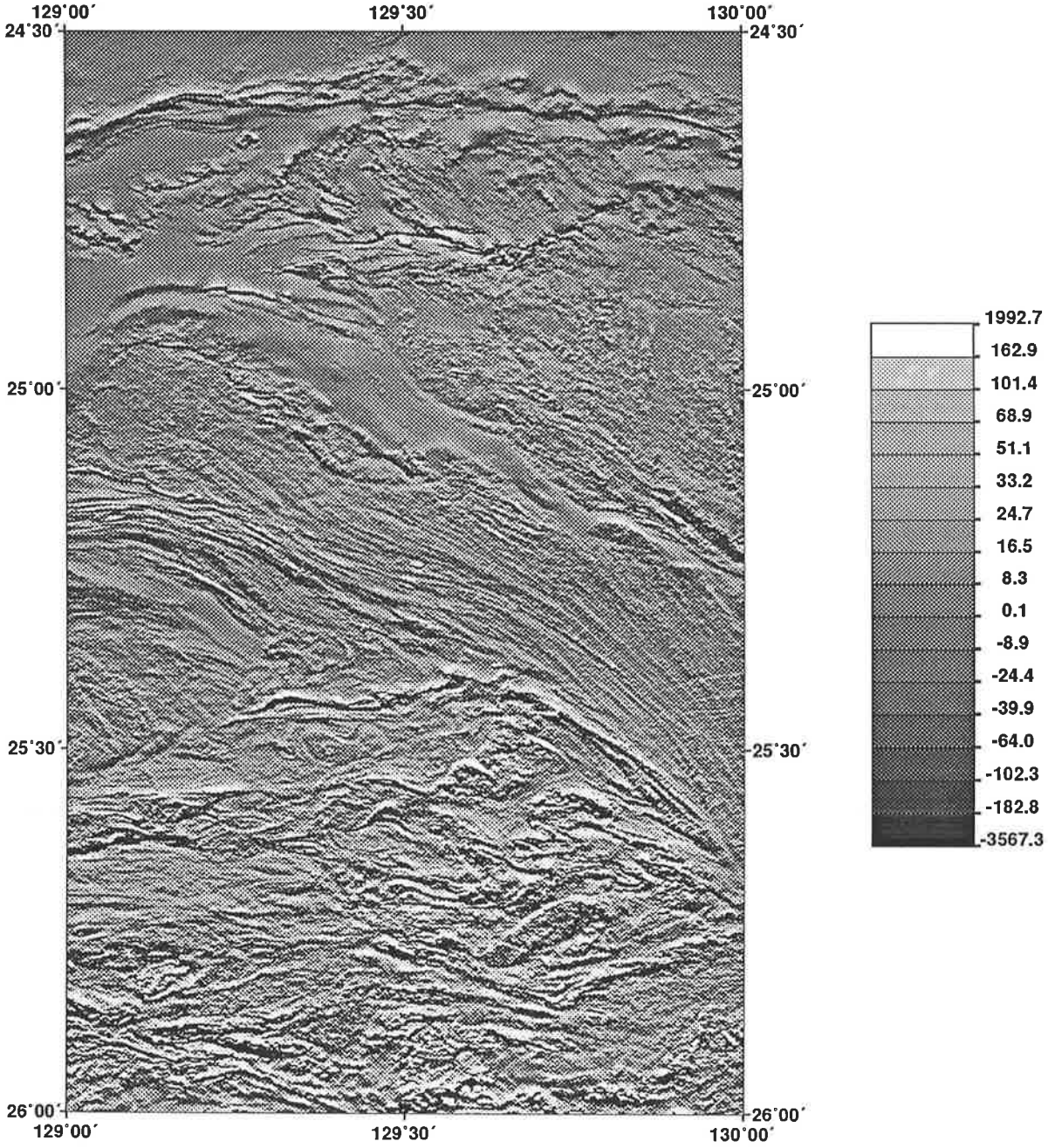

the circular and elliptical features in the study area are restricted to the Southern Domain. A detailed interpretation of the radiometric and magnetic data covering the two domains is set out in the following chapters.

Chapter 4

Radiometric Data

4.1 Introduction

The radiometric data over the study area correlates well with the interpreted magnetic domains and textural zones, however radiometric surveys only respond to the top few tens of centimetres of surface material and so parameters associated with the vertical dimension, such as depth and dip, are not relevant variables in radiometric interpretation. There are three main unknowns that are addressed in the interpretation of radiometric data:

1. the surface position of the source of radioactivity,
2. the surface dimensions of the source,
3. the radioactive strength of the source.

Thus the interpretation of radiometric surveys requires a different approach to that of magnetic or gravity data. This chapter presents the data and discusses the interpretation methods applied and the results obtained from the radiometric data over the study area. The survey specifications and corrections that have been applied are covered in Appendices B and C.

4.2 Interpretation Philosophy

Airborne radiometric data is generally collected for one of two important reasons. One of these reasons is to use the data as an exploration tool in the search for radioactive ore deposits, the second is to use the data as a geological mapping tool. Both these methods require a different approach to the interpretation of the data and it is important to decide how the data is to be used prior to embarking upon an interpretation project.

If the radiometric survey is to be used in the search for radioactive ore deposits it is almost mandatory that a detailed knowledge of the geology is available. One interpretation technique calculates the mean and standard deviation of the radioactive data set and uses these figures to highlight anomalies that are one, two or more standard deviations above or below the mean

LITHOLOGY	URANIUM (eppm)	THORIUM (eppm)	POTASSIUM (%)
Acid Igneous	4.8	18	3.8
Intermediate Igneous	2.6	9.7	2.2
Basic Igneous	1.1	3.2	0.8
Granulite	0.6	5.7	2.0
Amphibolite	1.2	6.0	2.4
Argillaceous	3.8	14	2.2
Arenaceous	0.9	3.9	1.2
Carbonates	1.3	1.4	0.25

Table 4.1: Typical Radioactive Element Concentrations
Compiled from Morse, 1977; Emerson, 1973; Aswathanarayana, 1985; Fahrig et al., 1967; IAEA, 1979; Darnley, 1982; Lambert and Heier, 1967

value, thus producing a so called significance factor map (Potts, 1976). Obviously this sort of technique must take into account the radiometric response of different lithologies in the study area and the calculated mean and standard deviation must be related to these lithologies. If this is not done any occurrence of a highly radioactive rock type such as a granite will always be highlighted as a statistically significant anomaly.

Individual radiometric anomalies can be interpreted on a semi quantitative basis if the parameters of an anomaly are studied in profile, such as the position of peak intensity, the area under the anomaly curve, the continuity of anomalies across flight lines. These parameters can be used to classify anomalies into various source classes, elementary, broad, line, slab and infinite sources (Sakakura, 1957). Analysis of this type can be useful in the search for ore bodies.

When using the radioactive data as a tool to aid in geological mapping, as is the case in this project, it is not so much the statistically significant anomalies that are of interest but rather the overall variations in radioactive strength with different lithologies. The basic premise of this type of interpretation is that the same lithology will produce similar radiometric responses, taking into account facies changes, both sedimentary and metamorphic and changes in the cover material. This premise has been shown to be applicable in many studies (e.g. Newton and Slaney, 1978; Pitkin, 1968).

Like many physical properties of rocks (density, magnetic susceptibility, seismic velocity) lithologies can be divided into broad sequences with typical or average radioactive element concentrations, although there are numerous exceptions and variations to the generalized scheme. Various authors have presented such information for the average radiometric response of generalized rock types; a compilation of such data is presented in Table 4.1.

4.3 Data Presentation

The process of radioactive decay, like most subatomic processes, is a statistical one. This means that there are measurable statistical errors associated with the collection, presentation and interpretation of radiometric data.

A series of radioactive count rates measured in unit time for a particular radioactive sample will follow a Poisson distribution (Løvborg and Mose, 1987). The mean or desired value of a Poisson distribution is the modal value and the standard deviation is given by the square root of the mean. By consideration of this simple relationship it is evident that as the mean count rate increases so the standard deviation decreases as a percentage of that mean count rate. This implies that the signal to noise ratio of a radiometric signal will decrease as the mean value of the signal decreases. The longer the time span (count time) over which the measurement is taken the more statistically significant will be that measurement because the number of counts will be large. Airborne surveys have count times that are necessarily short since the aircraft is in continuous motion and a long count time will cover a large tract of ground and possibly variable strength sources. Hence the trend for very large crystal volumes for data acquisition, which yield high count values in relatively small count times.

Due to the inherent statistical nature of the radiometric method there is destined to be noise on the records. The uranium channel, which in general has the lowest count rates, will be expected to be the noisiest channel, and this is often the case in surveys in the literature (e.g. Richardson, 1983) and also in this study. The total count channel, which has the highest recorded count rates, is expected to have the highest signal to noise ratio.

When using radiometric data as a tool to aid geological mapping the important parameters are the amplitude of the radioactivity and areal extent of radioactive zones, the form of individual anomalies is of much lesser importance. Contour maps of aeroradioactive data tend to be of limited use. If a contour interval is used which is in line with the range and distribution of the data there are necessarily a large number of small contour closures due to the inherent statistical noise contained within the data, resulting in a difficult map to interpret. Alternatively the contour interval can be unduly large to subdue these closures but then the finer details are lost, much of which is of the upmost importance. In general, contours tend to highlight the shape of anomalies but not their amplitudes. For these reasons digital images are a far more effective method of display.

The radiometric data, like the magnetic data, was gridded with a cell size of 100 metres (the original sampling intervals were approximately 20 m along flight lines and 500 m between flight lines, see Appendix B) and presented as greyscaled images. The total count channel is presented in Figure 4.1 as equivalent radioelement concentration units (ur).

Correlation with outcropping geology in the total count data is very good. Sediments of the Amadeus Basin Sequence in the Northern Magnetic Domain show up as total count lows (black areas), the most obvious being the Dean Quartzite and Winnall Beds in the far north of the

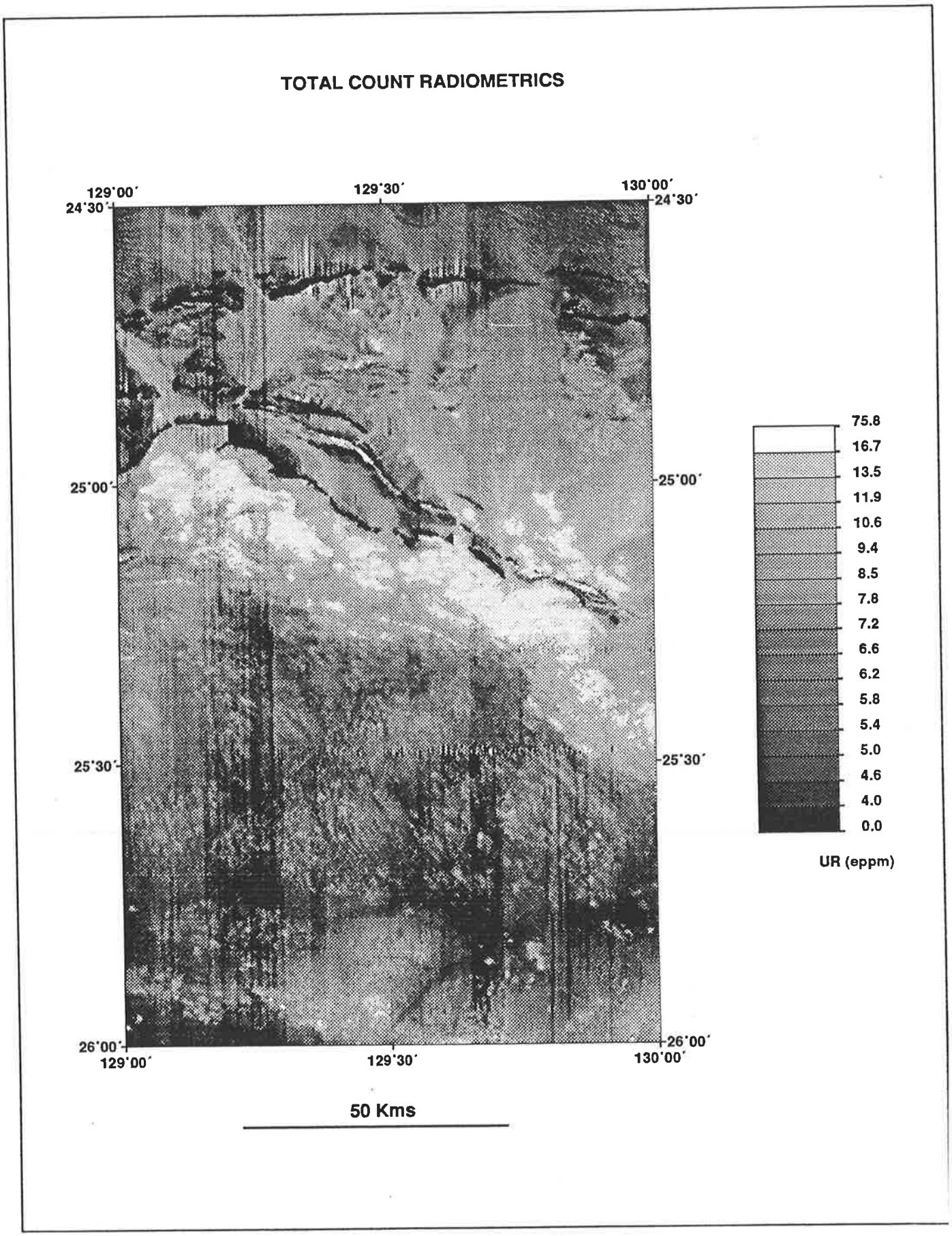

Figure 4.1: Total Count Radiometrics

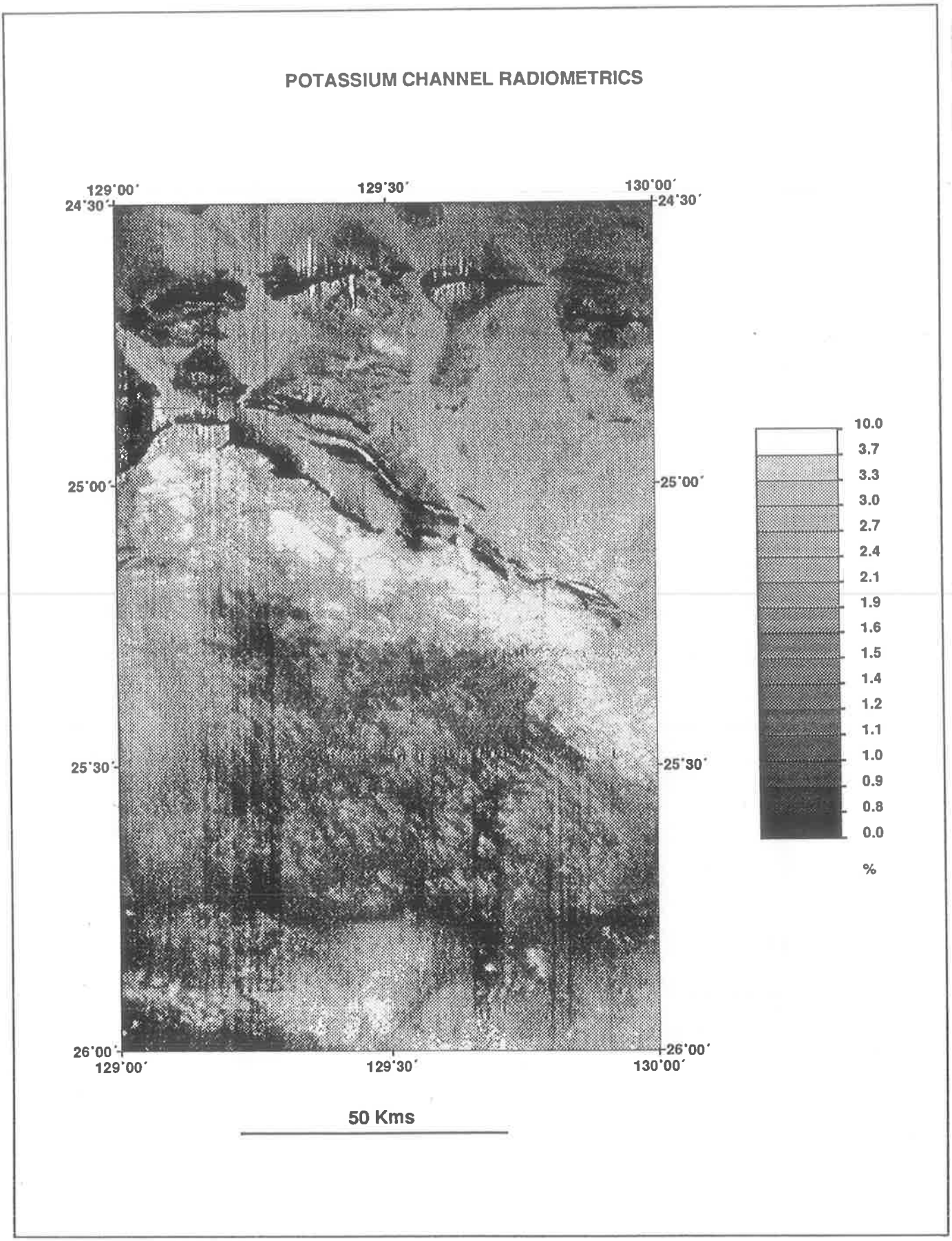

Figure 4.2: Potassium Channel Radiometrics

area. The granites, those in the north, the Pottoyu Granite Complex and those in the Southern Magnetic Domain all produce clearly defined total count highs. The Southern Magnetic Domain correlates with a general lowering of the overall radioactive level.

There are aspects of the data, in most or all of the four radiometric channels, that are caused by either surficial material or are artifacts of the data itself and are worthy of note before a more detailed discussion of the data is undertaken. In the far north quite strong southeasterly trending linear parallel anomalies are caused by sand dunes in that area. It is not clear from the digital images whether the anomalous regions are highs or lows, but on careful inspection of the profile and ground clearance data it becomes apparent that the radiometric lows are associated with the dune crests and the higher values are over the dune corridors. Dune crests generally have the mobile, active sand that is easily moved by the wind, whereas the corridors are much more stable (Tseo, 1986). It is evident from the geophysical data that the light windblown fraction of the sand has a lower proportion of grains of radioactive material than the more stable sediments found in the dune corridors. Similar curvilinear anomalies are also caused by dune fields in *Cockburn* and *Duffield.*

Low amplitude radiometric shadows are evident to the northwest of some of the major quartzite ranges in northern *Hull* and *Bloods Range.* These quartzite outcrops make up the prominent Bloods Range topographic highs. Material blown from the ridge tops by the prevailing southeasterly winds (Brookfield, 1970) has settled on the alluvium to the north, which has a higher background count rate, to form a thin blanket of lower radioactive material. A similar phenomenon of wind borne material affecting the results of an airborne survey has been reported by Gregory (1983) where highly radioactive waste rock from uranium mine workings were recorded three to five kilometres downwind from a mine dump near the Athabasca Basin, Canada.

The major river beds in the Northern Domain, the Docker, Hull, Irving and Chirnside creeks, are clearly visible as total count highs. Most of these water courses are sourced in the granitic Pottoyu Hills and the noticeably higher radioactive levels are due to detrital feldspar grains, high in potassium content, washed from the granite outcrops.

Noticeable north–south trending striping in the data is an artifact of the flight line direction of the survey, primarily due to the variation with time of the amount of radioactive atmospheric radon gas, coupled with instrumental drift. The banding is spatially correlated in all four channels. Some attempts to remove the banding using line averaging techniques and between channel correlation as proposed by Green (1987) were made. These efforts produced only minimal improvements and since the banding is not a major problem they were not applied to the data on a routine basis.

Two linear east–west trending features in southern and central *Petermann* are another artifact in the data caused by discontinuities in the flight line pattern. Between these two linear features the flight lines are short, and leveling mis-ties at either end of the flight lines cause the problem. The linear features are visible in all the radiometric channels and also some of the

processed magnetic images.

The corrected potassium channel data (Figure 4.2) shows good correlation with the outcrop geology, particularly in the Northern Domain. Several of the larger water ways (Hull River, Docker River, Irving Creek) are manifested as noticeable highs, due to the abundance of detrital feldspars as discussed above. The radiometric response of the sand dunes is not as obvious in this channel as it is in the total count and thorium channels (see below).

The thorium channel data (Figure 4.3) produces a lower quality image than the two previously discussed channels due to the effects of increasing statistical noise and this is particularly noticeable in areas of no outcrop. The response of the geological outcrop is well defined and follows a similar pattern to the total count and potassium data. The Pottoyu Granite Complex shows a clearer response in the thorium channel than in the potassium, and the alluvial cover over the granite in southern *Hull*, associated with the Hull River, is clearly defined as an area of lower thorium content. The response of the sand dunes in the northeast of the study area is also clear in the data. Subtle differences between the thorium and potassium channels can yield useful information and is discussed further in the next section.

The uranium channel (Figure 4.4) shows a marked deterioration in the quality of the data, the effects of statistical noise becoming quite prominent, as well as banding along the flight line direction. Some efforts were made to improve the appearance of the uranium image using processing techniques such as median filtering and averaging, however these did not improve the image quality greatly. Despite these problems the response of the geological outcrop is still discernible, particularly the highs produced by the granite outcrops of the Northern Domain and the lows associated with the quartzite ranges.

4.4 Data Processing and Analysis

As discussed in Appendix A there are numerous image processing techniques that can be applied to the gridded data, although the noisy nature of radiometric data restricts the usefulness of many of the methods.

One method commonly used with satellite imagery and radiometric data is the calculation of ratios of one band (channel) to another. These ratios exploit the overall similarity of the data in each channel, but highlight the small differences between channels. Ratios also have the added advantage of minimizing leveling problems in radiometric data. The strong correlation between the radiometric channels makes this ratio technique a useful one to apply here.

The commonly studied radiometric ratios are U/TH, TH/K and U/K. The best quality ratio image is presented in Figure 4.5 the TH/K ratio. The poor quality of the uranium channel means that the low signal to noise ratio will be propagated to any ratio image that involves the uranium data, and so the U/TH and U/K ratio data are not presented here.

Figure 4.5 highlights the sediments and metasediments in the north of the area as highs. The Dean Quartzite shows a variable response, with low ratios at the centre of outcrops, correspond-

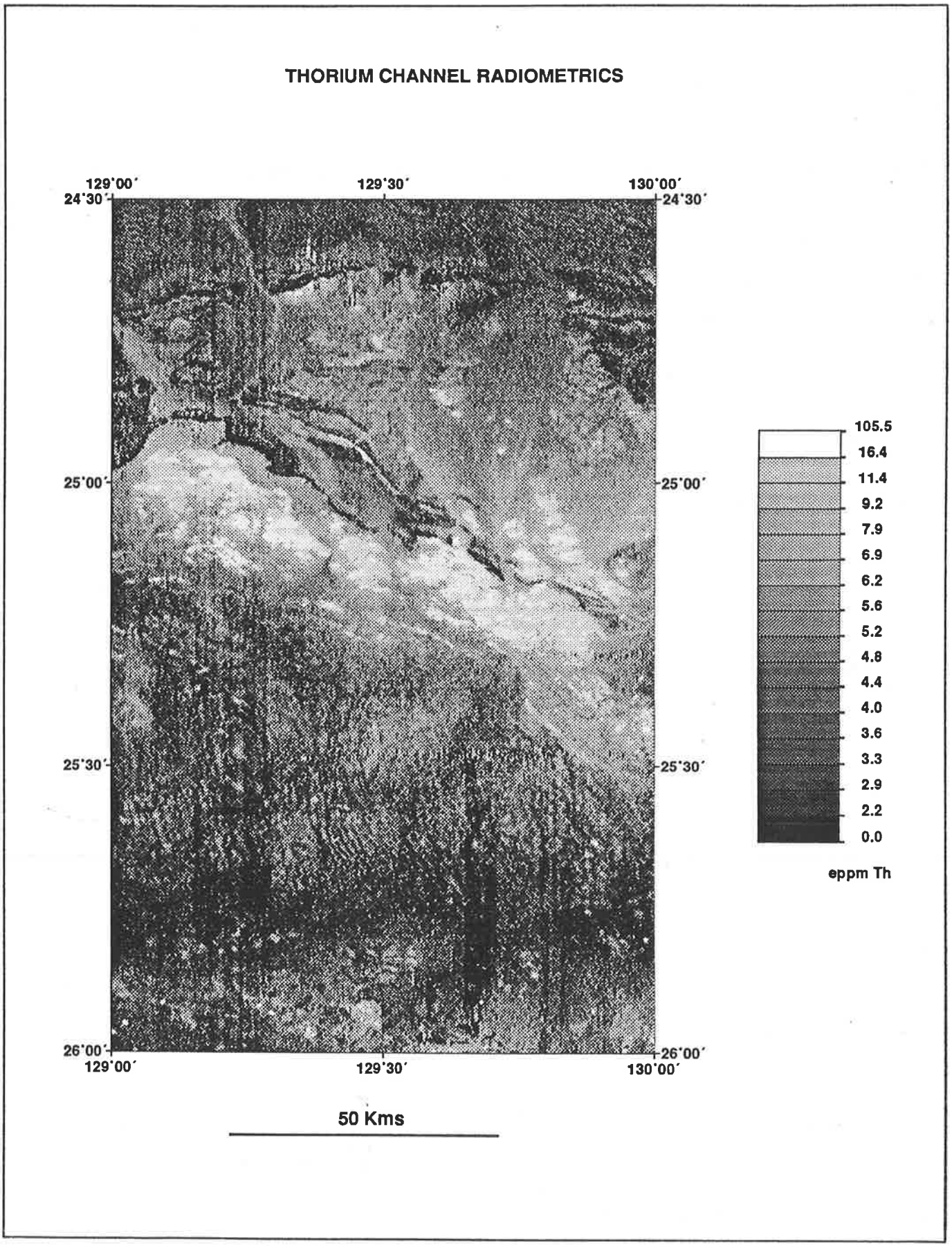

Figure 4.3: Thorium Channel Radiometrics

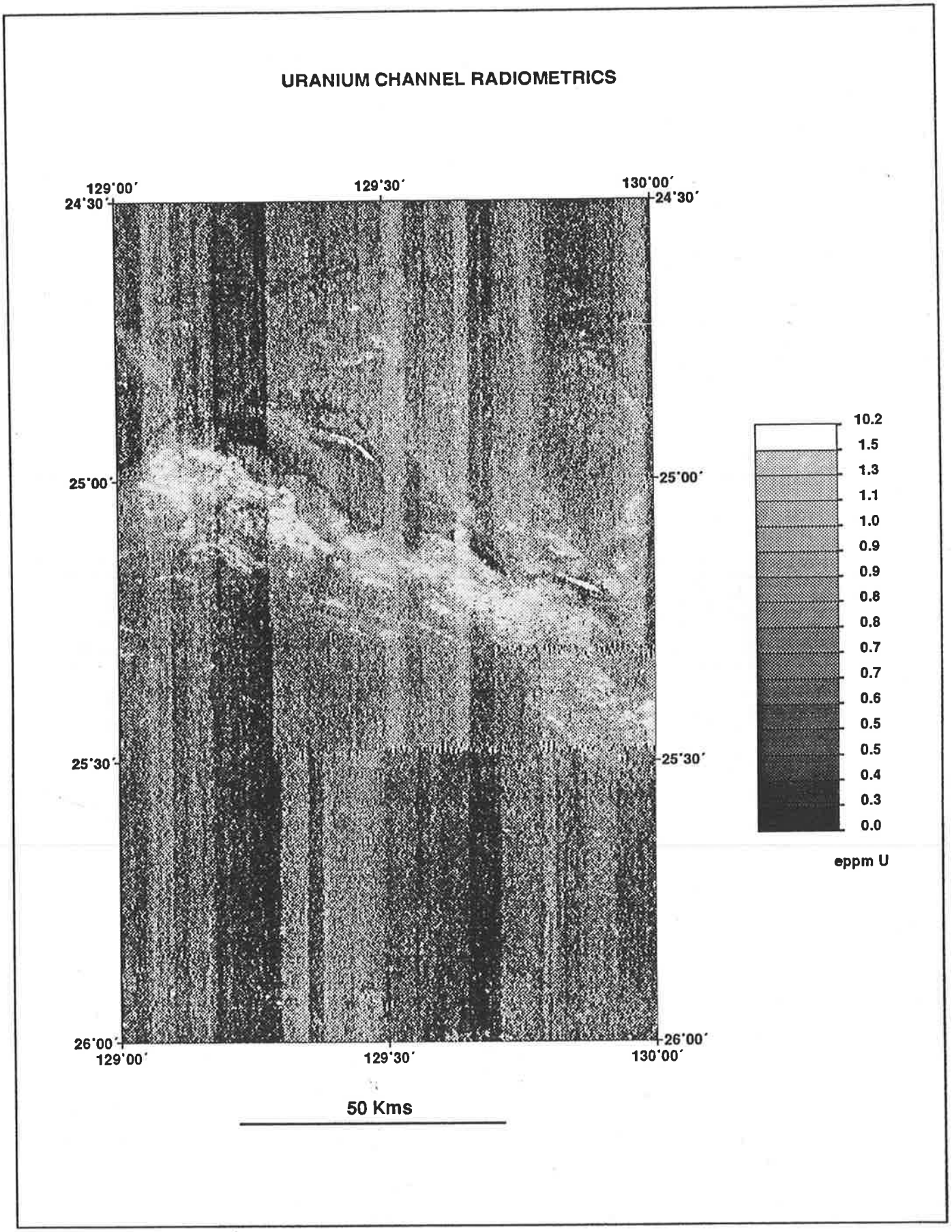

Figure 4.4: Uranium Channel Radiometrics

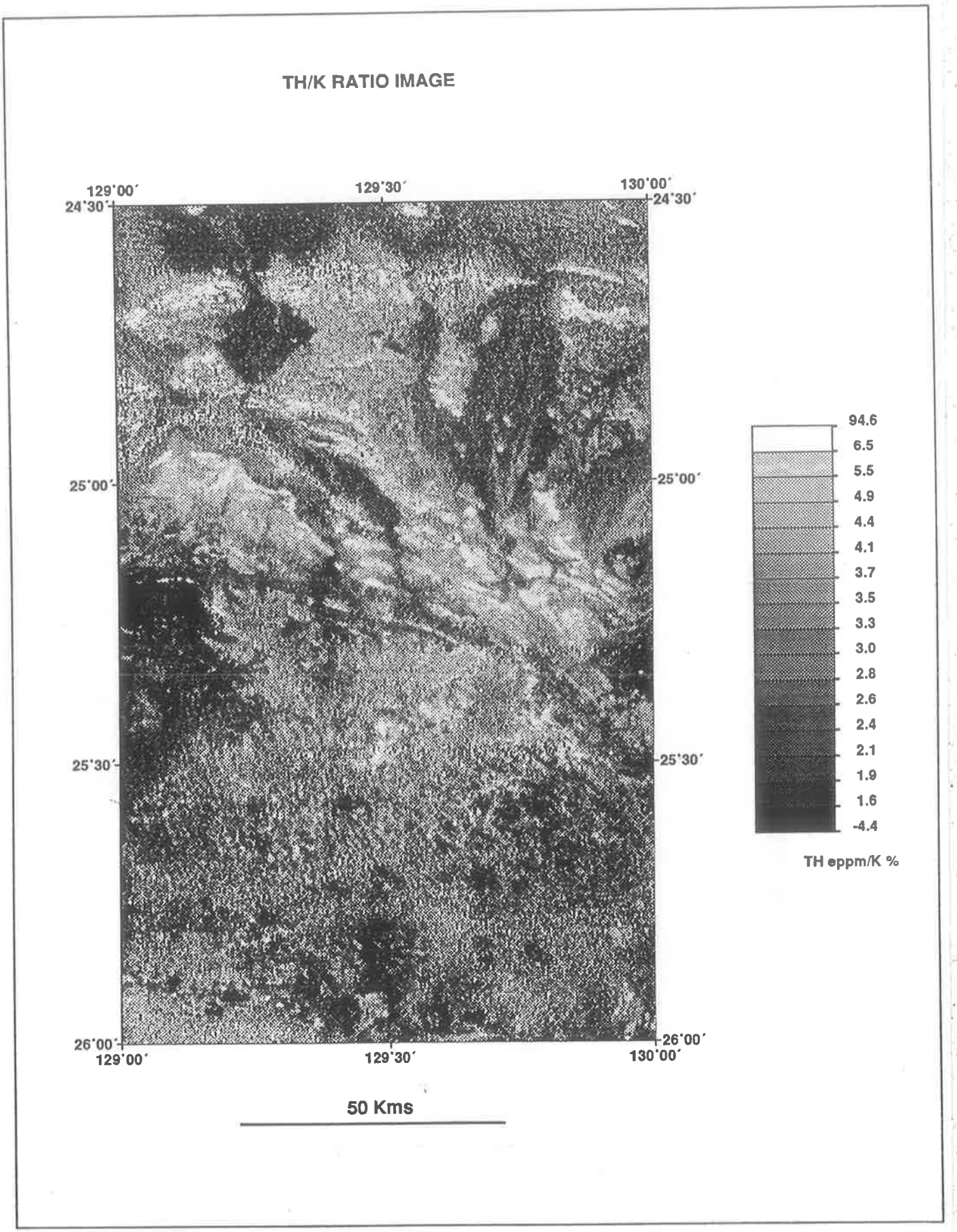

Figure 4.5: Thorium/Potassium Ratio Image

ing to the peaks of the topographic highs, and high ratios towards the edges of the outcrops. This effect is probably due to the build up of scree and Tertiary Conglomerate on the slopes of the quartzite ranges, which exhibit different radioelement concentrations. Marked differences are highlighted in the cover material, particularly in the vicinity of the Hull River where there is a large area with an anomalously low ratio, possibly related to occasional flooding and sediment deposition along the river.

A distinctive high ratio rim is visible around the northern edge of the Pottoyu Granite Complex in *Hull* and continuing southeastwards into *Petermann*. This thin rind is up to 500m wide and indicates that the granite is radiometrically zoned, enriched in thorium at the contact with the surrounding rocks. A border phase of medium grained granite noted in the field by Forman and Hancock (1964) (see Chapter 2) probably corresponds with this radiometric feature. Similar enrichment along the northern edge of the smaller pod of granite to the southeast is also evident. There is no evidence for a radiometric border phase along the southern edge of the granite.

Quite distinct southeasterly banding within the granite complex of the Pottoyu Hills parallels the strong linear magnetic anomalies seen in that region (magnetic zone **NL1**). This banding may be due to the abundance of gneissic material in the form of thin bands within the granite (Forman and Hancock, 1964 p.20)

The Olia Gneiss outcropping to the south of the Granite Complex is generally marked by distinct highs in the ratio image. Isolated outcrops of photointerpreted Olia Gneiss and Musgrave-Mann Metamorphics show up more clearly on the ratio image as lows than they do on any of the individual radiometric channels. The different responses of the Olia Gneiss will be discussed further in Section 4.4.1.

A large area of low radioactivity correlates with magnetic zone **NG2** on the western edge of *Pottoyu*, which corroborates the interpretation and suggests that there is a definite zone of different geophysical character in that area.

Overall the TH/K ratio image correlates well with the previously discussed magnetic zones (see Chapter 3). It also has the effect of removing the north–south striping which is evident in the individual radiometric channels. The striping is in the same positions in each channel, as is often the case (Green, 1987), and by dividing one channel by the other the low values defining the striping are effectively removed.

4.4.1 Data Analysis

A significant proportion of the outcrop mapped in the study area, particularly on *PETERMANN RANGES* is mapped on the basis of photointerpretation. This is because access to most of the area, particularly the south, is very difficult and helicopter support could not be organized by the field party at the time of mapping (Forman pers. comm.). It is with these outcrops that the radiometric data can be particularly useful as a geological mapping tool.

By calculating the statistics of the radiometric response produced by the individual rock types (i.e. mean, standard deviation, distribution) and comparing between known and unknown lithologies the data can be used to make inferences on rocks that are adequately represented as outcrop in the area. In order to obtain the radioactive information for individual lithologies each rock type must be digitized, as mapped on the 1:250 000 map sheets, as a polygon. The radioactive data from within all the polygons representing the same rock type can then be extracted from the whole gridded data set using a "point-in-polygon" computer algorithm (Saloman, 1978). Repeating this process for all the rock types mapped in the area will build up a picture of the radioelement distributions of each lithology, and these can then be compared with the average radioelement concentrations of unknown or photointerpreted outcrops.

There are a large number of mapped outcrops in the study area, and most of these were digitized. The airborne spectrometer system receives most of its signal from a finite circular area below the aircraft, known as the circle of investigation. The radius of this circle is dependent upon several factors, including air density and radioactive attenuation coefficients, but the flight ground clearance is by far the most important parameter (Duval et al., 1971). With a ground clearance of 100 m the radius of a circle in which 65 % of the radioactive signal originates is approximately 80 meters (Darnely, 1972). Thus the recorded signal will represent the mean count rate value over the area covered by that circle. If outcrops are very small they will only represent a small proportion of this circular area and the recorded signal will not adequately represent the radioactive properties of the rocks. For this reason some of the small outcrops marked on the geology map were not included in this analysis. Over 400 individual outcrops were included, most of which were also used to create the 1:1 000 000 geology map (Chapter 2, Figure 2.1) which gives an idea of the outcrops used.

The results of this study are presented in Tables 4.2–4.5 and the distributions of selected lithologies in Figures 4.6–4.8. Some important points have emerged from the analysis of this data and are discussed below.

Most of the sediments and metasediments which outcrop in the Northern Domain exhibit low average equivalent concentrations, as expected from their appearance in the radiometric images, and the distributions are typically smoothly varying unimodal curves (particularly where n, the number of samples, is large). The total count and thorium histograms generally have the largest standard deviations and similar shapes, the potassium and uranium channels produce much tighter distributions.

The younger basement lithologies (Bloods Range Beds and Mount Harris Basalt) which lie stratigraphically beneath the Amadeus Basin sequence, have contrasting radioelement concentrations. The Mt. Harris Basalt shows relatively high equivalent radioelement concentrations compared to the overlying sediments. The Bloods Range Beds have concentrations very similar to the younger sedimentary material. Further subdivision of these two lithologies could not be made on the basis of their radioelement distributions.

The Mannanana Porphyroblastic Schist, which according to Forman and Hancock (1964) is

LITHOLOGY	MEAN (Ur)	MAX (Ur)	MIN (Ur)	STAND. DEV.	SAMPLES
Ordovician Sst.	6.20	14.68	2.79	1.67	4382
Mt. Currie Conglom.	6.25	10.50	3.25	1.35	668
Winnall Beds	4.94	8.23	2.16	1.23	2344
Inindia Beds	-	-	-	-	-
Pinyinna Beds	6.65	17.21	0.00	2.14	4862
Dean Quartzite	4.90	47.53	0.00	2.96	45865
Mannanana Porphyry	12.05	28.26	1.09	3.77	11360
Qtz-Feld. Porphyry	10.00	25.58	2.51	4.56	1650
Bloods Range Beds	6.78	19.12	1.48	2.13	7921
Mt. Harris Basalt	8.10	23.47	2.04	2.68	10503
Pottoyu Granite	21.06	75.47	2.42	4.44	72415
Minor Granites	11.33	38.37	0.00	5.48	2250
Olia Gneiss	12.65	63.83	2.17	6.06	31245
Musgrave-Mann Met.	10.55	32.05	3.54	2.63	30662

Table 4.2: Total Count Equivalent Concentrations

LITHOLOGY	MEAN (%)	MAX (%)	MIN (%)	STAND. DEV.	SAMPLES
Ordovician Sst.	1.91	3.29	0.24	0.48	4382
Mt. Currie Conglom.	1.06	1.85	0.38	0.22	668
Winnall Beds	0.80	2.22	0.12	0.37	2344
Inindia Beds	-	-	-	-	-
Pinyinna Beds	1.28	3.78	0.08	0.59	4862
Dean Quartzite	0.77	5.70	0.00	0.59	45865
Mannanana Porphyry	2.82	8.59	0.00	1.03	11360
Qtz-Feld. Porphyry	1.90	4.48	0.16	0.95	1650
Bloods Range Beds	1.30	3.94	0.08	0.54	7921
Mt. Harris Basalt	1.53	6.48	0.15	0.67	10503
Pottoyu Granite	3.94	6.36	0.21	0.58	72415
Minor Granites	2.25	7.64	0.03	1.18	2250
Olia Gneiss	2.78	7.30	0.50	1.02	31245
Musgrave-Mann Met.	3.16	10.04	0.60	0.80	30662

Table 4.3: Potassium Equivalent Concentrations

LITHOLOGY	MEAN (eppm)	MAX (eppm)	MIN (eppm)	STAND. DEV.	SAMPLES
Ordovician Sst.	0.82	2.34	0.00	0.32	4382
Mt. Currie Conglom.	0.87	1.81	0.00	0.34	668
Winnall Beds	0.76	1.76	0.00	0.28	2344
Inindia Beds	-	-	-	-	-
Pinyinna Beds	0.78	1.96	0.00	0.27	4862
Dean Quartzite	0.67	5.22	0.00	0.35	45865
Mannanana Porphyry	0.82	3.06	0.00	0.41	11360
Qtz-Feld. Porphyry	1.03	2.96	0.00	0.45	1650
Bloods Range Beds	0.84	2.18	0.00	0.29	7921
Mt. Harris Basalt	0.95	2.74	0.00	0.32	10503
Pottoyu Granite	1.82	5.69	0.00	0.59	72415
Minor Granites	1.04	4.27	0.00	0.57	2250
Olia Gneiss	1.15	7.61	0.00	0.60	31245
Musgrave-Mann Met.	0.64	3.29	0.00	0.33	30662

Table 4.4: Uranium Equivalent Concentrations

LITHOLOGY	MEAN (eppm)	MAX (eppm)	MIN (eppm)	STAND. DEV.	SAMPLES
Ordovician Sst.	5.62	20.16	0.86	2.17	4382
Mt. Currie Conglom.	6.40	16.63	3.00	1.97	668
Winnall Beds	4.41	13.00	0.00	1.36	2344
Inindia Beds	-	-	-	-	-
Pinyinna Beds	6.24	16.67	0.00	2.19	4862
Dean Quartzite	4.99	74.99	0.00	3.93	45865
Mannanana Porphyry	11.12	31.06	0.00	4.02	11360
Qtz-Feld. Porphyry	10.06	32.57	0.74	5.59	1650
Bloods Range Beds	5.84	17.52	0.65	2.02	7921
Mt. Harris Basalt	7.73	31.98	0.00	3.60	10503
Pottoyu Granite	22.60	68.50	1.00	7.20	72415
Minor Granites	11.73	57.07	0.00	7.93	2250
Olia Gneiss	11.46	104.16	0.76	9.43	31245
Musgrave-Mann Met.	6.56	39.41	0.00	3.71	30662

Table 4.5: Thorium Equivalent Concentrations

derived in part from the Bloods Range Beds, has a considerably higher radioactive concentration than either the Bloods Range Beds or the Mount Harris Basalt in most of the channels. The Mannanana Schist has been mapped on *BLOODS RANGE* but it is discontinued on *PETERMANN RANGES*, where it is mapped as Pottoyu Granite Complex. The radiometric concentrations of the Mannanana Schist are significantly lower than those of the Pottoyu Granite Complex. This difference in the radioactive equivalent concentrations and the fact that there is a well defined zone of increased magnetic activity closely correlated to the mapped Mannanana Porphyroblastic Schist on *BLOODS RANGE*, and its assumed continuation onto *PETERMANN RANGES*, indicates that the Mannanana Schist has significantly different physicochemical properties from the Pottoyu Granite Complex and should be differentiated from it on the mapped geology. The two lithologies have been differentiated on the interpretation maps (plates 1–4) at the back of this thesis.

The Pottoyu Granite Complex stands out in the radioactive images as a dominant area of high concentrations and analysis of the data confirms that the granite complex has the highest equivalent radioelement concentrations of all the mapped lithologies. Although the granite is the most radioactive unit in the study area it has concentrations similar to those of an "average" granite, and is somewhat lower in uranium content than most granites. The large area of mapped granite falls into two very distinct magnetic zones, **NL1** and **NG1** (see Chapter 5). The granitic outcrop was divided into these individual zones to determine if any radioactive concentration differences exist between the two groups; no significant differences were found.

The Olia Gneiss has relatively high radioactive concentrations in all channels, however the histograms show that the distributions are complex with at least two distinct populations in most of the channels (Figure 4.6). This is uncharacteristic of a single lithology which generally show a smooth, unimodal distribution similar to that illustrated in Figure 4.8.

The mapped Olia Gneiss can be divided into two main groups based on the 1:250 000 geology maps:

1. those outcrops which have *not* been visited in the field and have been assigned the lithology of Olia Gneiss on the basis of airphoto interpretation,

2. those outcrops that have been visited and definitely mapped as Olia Gneiss.

Group 1 occurs mainly in the central section of *PETERMANN RANGES*, south of the Pottoyu Granite, where outcrops are widely separated and ground access is extremely difficult. Group 2 is made up of outcrops further north and into *BLOODS RANGE*. If individual distributions are calculated for each of these groups it becomes evident that group 1, the photointerpreted outcrops, make up the populations with the lower average values (Figure 4.7) that can be clearly seen in the distributions of all the Olia Gneiss outcrops (Figure 4.6). This information suggests that the outcrops mapped as Olia Gneiss are probably two distinct lithologies. From consideration of the outcrop pattern and the magnetic information it seems likely that

the majority of group 1 outcrops should be mapped as higher grade Musgrave-Mann Metamorphics, which outcrop along the southern edge of *PETERMANN RANGES* and show a similar radiometric response in all channels to that of the group 1 Olia Gneiss.

The higher metamorphic grade Musgrave-Mann lithologies have lower average equivalent radioelement concentrations than the amphibolite grade group 2 Olia Gneiss. This is in agreement with the data collected by Lambert and Heier (1967) whose radioactive measurements on samples from the granulite and amphibolite facies rocks from the Musgrave Block and the Fraser Range in Western Australia indicate that the granulite facies is depleted in uranium and thorium by factors of 5 and 9 respectively relative to the lower grade lithologies. Similar conclusions were reached by Fahrig et al. (1967) in their study of crystalline surface rocks in the Canadian shield.

The lithological distributions suggested by this radioactive evidence has important implications on the position of the Woodroffe Thrust (see Chapter 2 Section 2.4) and will be further discussed in Chapter 6.

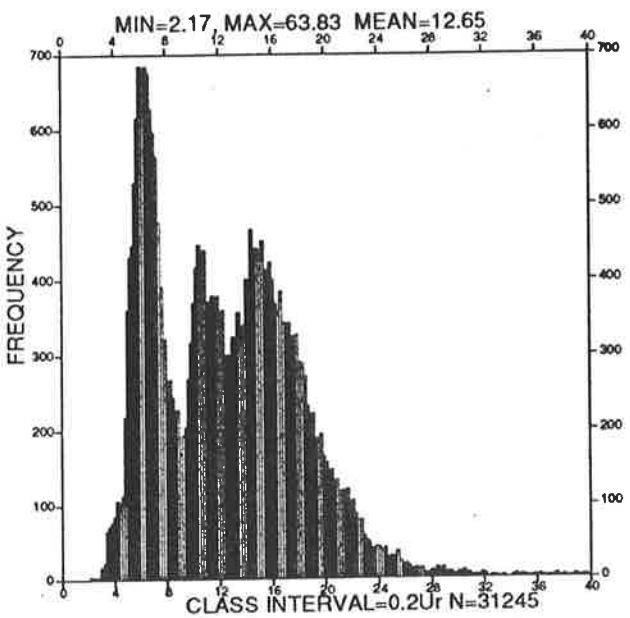

TOTAL COUNT

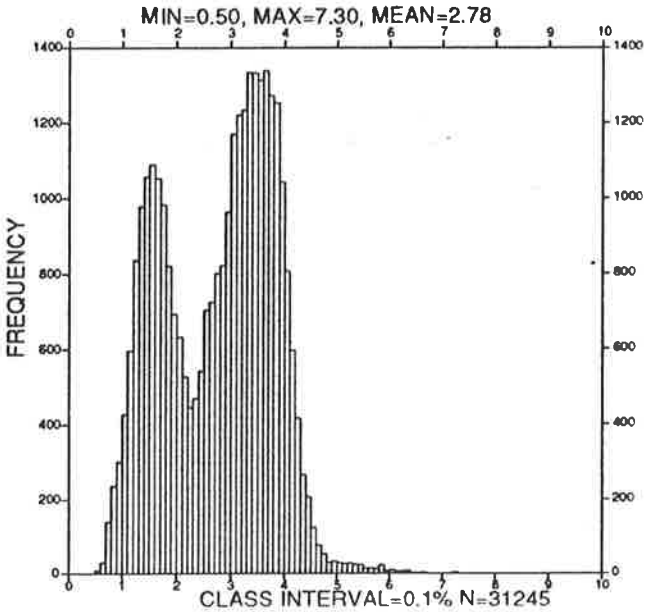

POTASSIUM

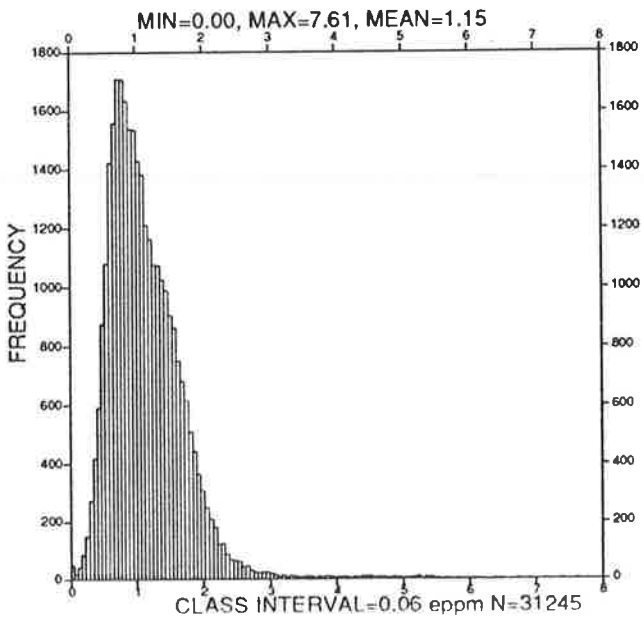

URANIUM

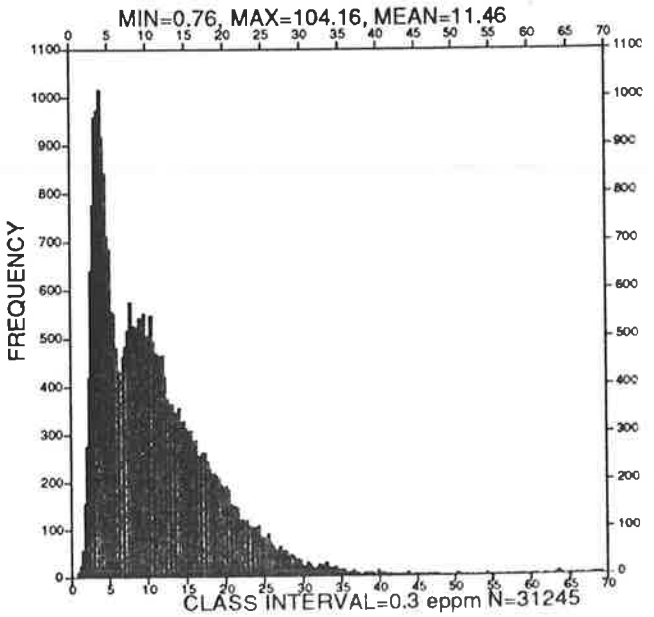

THORIUM

Figure 4.6: Radiometric Histograms for All Mapped Olia Gneiss

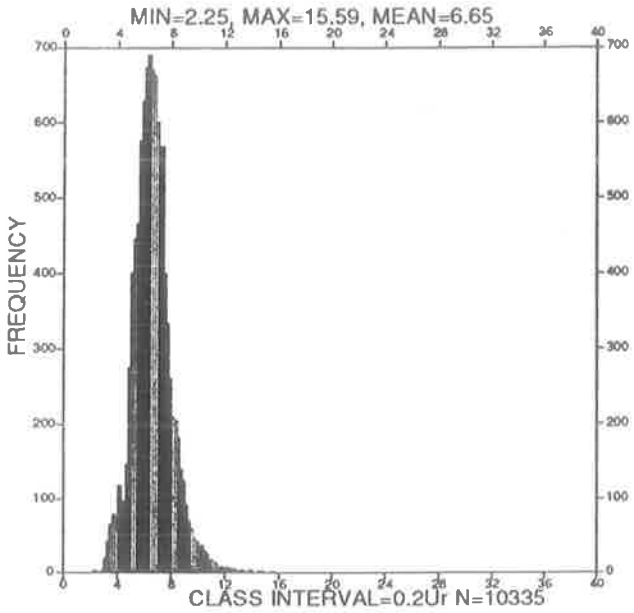

TOTAL COUNT

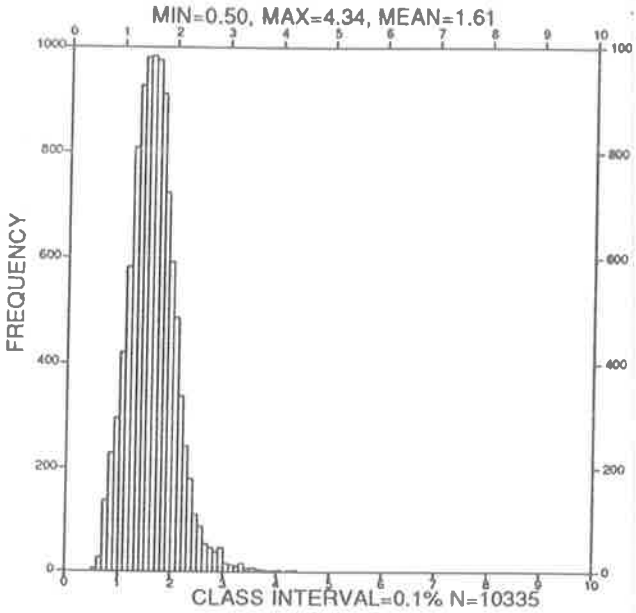

POTASSIUM

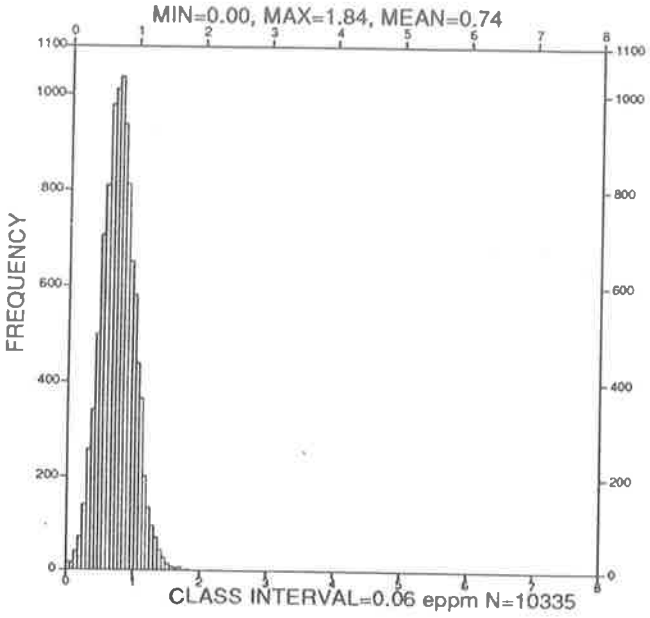

URANIUM

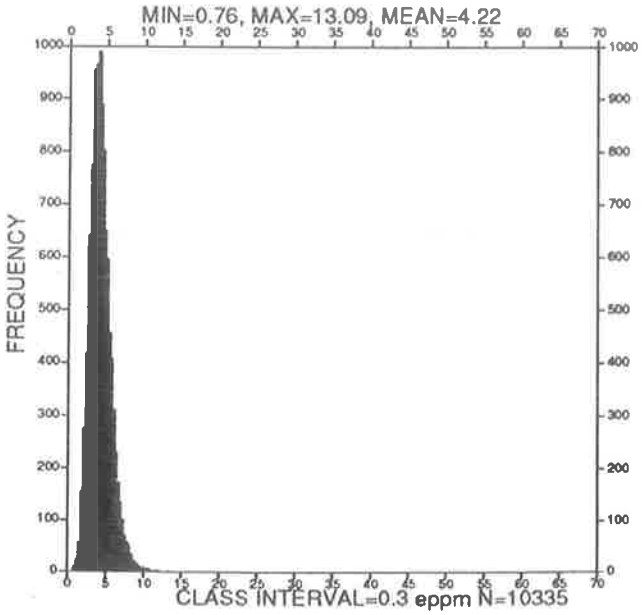

THORIUM

Figure 4.7: Radiometric Histograms for the Photointerpreted Olia Gneiss

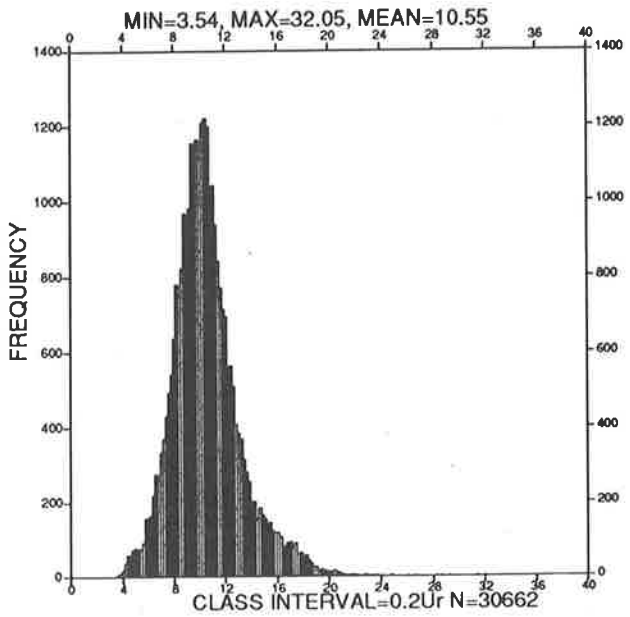

TOTAL COUNT

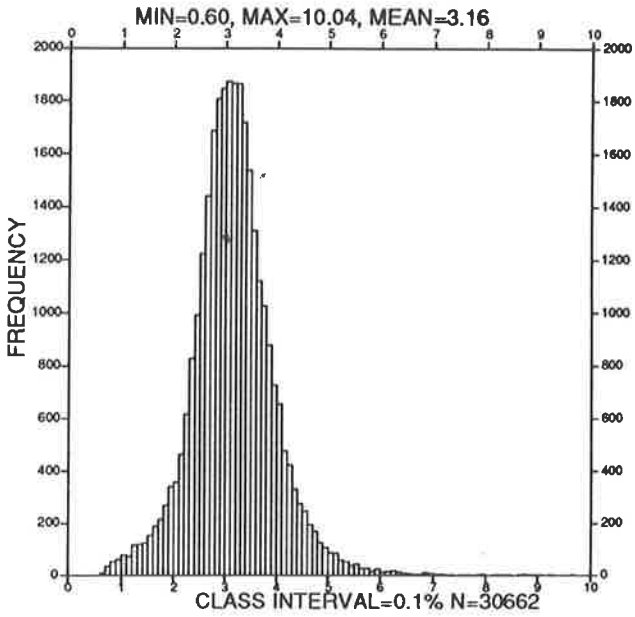

POTASSIUM

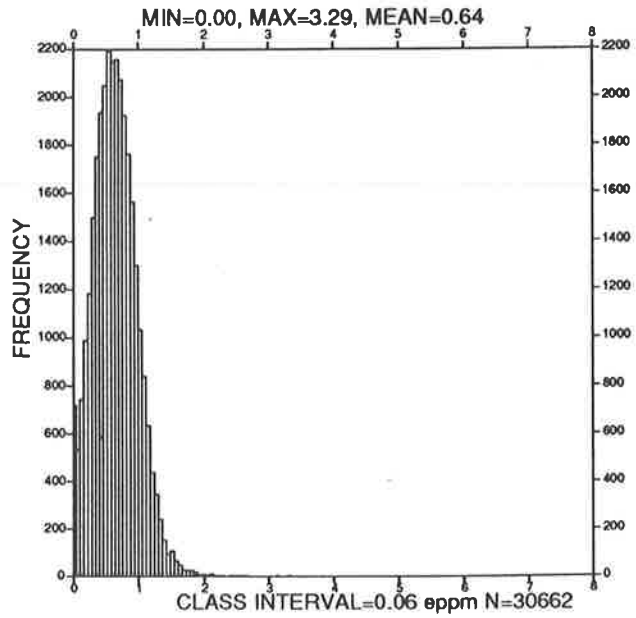

URANIUM

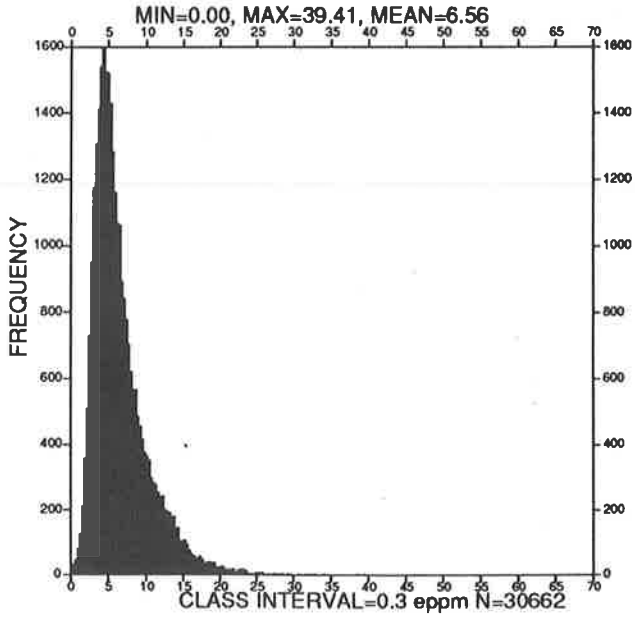

THORIUM

Figure 4.8: Radiometric Histograms for Musgrave-Mann Metamorphics

Chapter 5

Northern Magnetic Domain

5.1 Introduction

The Northern Magnetic Domain, as defined in Chapter 3, covers most of the four northerly map sheets of the survey area (*Hull*, *Bloods Range*, *Pottoyu* and *Petermann*). The Domain includes smooth, mottled, linear and broad linear magnetic textural zones. In the context of the regional structure (see Chapter 2) the Northern Domain can be subdivided into three sections:

1. Amadeus Basin proper,
2. Regional Fold Nappe,
3. Original Basement.

The Amadeus Basin proper and the Petermann fold nappe make up a cover sequence in the north of the Domain. To the south is a region of original gneissic and granitic basement interpreted on the basis of mapped lithologies and the magnetic patterns.

This chapter discusses the interpretation of the geophysical data in the context of these three subdivisions, and includes both the geological significance of the magnetic signatures and the structural information which has been extracted from the geophysical data. The chapter is designed to be used in conjunction with the interpretation maps (plates 1–4) which have been produced by a synthesis of all the available forms of the geophysical data (see Appendix A) as well as other available geological/geophysical data and literature.

Throughout the chapter symbols in upper case bold (e.g. **NS1**) refer to magnetic textural zones as defined in Chapter 3. Symbols in normal type (e.g. G1) are lithomagnetic units referred to on the interpretation maps. The locations of the magnetic zones referred to in the text are reproduced on figure 5.1.

5.2 Amadeus Basin Proper

The smooth textural zone **NS1** which forms an east–west trending belt across far north *Hull* and *Bloods Range* is the magnetic response of the Amadeus Basin. The edge of the basin is mapped

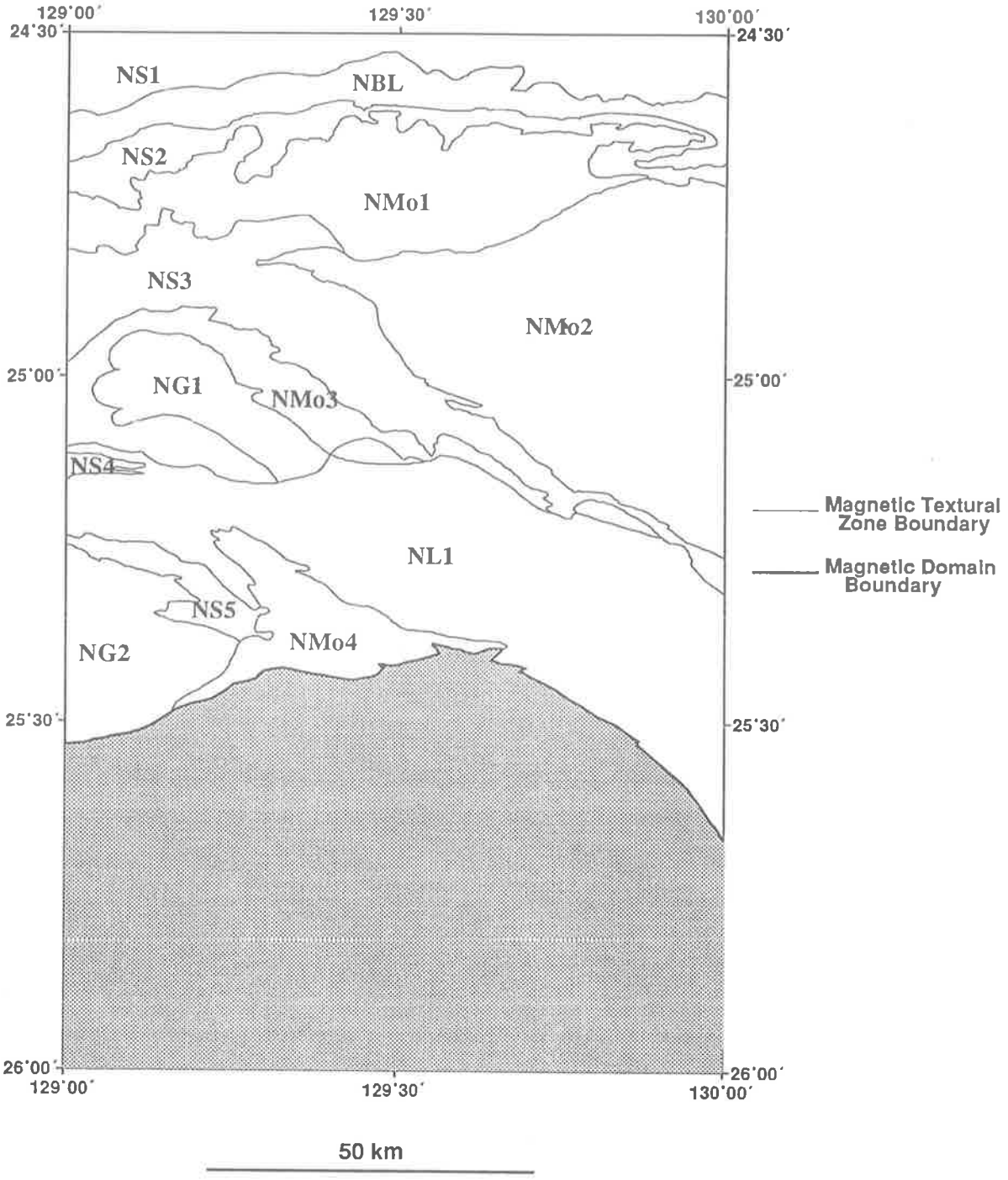

Figure 5.1: Interpreted Magnetic Zones in the Northern Domain

as the boundary between **NS1** and **NBL**. Outcrop is restricted to two basinlike occurrences of Winnall Beds, one at Mt. Cowle and another further west. The majority of the zone is dominated by sand dunes.

An increasing thickness of nonmagnetic Winnall and Inindia Beds make up the zone, thickness increasing to the north (Young and Shelley, 1977). The area covered in this study is not large enough to define the low frequency anomalies originating from magnetic basement underlying the Amadeus Basin.

Processed versions of the magnetic data show several low amplitude linear magnetic anomalies with depths to source of the order of 150 metres. The origin of these anomalies is assumed to be from lenses of increased magnetic mineral content within the nonmagnetic sediments. The zone is generally lacking in high frequency anomalies so it is not possible to resolve a large amount of structural detail from the magnetic data covering the area.

5.3 Petermann Fold Nappe

The Petermann fold nappe dominates the northern section of the study area and is covered by the *Hull* and *Bloods Range* sheets. It is characterized by variable magnetic activity mainly of smooth and mottled zones, **NS2**, **NS3**, **NMo1**, **NMo2**, **NMo3**.

The lithologies within the fold nappe include Dean Quartzite and Pinyinna Beds, as well as the underlying metavolcanics and metasediments of the younger basement and also Olia Gneiss. The discussion of this area will be treated in three main parts covering the sediments, the younger basement and the older basement core of the regional fold.

Sediments

The smooth magnetic response of nonmagnetic sediments is a dominant feature of the Northern Magnetic Domain and can be separated into zones **NS2** and **NS3**.

Zone **NS2** is an east–west trending band across northern *Hull* and *Bloods Range*. The main lithologies contained within the zone are Dean Quartzite and Pinyinna Beds. The zone is of variable width, thickest on its western side. Magnetic interpretation confirms a large scale fold pair on the eastern boundary of the area which has been previously inferred from the outcrop pattern of Dean Quartzite (Forman and Hancock, 1964 Figure 19). Several previously unrecognized north-northwest trending strike-slip faults cut the zone towards the east, and will be discussed in further detail in Section 5.6.

NS3 lies in central *Hull* and thins southeast across *Petermann*. The zone correlates closely with the mapped outcrop of Dean Quartzite and Pinyinna Beds. Magnetic susceptibilities measured from hand samples in the B.M.R. rock collection in Canberra (using a Geoinstruments JH-8 Susceptibility meter) are consistent with the low to nonmagnetic nature of the smooth textural zones (see Table 5.1).

A prominent high amplitude curvilinear anomaly, 40 kilometres long, occurs within **NS3** in south central *Hull* in an area of no outcrop. Modeling this two dimensional horizon yields a moderate to steep northerly dipping sheetlike body with a susceptibility in the range 0.02–0.105 S.I. units, and a depth to the top of between 50–460 metres. Modeled dips of the horizon are in close agreement with the measured dips on nearby Dean Quartzite outcrops, suggesting that the magnetic horizon is stratabound and that remanence is not a significant component of the magnetization. The magnetic horizon is placed stratigraphically near the contact between the Dean Quartzite and Pinyinna Beds, and the most likely source for the anomaly is the hematite-goethite schist (unit 2) within the Pinyinna Beds (see Chapter 2). The Kay Valley gossan, iron-rich cappings reported by Wilson (1966), possibly represent the weathered surface expression of the magnetic horizon. The horizon is cut in several places by strike-slip faults and at least one obvious dip-slip fault. Modeling either side of the dip-slip fault indicates that a sheetlike body of very similar parameters (except depth to top) will closely match the observed anomaly. The throw of the fault has been modeled as about 400 metres downthrown on the western side, see Figure 5.2.

The modeled profiles in this thesis are presented as two-page figures. The left hand page shows a total magnetic field image to illustrate the position of the profile and the magnetic distributions in the neighbourhood of the profile. Also on the left hand page is a tabular list of the body specifications of the model. The right hand page shows the modeled (dashed) and observed profile in cross section. The profile positions are also marked on the interpretation plates.

Zone **NS3** thins considerably to the southeast where some small amplitude anomalies in the zone have their source within the sedimentary units.

Zone **NS4** on the western edge of northern *Pottoyu* is a small triangular shaped smooth textural zone over mapped Dean Quartzite and Bloods Range Beds. The zone is the continuation of **NS3** which has been folded around in a large structure mapped on *SCOTT* in Western Australia.

A prominent broad linear zone **NBL** forms an east–west trending belt stretching across northern *Hull* and *Bloods Range*. The zone is north of the Bloods Range and is predominantly in an area of no outcrop, although one small outcrop of Winnall Beds lies within the zone. The anomalies making up **NBL** are high amplitude, complex multiple source features.

The zone consists of a number of anastomosing continuous magnetic highs, cut in several places by north-northeast trending faults which continue through **NS2**. Modeled source depths are of the order of 150–200 metres with a dip trend steeply to the south in the centre of the zone but trending northerly towards the southern and northern edges of the zone. Figure 5.3 shows modeled sections through the zone along flight lines 1411 and 1641 in *Hull*.

The anastomosing nature of the anomalies suggests that there is complex structure and folding of the sources towards the eastern and western edges of the study area. Poor resolution

Body	Depth (m)	Strike	Suscep.(S.I.)	Dip	Depth Extent	Width
1	461	90	0.052	105	1200	291

Body Specifications, Hull 1312

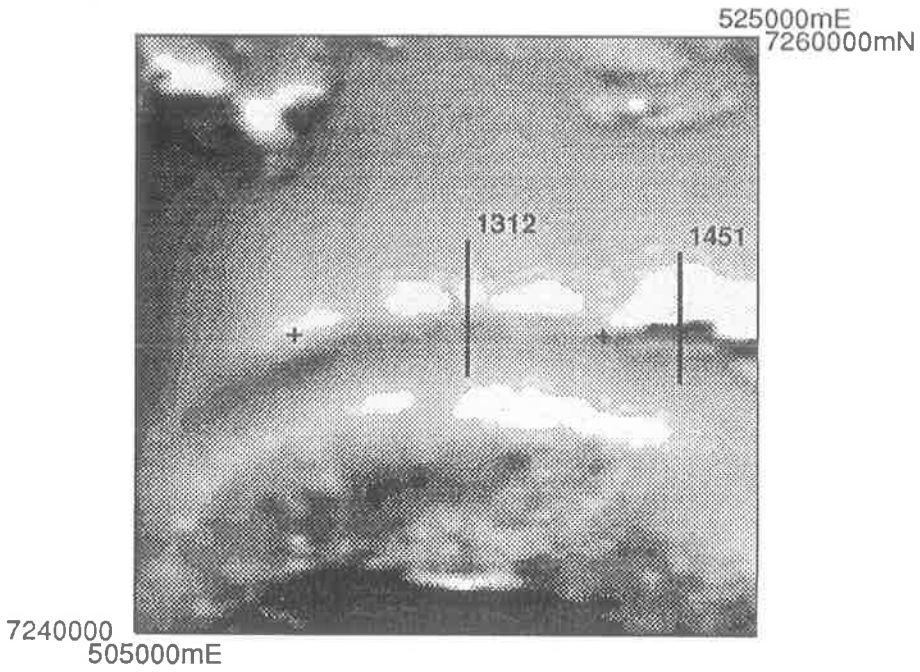

Body	Depth (m)	Strike	Suscep.(S.I.)	Dip	Depth Extent	Width
1	51	90	0.054	95	1119	243

Body Specifications, Hull 1451

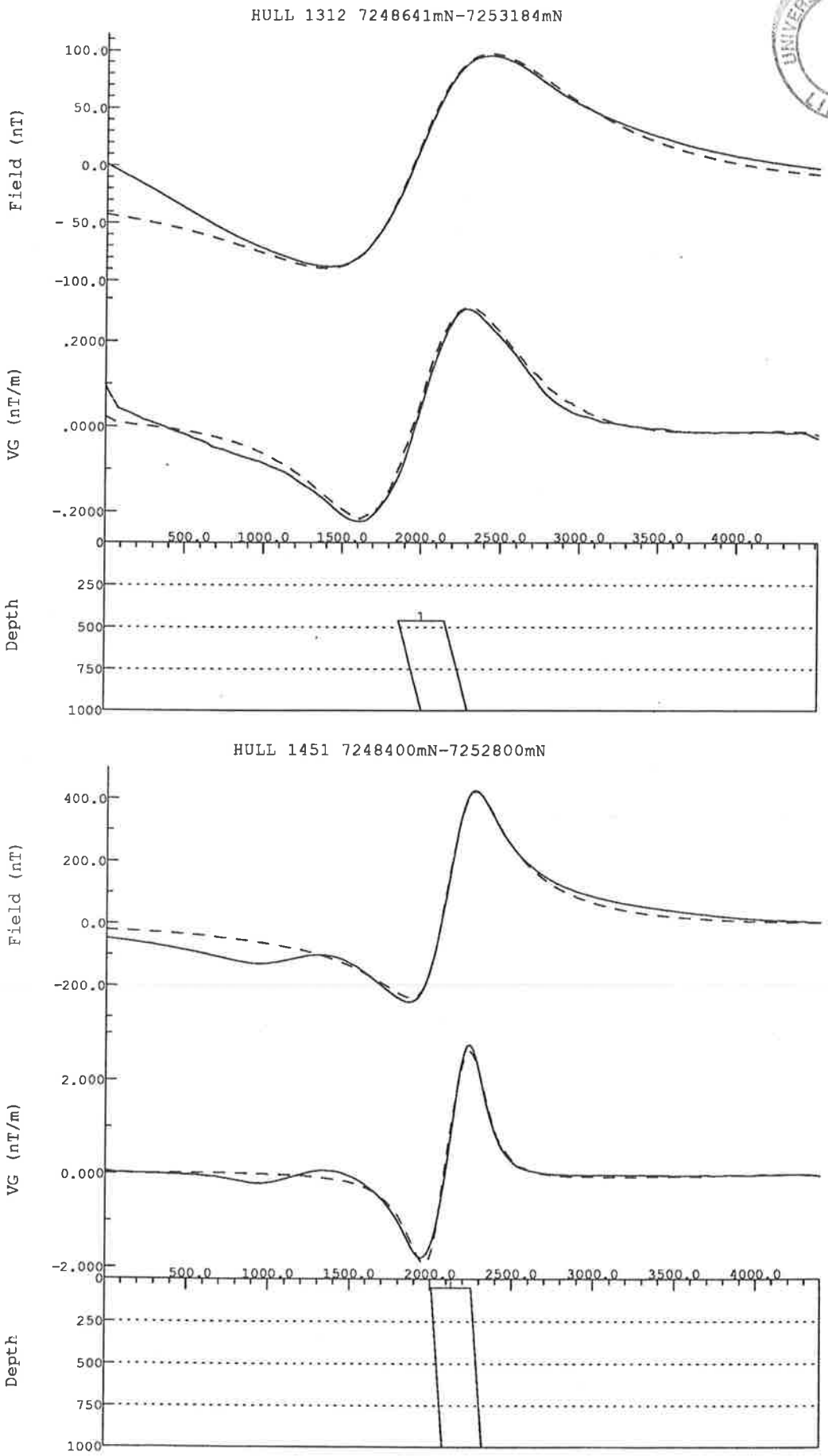

Figure 5.2: Modeled Sections Lines 1312 and 1451, *Hull* (dashed line is modeled profile, solid line is observed data). *Note that the scales differ on each profile*

Body	Depth (m)	Strike	Suscep.(S.I.)	Dip	Depth Extent	Width
1	338	90	0.108	50	1839	153
2	209	90	0.070	50	471	251
3	157	90	0.067	50	171	54
4	135	90	0.028	50	∞	48
5	157	90	0.071	50	328	107
6	43	90	0.004	102	5000	77
7	34	90	0.018	124	5000	90
8	155	90	0.012	100	507	143
9	107	90	-0.013	45	9126	111

Body Specifications, Hull 1411

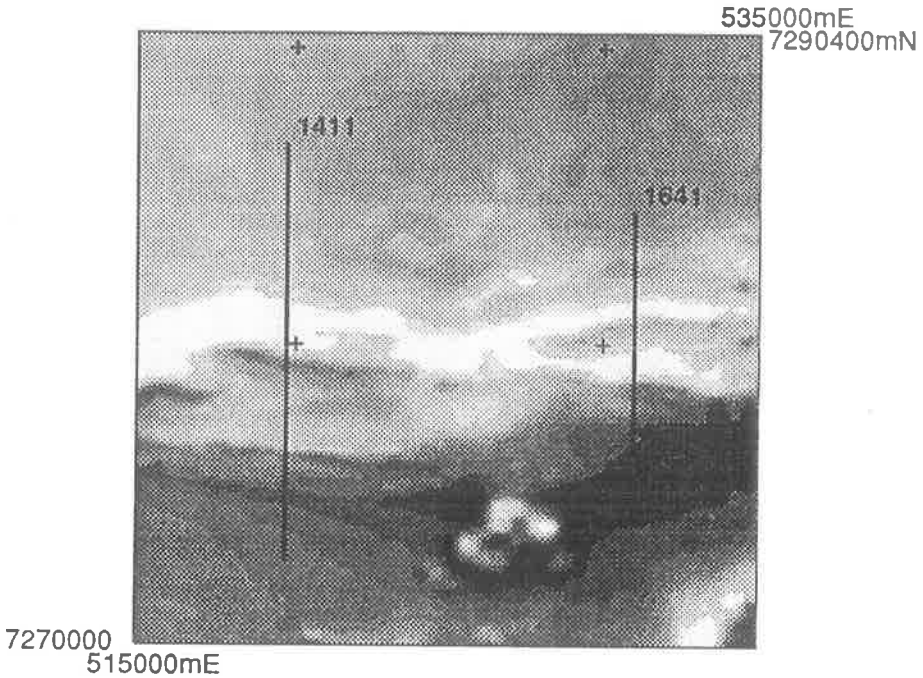

1:250 000

Body	Depth (m)	Strike	Suscep.(S.I.)	Dip	Depth Extent	Width
1	216	90	0.077	50	277	263
2	119	90	0.006	50	∞	317
3	107	90	0.006	50	∞	280
4	189	90	0.041	50	596	303
5	225	90	0.052	50	691	279
6	138	90	0.007	92	340	322
7	200	90	0.025	50	2000	100
8	200	90	0.013	50	2000	100

Body Specifications, Hull 1641

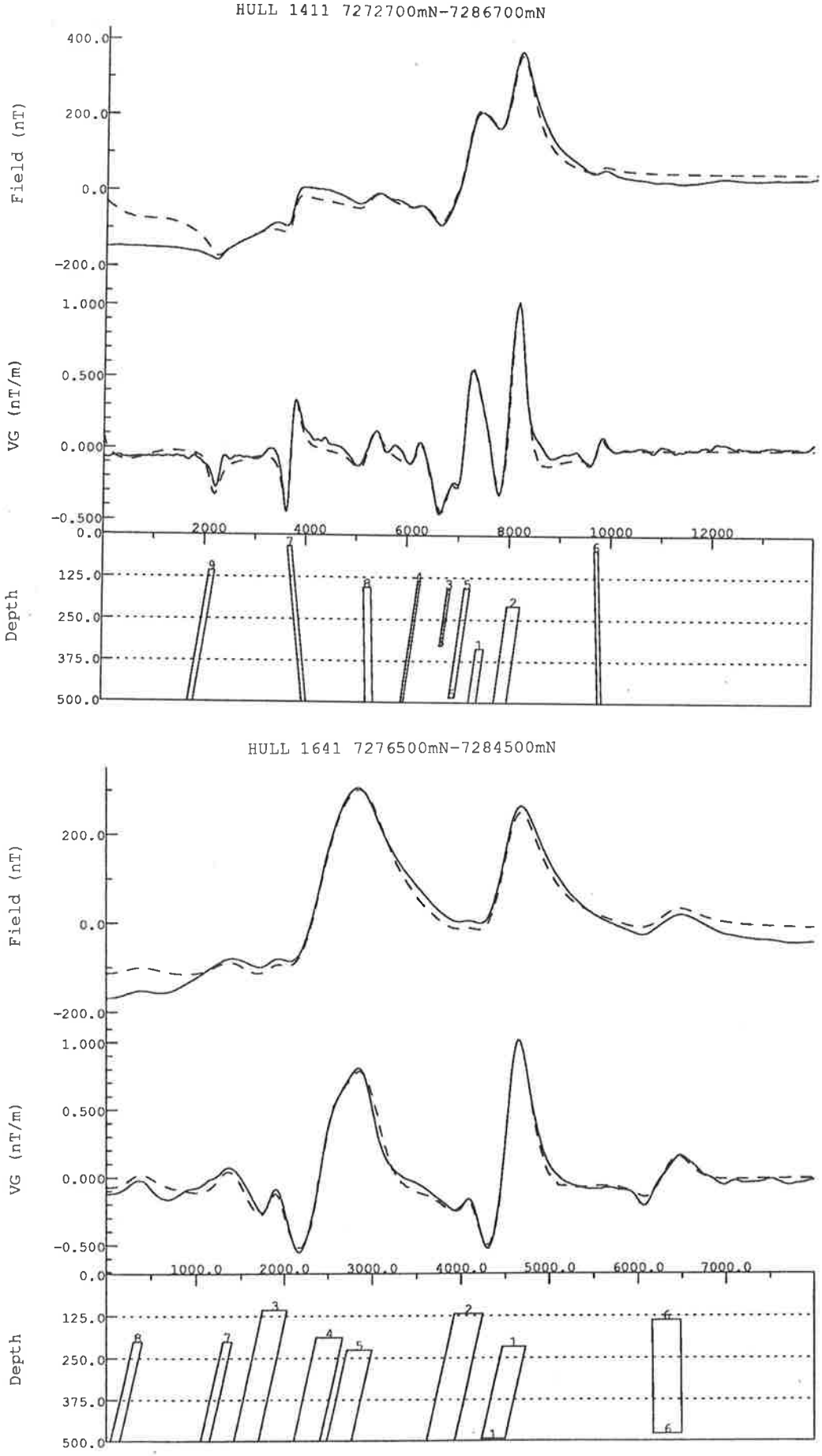

Figure 5.3: Modeled Sections Lines 1411 and 1641 through **NBL**, *Hull. Note that the scales differ on each profile*

ROCK TYPE	MEAN SUSCEP.	MODE	RANGE	STD. DEV.	N
Ordovician Sst.	130	0	0–2000	384	33
Mt. Currie Conglom.	-	-	-	-	-
Winnall Beds	5	0	0–150	22	5
Pinyinna Beds	5	0	0–10	6	20
Dean Quartzite	37	0	0–800	166	23
Minor Granites	75	-	10–150	73	4
Pottoyu Granite	256	0	0–2000	601	34
Porphyroblastic Schist	761	20	0–5000	1541	31
Q-F Porphyry	1008	-	15–2000	1404	2
Bloods Range Beds	13	5	0–30	8	16
Mt. Harris Basalt	5	-	0–10	5	3
Olia Gneiss	560	1000	0–3500	1111	10
M-M Metamorphics	738	1100	10–5000	864	50

Table 5.1: Measured Magnetic Susceptibilities (S.I. units $\times 10^5$) Measured from the B.M.R. rock collection by A.M.Lewis.

due to the depth of the sources means that as magnetic units converge their individual responses merge into one anomaly.

The stratigraphic position of the magnetic unit within the regional recumbent fold places it close to where Pinyinna Beds are folded around and become near vertical. If this is the case then it is probable that the source of the broad linear anomalies is the same magnetic hematite-goethite schist unit attributed to the source of the prominent curvilinear magnetic anomaly within **NS3** discussed above. Where noted in **NS3** the horizon was a relatively thin well defined single horizon; in **NBL** there are a number of separate horizons.

Another possible source could be the chert unit within the Inindia Beds which, if enriched in magnetic iron bearing minerals, could produce such an anomaly pattern. The magnetic layering would need to be relatively steeply dipping as indicated in the magnetic models, unless remanence contributes a significant amount to the overall magnetization of the unit. Without further evidence it is difficult to attach a definite geological source to the zone.

Younger Basement Core

Much of the basement core of the regional fold is occupied by the younger basement metasediments and metavolcanics (see Figure 2.2 in Chapter 2). The magnetic expression of these lithologies is variable. The majority of the outcropping Bloods Range Beds within the younger basement are nonmagnetic quartzites, and a significant amount of outcrop is mapped in the

smooth textural zone **NS2**. Consequently these nonmagnetic units of the Bloods Range Beds cannot be distinguished from the nonmagnetic overlying sediments. In contrast to the smooth zones, most of the younger basement outcrop lies within **NMo1**, a mottled magnetic zone with distinct boundaries visible on the processed versions of the magnetic data.

Bloods Range Beds outcropping in the south of **NMo1** near the *Hull/Bloods Range* boundary are associated with magnetic anomalies in places, although most appear weakly magnetic, as suggested by the measured average susceptibility. Limited magnetic susceptibility measurements (Table 5.1) on the Mt. Harris Basalt do not indicate that the unit has a significant magnetic susceptibility. Since the aeromagnetic data clearly shows that there are quite strongly magnetic lithologies in the vicinity of mapped Mt. Harris Basalt it is considered that the measured susceptibility samples are a biased representation of the unit, with most samples coming from the basal quartzite of the Mt. Harris Basalt which would be expected to be only weakly magnetic. The main magnetic rock type within the Mt. Harris Basalt is interpreted to be the upper basaltic unit.

The Mt. Harris Basalt has not been subdivided into the quartzite and basalt members on the available geological maps but the distinction has been made between two lithomagnetic units on the magnetic interpretation maps (V1 and V2, see Plates 1 and 2). V1 is manifested as the areas within **NMo1** showing moderate amplitude magnetic anomalies attributed to the basalts. V2 is interpreted in the weakly magnetic areas as the basal quartzite and probably includes a significant proportion of the nonmagnetic units of the Bloods Range Beds.

The distribution of these lithomagnetic divisions can be used to make inferences on basement structure. Since the younger basement occurs in the overturned limb of the regional recumbent fold, areas of nonmagnetic V2 (basal quartzite) can be interpreted as basement lows and areas of magnetic V1 (basalt) as basement highs.

The quartz-feldspar porphyry situated near the top of the Mt. Harris Basalt (Wilson,1966) makes a prominent magnetic horizon along the southern boundary of **NMo1** on eastern *Hull* and western *Bloods Range*. The anomaly is marked in the interpretation maps as lithomagnetic unit P. The horizon can be modeled as a shallow northerly dipping sheetlike body (see body 2 in Figure 5.4). Further to the east the horizon is abruptly truncated against the magnetic zone boundary. The quartz-feldspar porphyry outcropping at the northern boundary of the zone does not produce such a marked magnetic anomaly and is probably a different lithological variant of the magnetic porphyry.

The prominent anomaly group within **NMo1** on the western edge of *Hull* is caused by the magnetic V1 units of the Mt. Harris Basalt below nonmagnetic cover. The southern edge of this anomaly group can be seen in the northwest of the image in Figure 5.2. Modeled dips are consistently southerly, except along the southern edge of the anomaly group where they change to northerly, indicating the presence of a possible synformal structure. This group of anomalies has been discussed by Woyzbun (1968) and was attributed to uplift of the magnetic basement.

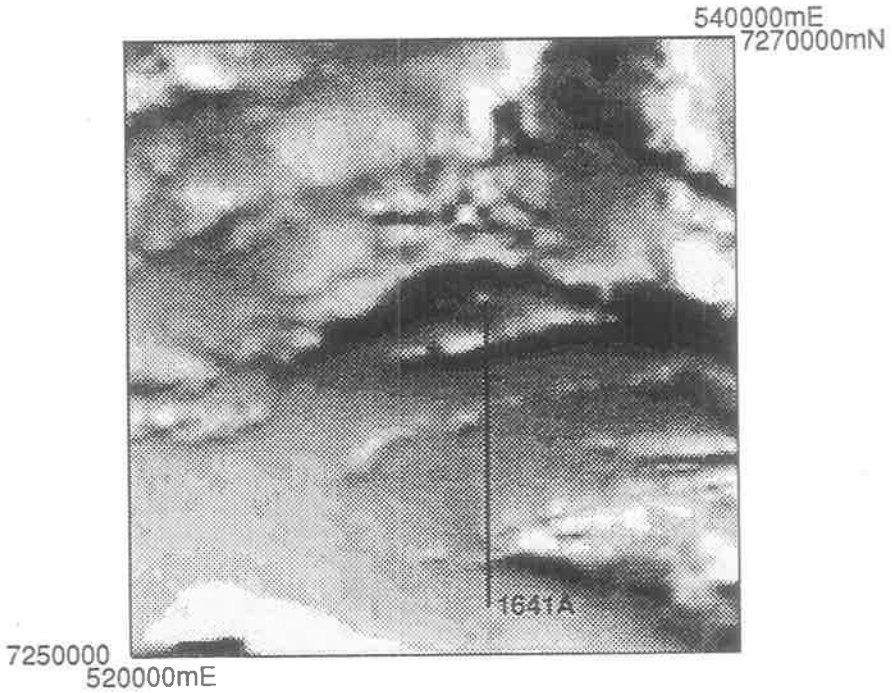

1:250 000

Body	Depth (m)	Strike	Suscep.(S.I.)	Dip	Depth Extent	Width
1	68	75	0.029	38	120	56
2	53	75	0.101	96	83	46
3	57	75	0.127	118	51	20
4	107	75	0.135	155	182	134
5	45	75	0.043	157	101	31

Body Specifications, Hull 1641a

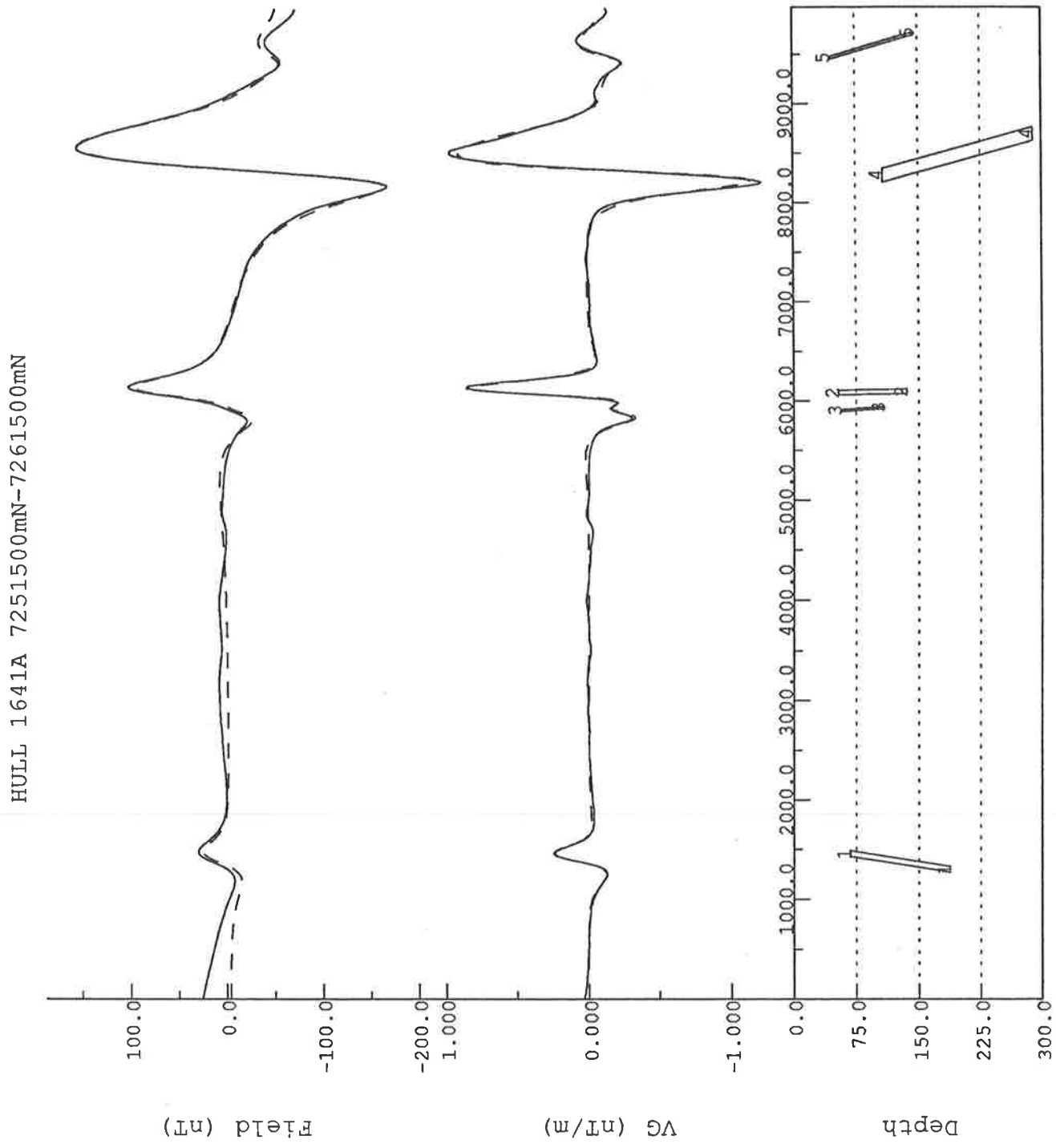

Figure 5.4: Modeled Section Line 1641a, *Hull*

The depth estimates of these anomalies made by Woyzbun (1968) at 750 m (2500 feet) would appear to be too deep from the work done here, which suggests a depth of the order of 250 metres.

Also grouped within the younger basement is the Mannanana Porphyroblastic Schist. A distinct zone of mottled magnetic texture **NMo3** is closely associated with the mapped arcuate outcrop of the Schist in southern *Hull*. Measured magnetic susceptibilities indicate that the Schist is considerably more magnetic than the surrounding lithologies in agreement with the observed magnetic patterns.

NMo3 stretches southeasterly into *Pottoyu* and also has isolated occurrences in *Petermann*. All occurrences of this magnetic zone are interpreted as the magnetic response of the Mannanana Porphyroblastic Schist, even though lithologies which fall within the zone are mapped as Pottoyu Granite Complex on *PETERMANN RANGES* (as noted in Chapter 4). The northern boundary of **NMo3** is transitional, suggesting that it is dipping northwards beneath an increasing thickness of nonmagnetic sediments.

Older Basement Core

A large mottled zone, **NMo2**, in southern *Bloods Range* and northern *Petermann* continues over the eastern edge of the study area to form a well defined triangular zone of increased magnetic activity. Within this zone outcrop is limited, but older basement Olia Gneiss is most common, together with some minor Mt. Harris Basalt, Dean Quartzite and overlying Ordovician Stairway Sandstone.

The southern boundary of the zone is sharply defined against **NS3**, the northern boundary has a sharp edge but becomes more diffuse towards the south, suggesting that the contact has a regional southerly dip. Several linear horizons within **NMo1** have been truncated against the northern boundary. A distinct linear sloping regional trend is a characteristic of the zone with a magnitude of approximately 10 nT/kilometre, increasing to the east.

The entire zone is interpreted as the older basement Olia Gneiss core of the regional recumbent fold. Both the younger and older basement sections of the core area of the regional fold correlate with the Bloods Range Gravity High (see Figure 6.1 in Chapter 6). The minor occurrences of Dean Quartzite within this area are likely to have been downfolded from the upper limb of the regional fold. If the outcrops were the result of upfolding from below, a significant nonmagnetic zone would be expected in association with the outcrops. Since no such zone is present the Quartzite is interpreted as the root zone of a synform, the upper part of which has been eroded.

The amphibolite facies Olia Gneiss has been postulated as having two distinct and separate modes of formation by Forman and Hancock (1964):

- The result of granitization and metamorphism of Mt. Harris Basalt and Bloods Range

Beds.

- Original gneissic basement unrelated to Mt. Harris Basalt and the younger basement.

The magnetic data also indicates that the Olia Gneiss can be divided into two lithomagnetic units. The different magnetic responses of the two units are considered to be caused primarily by their differences in origin, although differences in their later deformation history must also contribute in part to their magnetic character. The magnetic evidence can be used to subdivide the gneiss into two lithomagnetic groups, AM and AB. Unit AM is interpreted as Olia Gneiss that is the result of metamorphism and granitization of younger rocks, AB is considered to be original gneissic basement.

The gneiss within **NMo2** is classed as lithomagnetic unit AM due to its similar magnetic response to the younger basement and its close association (in outcrop) with the younger basement (see the interpretation maps where the distinction has been made between the two lithomagnetic variants). AB type Olia Gneiss is interpreted further south and is discussed in more detail below.

Granites within the Fold Nappe

The granites which outcrop within the fold nappe have variable magnetic characteristics. As well as outcropping granites, several anomaly groups in **NMo1** have been interpreted as granitic bodies though no geological evidence exists.

The granites within the fold nappe can be subdivided into two lithomagnetic groups. The first, G1, are generally equidimensional in shape and have significant magnetic anomalies or groups of anomalies associated with them. The second, G2, are generally elongate or sheetlike in form and weakly magnetic. Where outcropping, all the granites are correlated with radioactive highs.

The G1 magnetic granites outcrop just south of the Bloods Range, near the eastern boundary of *Hull*. The associated magnetic anomalies are complex and more extensive than the mapped outcrop suggests. Another example of this class of granite has been interpreted in central *Hull* near the Hull River within **NMo1**. This anomaly group has no associated outcrop.

The weakly magnetic granites (G2) occur as elongate outcrops near the southern boundary of the fold nappe complex within **NS3** on eastern *Hull*, continuing into *Petermann*. Small amplitude magnetic anomalies are associated with some of these granites, and are discernable in the nonmagnetic background of **NS3**. Modeling indicates a northerly dip for these sheetlike granites.

It seems likely, both from the weak magnetic character and stratigraphic position, that the G2 granites are related to the Pottoyu Granite Complex, which is in general also weakly magnetic. The magnetic G1 granites, which occur in the core area of the fold nappe appear to be unrelated to the Pottoyu Granite Complex due to their different form, contrasting magnetic character and

different stratigraphic position. Since the G1 granites appear to belong to a different suite than the Pottoyu Granite Complex and some outcrops show intrusive contacts they are perhaps the result of local melting and intrusion into younger basement lithologies during the Petermann Ranges Orogeny.

5.4 Original Basement

Immediately south of the zones discussed above is a large area of contrasting geophysical and geological character. This area is interpreted as a window of original autocthonous basement situated between the metasediments and metavolcanics of the fold nappe cover sequence and the overthrust higher grade granulite basement to the south (see Chapter 6). This original basement covers most of *Pottoyu* and *Petermann* and is dominated by the Pottoyu Granite Complex and Olia Gneiss lithologies. The area includes several magnetic textural zones ranging through granular, mottled and linear. The magnetic patterns and geological evidence in **NL1** suggest that large scale basement shearing may dominate much of the structure in this area, and relative ages can be assigned to the lithomagnetic units according to their development in relationship to this proposed shearing.

5.4.1 Basement Shearing

Evidence for recrystallization and shearing within the Olia Gneiss from the Pottoyu Hills in **NL1** has been noted by Forman and Hancock (1964) (see Chapter 2). However the scale of the sheared zone was not evident from the ground based geological data, which was necessarily collected from isolated outcrops. The magnetic data gives a much broader and complete picture of the extent of the postulated shearing. The interpreted shear belt stretches as a curvilinear feature trending roughly east–west across the entire width of the study area. It is manifested as the linear magnetic zone **NL1**, characterized by elongate anomalies, individual examples of which can be traced for up to forty kilometres. Such linear magnetic patterns can be produced by banding and intercalations of thin magnetic horizons without shearing, but the available evidence suggests that basement shearing is involved in this case. The proposed shear zone in **NL1** is possibly caused by deep seated east–west trending left-lateral transcurrent faulting in the basement rocks.

Large scale Precambrian basement shear belts are not uncommon in the geological record. A similar shear has been postulated, on the basis of aeromagnetic evidence, in the Musgrave Block of South Australia by Shelley and Downie (1971) between Mt. Harcus and Mt. Tietkens (on *MANN* in South Australia). This zone is characterized by strong positive and negative magnetic lineations which extend for up to 32 kilometres. It would appear that this zone is not related to a continuation of the feature in the Petermann area. Other large scale shear zones have been mapped in the Harts Range to the northeast of the study area (James and Ding, 1988).

Two spatially separated shears, the Florence and Leaky Shear Zones are each approximately 20 kilometres long and 2 kilometres wide, however it is considered by James and Ding (1988) that the two shears represent the remnants of a single much larger zone, up to 60 kilometres long.

The postulated shear zone in the study area affects the Olia Gneiss and a large section of the Pottoyu Granite, mainly the granite in *Petermann*. The contact between these two rock types on *Petermann* can be discerned on stereo air photographs as a topographic feature. Only a subtle difference exists between the two rock types on the magnetic data and the contact appears gradational. The Olia Gneiss is associated with larger amplitude, better defined anomalies and is interpreted as original gneissic basement (lithomagnetic unit AB). The Pottoyu Granite Complex exhibits lower amplitude magnetic anomalies.

Both measured dips from the geology and calculated dips from two dimensional modeling are variable, but profiles from within **NL1** indicate that the majority of anomalies can be modeled with southerly dipping sheets within 100 to 150 metres from the surface (see Figures 5.5). There are several large amplitude (700–1600 nT) single line anomalies which are prominent within the zone. Most of these anomalies can be modeled as strongly magnetized near surface strike limited southerly dipping sheets which are conformable with their neighbouring anomalies.

Near the southern boundary of **NL1** in *Petermann* several horizons are truncated, suggesting evidence for individual shear planes within the belt. Northwest trending isoclinal folding is also evident in this area. A number of northeasterly trending faults have been interpreted within the zone in *Petermann*

East–west trending linear features are clearly defined, both from the magnetic data and aerial photographs within the Pottoyu Granite Complex in southeastern *Petermann*. These have been interpreted as a swarm of dykes which were emplaced after the main shearing event since they appear unaffected by the shearing. Differential weathering of the softer dyke lithologies within the more indurate granites may have produced these prominent airphoto features.

The Pottoyu Granite Complex has been described as a variable granite (Forman and Hancock, 1964) which is in part gneissic. However on the geological maps the granite is not differentiated into its different lithological variants. The granite complex which lies within the sheared zone (**NL1**) is perhaps better described as a gneissic granite on the basis of the magnetic evidence and the geological description and has been identified as such on the interpretation maps.

South of **NL1** is an indistinct triangular shaped zone of mottled magnetic texture, **NMo4**. In the northern section of the zone the magnetic trend directions are parallel to those within **NL1**. As the distance from the contact with **NL1** increases so the magnetic trends tend to diverge from the strong southeasterly direction so typical of the shear belt. Towards the southern boundary of **NMo4** is a well defined thin magnetic horizon which is clearly complexly folded into a number of fold structures. Modeling on this horizon suggests bodies similar to those found within **NL1**. A prominent single line magnetic anomaly in central **NMo4** also resembles the single line anomalies in the sheared zone.

Body	Depth (m)	Strike	Suscep.(S.I.)	Dip	Depth Extent	Width
1	6	110	0.114	34	145	36
2	93	110	0.119	49	127	77
3	155	110	0.209	31	90	35
4	14	110	0.037	24	138	30
5	158	110	0.099	48	193	43
6	125	110	0.146	20	532	40
7	123	110	0.086	30	52	20
8	40	110	0.014	61	1011	44
9	18	110	0.008	69	215	22

Body Specifications, Petermann 2152

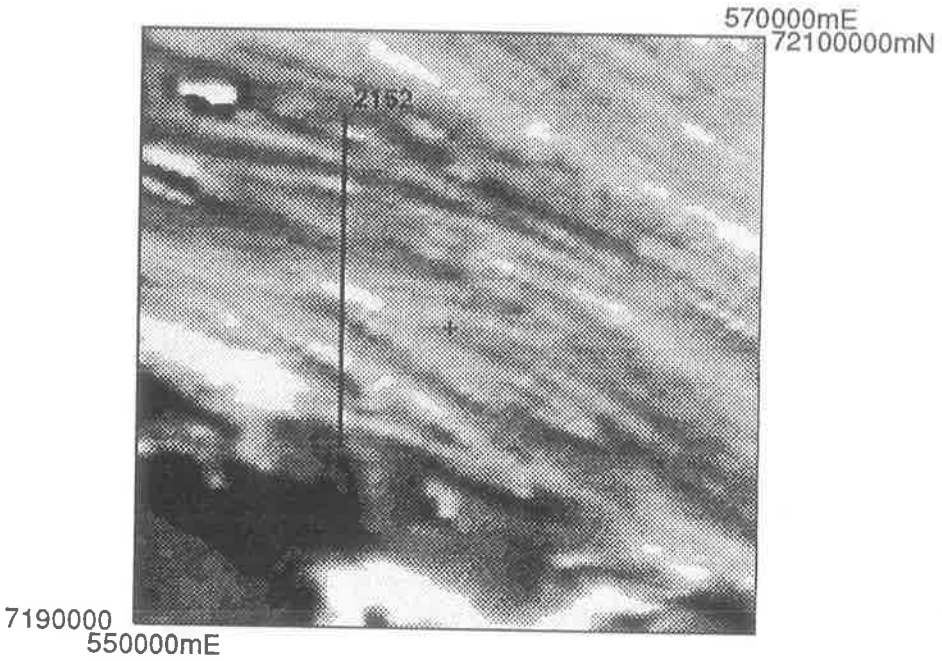

1:250 000

Body	Depth (m)	Strike	Suscep.(S.I.)	Dip	Depth Extent	Width
1	138	110	0.132	33	903	57
2	139	110	0.050	21	127	63
3	199	110	0.250	79	396	37
4	93	110	0.055	51	280	44
5	100	110	0.078	62	130	46
6	126	110	0.142	49	304	59
7	79	110	0.074	32	199	50
8	104	110	0.030	57	∞	32
9	77	110	0.027	32	2201	53

Body Specifications, Petermann 2152

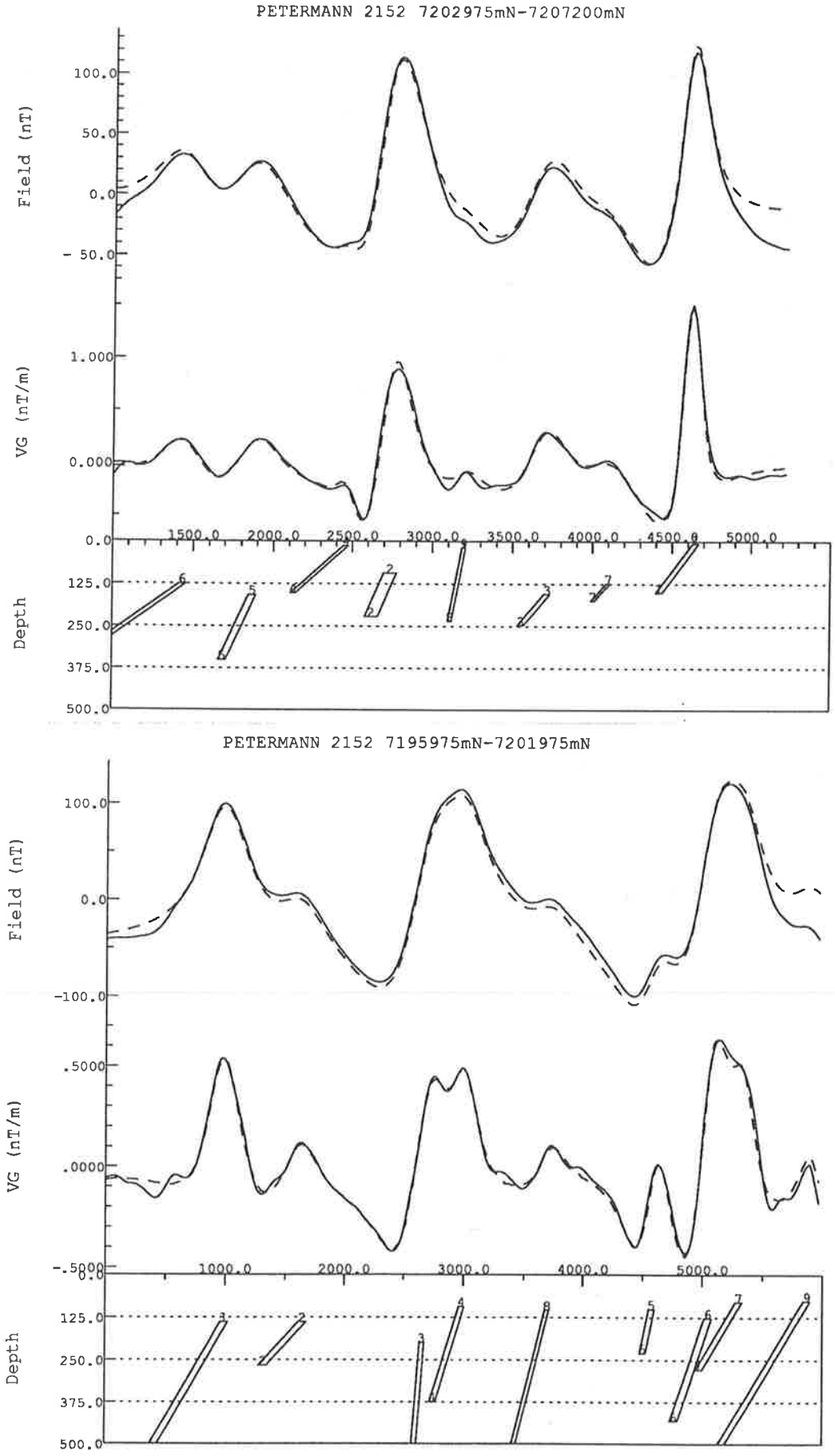

Figure 5.5: Modeled Sections Line 2152 *Petermann*

This evidence suggests that zone **NMo4** is a remnant of the original basement at the edge of the shear belt which has been unaffected by the shearing. If this is indeed the case then it indicates that folding had taken place within the original basement along northeasterly axial trends prior to the shearing. Unfortunately there is only very limited outcrop within the zone and no ground observations on those outcrops to confirm this hypothesis.

5.4.2 Late Stage Granites

The granular textural zone **NG1** in southern *Hull* and northern *Pottoyu* correlates closely with mapped outcrop of Pottoyu Granite Complex. The zone shows no evidence for the distinct long linear magnetic horizons found within the sheared gneissic granite section of the Granite Complex further east in *Petermann*, although **NG1** directly adjoins the latter zone.

It is proposed that the granite corresponding to zone **NG1** is a later stage intrusion than the sheared **NL1** granite, and was emplaced after the shearing event. The emplacement of this granite may have been controlled by crustal weaknesses resulting from the shear. The southern boundary of **NG1** is a distinct linear magnetic low, best seen in processed versions of the magnetic data (Appendix A). The northern boundary has, in places, large amplitude anomalies (e.g. in southern *Hull*) suggesting the granite is of an intrusive nature, emplaced into relatively cooler country rocks at a high crustal level; the notable large amplitude anomalies perhaps produced by contact metamorphism.

The easternmost boundary is a distinct linear magnetic feature which separates the sheared (**NL1**) and unsheared (**NG1**) members of the Pottoyu Granite Complex. Several weak south-easterly trending linear magnetic features have been interpreted as dykes within the late stage granite intrusion.

On the western edge of southern *Pottoyu* and continuing into *Cockburn* is a distinct semi-circular granular magnetic zone **NG2**, with a smooth zone **NS5** on its northern boundary. Both these zones fall within the area of the Cobb Gravity Depression (Lonsdale and Flavelle, 1968) (see Figure 6.1 in Chapter 6). The Cobb Depression is an elongate gravity low which begins within the study area and stretches several hundred kilometres northwest across Western Australia. In the study area the Depression is a 35–40 mGal gravity low.

The source of the Cobb Gravity anomaly has been attributed to a Permian basin filled with sediments of glacial origin (Lonsdale and Flavelle, 1968; Daniels, 1974). This hypothesis is based on outcrop and borehole evidence (Farbridge, 1967) from Western Australia. Drillhole D59 intersected at least 120 metres (400 feet) of sediments in the Cobb Depression approximately 50 kilometres southeast of the Giles Meteorological station.

It seems likely that the smooth magnetic zone **NS5** which lies in the northern section of the Cobb Depression is the magnetic response of a shallow basin filled with these Permian sediments, which deepens towards the east. The majority of the Cobb Depression in the study area is dominated by the granular zone **NG2**, which is not the typical magnetic expression

of a sedimentary basin. **NG2** is interpreted as a weakly magnetic granitoid which has been emplaced after the shearing event. This interpretation is confirmed by drillhole D58 (Farbridge, 1967) which encountered weathered acidic gneiss at a shallow depth. The granite is possibly related to the granite on the northern side of the shear zone (**NG1** discussed above). Linear trends within **NG2** have similar southeasterly orientation to those within **NG1**, and have been similarly interpreted as dykes within the granite. A series of strong anomalies near the northern boundary of **NG2** correlate with mapped outcrops of Olia Gneiss. These outcrops are considered to be large scale xenoliths or roof pendants of original gneissic basement within the granitoid, the remnants of the sheared basement through which the granite intruded.

Though no surface evidence for the granite is available, either in the Northern Territory or Western Australia, the interpretation is corroborated by the radiometric data. On the total count and potassium channel images (see Chapter 4, Figures 4.1 and 4.2) a zone of higher radioactivity is evident in the area of the interpreted granite. This would be expected from a subcropping granite with a cover derived in part from residual material from the granite, since granites are typically more radioactive than other lithologies in the study area (see Tables 4.1 and 4.2–4.5, Chapter 4).

If standard densities for granites (2.65 $g\,cm^{-3}$), sediments (2.63 $g\,cm^{-3}$) and amphibolite country rock (2.7 $g\,cm^{-3}$) are used in a $2\frac{1}{2}$ dimensional gravity model the granite must extend to a depth of the order of 20–25 kilometres to produce an anomaly of the magnitude of the Cobb Depression within the study area.

To confirm the interpretation of this subcropping granite, the outcrops in the area should be examined carefully and some suitably placed drillholes would be useful. Good quality semidetailed aeromagnetic data from the Western Australian section of the Cobb Gravity Depression would also be helpful.

5.5 Folding within the Northern Domain

Folding discernable from aeromagnetic interpretation is not abundant within the Northern Domain. In order to interpret folded horizons they must produce magnetic anomalies which register on several flight lines (each flight line being 500 metres apart). This means that folding must be quite large scale. The sense of folding (synform, antiform) can be determined by modeling the anomalies in each limb of the interpreted fold for dips, though this cannot always be done successfully. Hence large scale (kilometre or larger) plunging folds within magnetic rocks can be located. Much of the Northern Domain is covered by nonmagnetic sediments which preclude the location of many folds using aeromagnetics which are possibly clearly visible in aerial photographs or in outcrop within the sediments.

This survey confirms the regional scale antiform-synform pair which had been previously interpreted from the outcrop pattern on northeastern *Bloods Range*. This prominent fold pair, at the edge of the Amadeus Basin, has an east–west trending axis and clearly folds the magnetic

zones, **NBL**, **NS2** and **NMo1**.

A previously unrecognized regional scale fold is interpreted within the basement core (**NMo2**) in southern *Bloods Range* and northern *Petermann* and is clearly discernable on the local contrast stretched version of the total field magnetics. (see Figure A.5 in Appendix A). The fold has a north-northwest trending axial plane and closes to the south. The eastern limb dips to the west; dips on the western limb could not be determined due to the poor definition of the anomalies in that area. The consistent westerly dips for the eastern limb suggest that the fold is a synform. The magnetic trends in the fold structure agree closely with the gneissosity trends on the geological map, however lack of outcrop in the nose of the fold prevented the structure from being defined from the ground based data.

Variable calculated dips from the western end of **NBL** (northern *Hull* and *Bloods Range*) suggest complex structure, possibly marked by upright folding within the zone. Individual folds can not be defined due to the difficulty of delineating upright folds at depth from aeromagnetic data where an anticline can produce a similar magnetic response to a single dipping horizon. Another upright synform is postulated within **NMo1** in the anomaly group at the far western edge of *Hull* where modeled dips show marked changes from south to north.

Folding within the original basement is more easily distinguishable due to the higher magnetic activity of the lithologies. A number of tight to isoclinal folds have been delineated in **NL1**, particularly near the southern boundary of the zone. The axes trend northwest. It is probable that some of the elongate horizons within that zone are isoclinaly folded, but the fold closures are not resolved.

Folding in **NMo4** in the form of several open, easterly plunging synforms on a single well defined magnetic horizon suggest that the original Olia Gneissic basement had undergone folding prior to the shearing event.

5.6 Faulting within the Northern Domain

Only occasionally are faults directly observable as aeromagnetic anomalies. Magnetic lows can develop within fault zones due to near surface martitization and hydration of magnetite in the zones, mainly due to the presence of water (Henkel and Guzman, 1977). Magnetic highs are also noted associated with faults, perhaps as the result of fluid movement from depth precipitating magnetic minerals, as is the case with the Mann Fault, which is discussed in more detail in Chapter 6. Where anomalies are the direct result of faulting they have been marked on the interpretation maps with the symbol F. More commonly faults can be defined by the alignment of magnetic highs, lows or gradients into linear features (Parker Gay, 1972, 1973) or by displacements of magnetic horizons.

Faults are common in the Northern Domain. Within the cover sequence fold nappe they trend predominantly northerly. Several large, well defined strike-slip faults cut zone **NBL**, **NS1** and **NS2** and continue into **NMo2** in northern *Bloods Range*. These faults displace both

magnetic horizons and zone boundaries with approximately 1 kilometre of movement, suggesting that they developed after the regional fold structure.

A series of en echelon, predominantly left lateral strike-slip faults are prominent within **NMo1** in western *Hull.* Displacements on these faults are of the order of several kilometres. A similar series of faults has been mapped in the nonmagnetic Dean Quartzite outcrops within **NS2** on *BLOODS RANGE* just north of the interpreted faults, confirming that the features continue into the nonmagnetic areas.

The northern boundary of **NMo2** in central *Bloods Range* is marked by a complex system of cross cutting interpreted faults with evidence that a series of northwest trending faults have been displaced by a later developed system of northeast trending strike-slip faults.

Another group of northeast trending strike-slip faults displaces the eastern limb of the regional scale fold in **NMo2** in southeastern *Bloods Range* and northeastern *Petermann* which has been discussed in Section 5.5. It is probable that these features are of the same system as those with similar trends noted further north in the zone, and may be related to the development of the large scale fold which dominates the mottled zone.

Faulting within the original basement is restricted to short (2–4 km) northeast trending features within zone **NL1** and some southeasterly faults in the south of the zone. The well defined curvilinear feature which separates the two types of granitic lithomagnetic units (zones **NG1** and **NL1** within the area of original basement on northern *Pottoyu*) may be a deep seated bounding fault which has acted to control the emplacement of the younger **NG1** granite.

Chapter 6

Southern Magnetic Domain

6.1 Introduction

The Southern Magnetic Domain covers most of the southern two map sheets (*Cockburn* and *Duffield*). The magnetic activity in the Domain is much higher than that of the Northern Domain, and reflects the near surface high grade metamorphic rocks which make up much of the southern area. Large zones of muricate magnetic textures are interpreted within the Domain, as well as a number of circular/elliptical features and less magnetically active zones.

The magnetic response in the Southern Domain is complex, and the available geological control is severely limited by lack of outcrop. These two factors make the interpretation of the data a difficult problem and in the absence of any well defined regional structural picture the Southern Domain will be discussed in terms of the interpreted lithomagnetic units. Two major lithomagnetic units have been identified in the Domain:

1. Strongly Magnetic Basement Complex (B1),
2. Moderately Magnetic Basement Complex (B2).

Further areas of weakly magnetic lithologies are delineated as well as a number of circular and elliptical features.

This chapter is designed to be used in conjunction with the interpretation maps (plates 5 and 6 at the back of this thesis).

6.2 The Domain Boundary

The boundary between the Northern and Southern Magnetic Domain is a prominent geophysical feature. In the magnetic data it is manifested as a high amplitude magnetic anomaly along part of its length, which decreases in amplitude to the west and eastern edges of the study area, where it becomes a contact between high magnetic relief to the south and lower relief to the north.

The Southern Domain is also marked by prominent regional anomalies in both the radiometric and gravity data. The radiometrics show a general lowering of the radioactivity level over the Southern Domain (see Chapter 4, Figures 4.1–4.3). This is consistent with both the decrease in amount of outcrop and the expected decrease in radioelement concentrations in lithologies of higher metamorphic grade (Lambert and Heier, 1967). The gravity data exhibits a large high, the Blackstone Gravity Plateau (Lonsdale and Flavelle, 1968), which correlates closely with the Southern Magnetic Domain (see Figure 6.1). A steep gravity gradient is centred on the Domain boundary, although the exact form and position of the gradient is difficult to define due to the wide gravity station spacings. All of these geophysical features tend to confirm that the Southern Magnetic Domain is the higher density, higher metamorphic grade granulite terrain within the Musgrave Block which is separated from the lower grade amphibolite facies gneisses by the Woodroffe Thrust. Smith (1979) notes that the mylonites of the Woodroffe Thrust in South Australia have no distinct magnetic signature, but the Woodroffe Thrust appears to separate a zone of lower magnetic relief to the north from higher relief to the south. The magnetic data analysed in this project confirms that the Woodroffe Thrust has a similar magnetic expression in the Northern Territory, although it is associated with a magnetic high of 300–550 nT along some of its length.

Attempts to model the magnetic and gravity data across the Domain boundary as simple geological contacts were not successful. The gravity stations are widely spaced (11 kilometre grid) which makes it difficult to model near surface features. Mathur (1976) considered the gravity field in this part of central Australia to be strongly influenced by deep crustal/mantle sources. The gravity data available to the author was obtained from digitizing and gridding 1:250 000 scale gravity maps obtained from the N.T.G.S. and detailed modeling was felt to be inappropriate due to the nature of the data. A closely spaced gravity profile across the magnetic Domain boundary would better define the details and form of the large gravity gradient in that area. Such a profile would yield much useful information on the nature of the geological contact by accurately locating the position of the contact, defined from the magnetic data, relative to the gravity gradient and so yield accurate information on the dip of the contact. Modeled dips on individual magnetic anomalies in the area of the Domain boundary are variable, as may be expected in the highly deformed zone associated with a near horizontal thrust fault.

On the western edge of the study area the Woodroffe Thrust follows the southern boundary of the interpreted **NG2** granite and crosses into Western Australia. The Thrust has not been recognized in geological mapping in Western Australia, although a poorly defined structural discontinuity has been postulated in the area (Horwitz et al., 1967; Daniels, 1972; Daniels, 1974). This structure, known as the Giles Discontinuity, has been proposed to explain the contrasting metamorphic and structural character seen on either side of a northeasterly linear trend approximately 40 kilometres west of the Western Australian border. Daniels (1974) considered that this feature is a transcurrent fault which continues northward beneath the Cobb Depression and

LOCATION	GRAVITY UNIT/FEATURE
A	Amadeus Gravity Depression
B	Bloods Range Gravity High
C	Katamala Gravity Embayment
D	Cobb Gravity Depression
E	Blackstone Gravity Plateau

Main Gravity Features (Lonsdale and Flavelle, 1968)

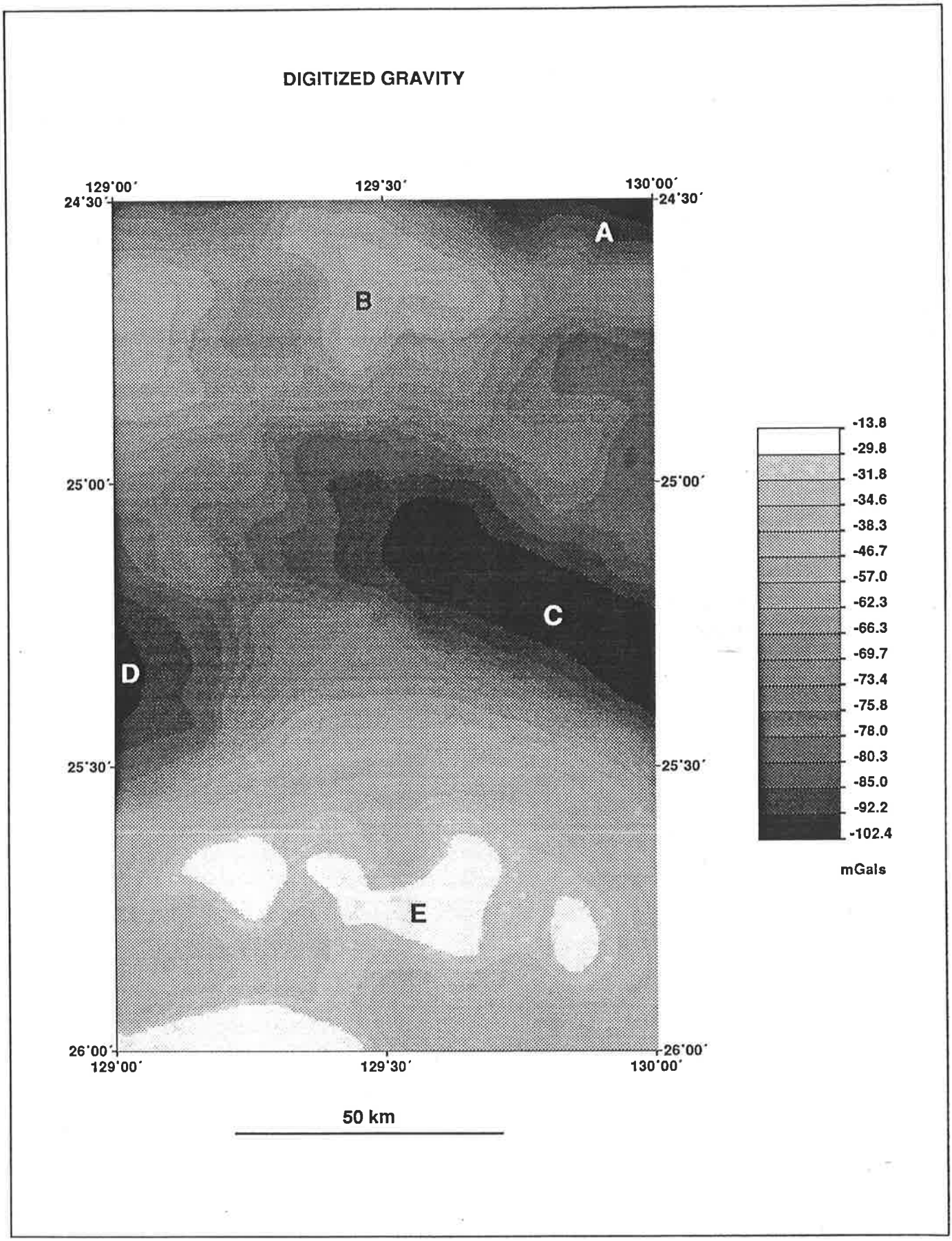

Figure 6.1: Regional Gravity Field in the Study Area

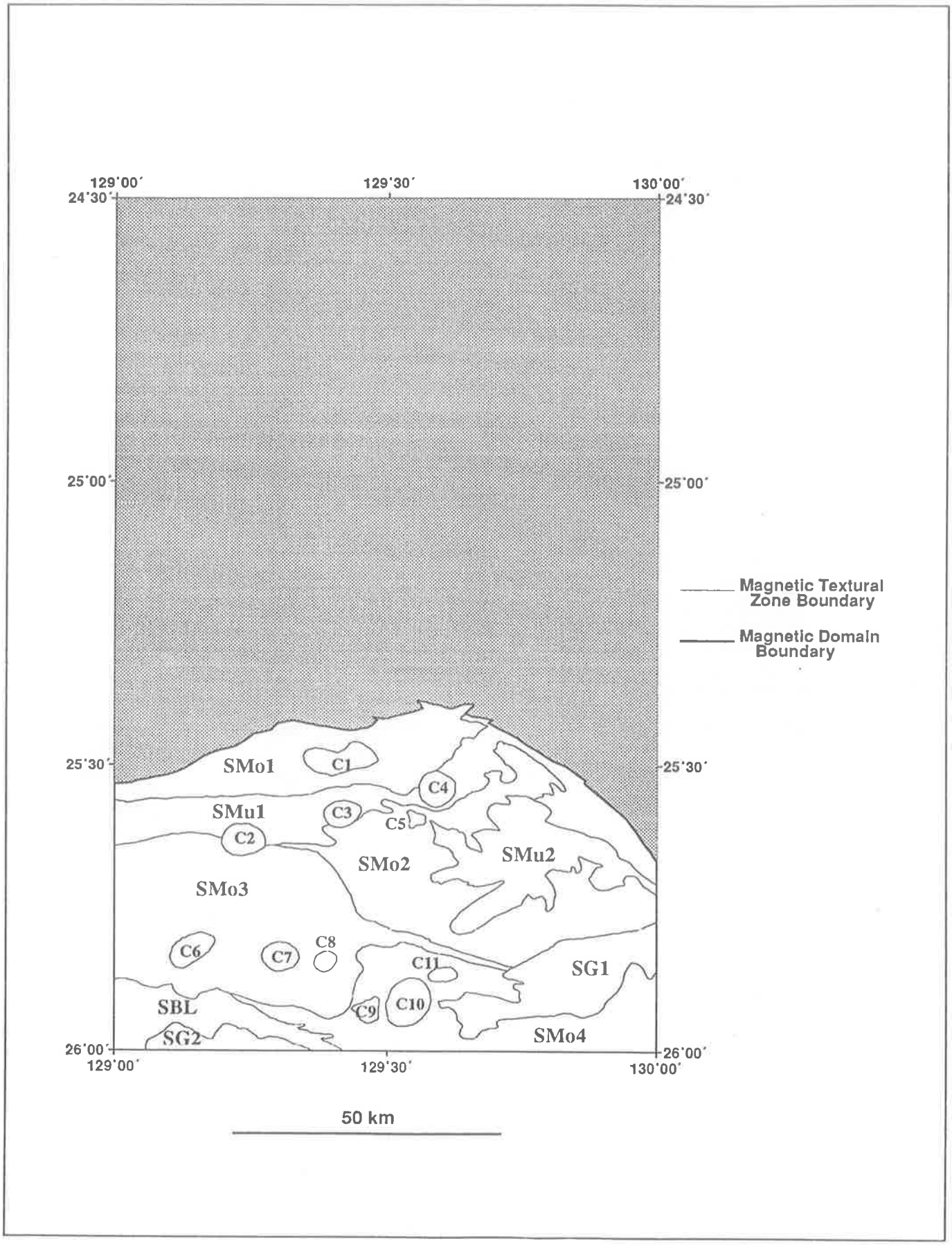

Figure 6.2: Interpreted Magnetic Zones in the Southern Domain

joins a bounding fault northwest of the Dean Range. Unfortunately it is covered along most of its length by an extensive sheet of calcrete. The bounding fault in the Dean Ranges on *SCOTT* does not show marked structural or metamorphic differences on either side.

The information revealed in the geophysical data in this study suggests as an alternative explanation that the Giles Discontinuity is the possible continuation of the Woodroffe Thrust into Western Australia. This implies that the Discontinuity does not trend northwards beneath the Cobb Depression, but swings to the east along the southern edge of the Depression. Further evidence is required to confirm this interpretation, and a semidetailed aeromagnetic survey would probably be the most useful information to help solve the problem, together with careful study of the metamorphic grade and structural conditions on either side of the discontinuity.

To the east of the study area the Woodroffe Thrust enters a region of very complex magnetic character and is discussed in more detail below (see section 6.5).

6.3 Strongly Magnetic Basement Complex

The Southern Domain can be subdivided into two lithomagnetic units, a strongly magnetic basement complex and a moderately magnetic complex. The strongly magnetic basement complex is characterized by large amplitude magnetic anomalies and complex magnetic patterns restricted to the muricate magnetic textural zones and has been marked on the interpretation maps as lithomagnetic unit B1. The high magnetic activity of the strongly magnetic basement complex suggests that this unit may be predominantly mafic granulite basement. Mafic granulites have been noted by Collerson et al. (1972) to make up to 9% of the granulite rocks in parts of the Musgrave Block in S.A.

The most distinct zone is **SMu2** in central *Duffield* (see figure 6.2). This zone forms an envelope around a number of apparently isolated outcrops which have been interpreted on the geological maps as Olia Gneiss, but re-interpreted in this work as Musgrave-Mann Metamorphics (see Chapter 4). Strongly magnetic basement complex is also located in zone **SMu1** in northern *Cockburn* which continues across southern *Petermann* and into *Duffield*. Mapped outcrop within **SMu1** is restricted to photointerpreted Olia Gneiss. The zone runs along the Domain boundary on the eastern side of the study area.

Modeled susceptibilities of individual horizons within **SMu2** are in the range 0.015–0.245 S.I. and part of the zone can be modeled as a vertical sided block of higher magnetic susceptibility within a lower susceptibility background (see Figure 6.3).

The magnetic data and limited outcrop in **SMu2** suggest a basement core structure of mafic granulite rocks, which have a higher concentration of magnetite than surrounding lithologies, as the source. The zone possibly defines a regional structural high in the form of a dome in which extensive early folding and faulting have taken place. Much of the subsequent structure defined by the magnetic data (**SMu1, SG1, SMo3**) appears to wrap around this prominent basement unit, suggesting that it is a central structural feature.

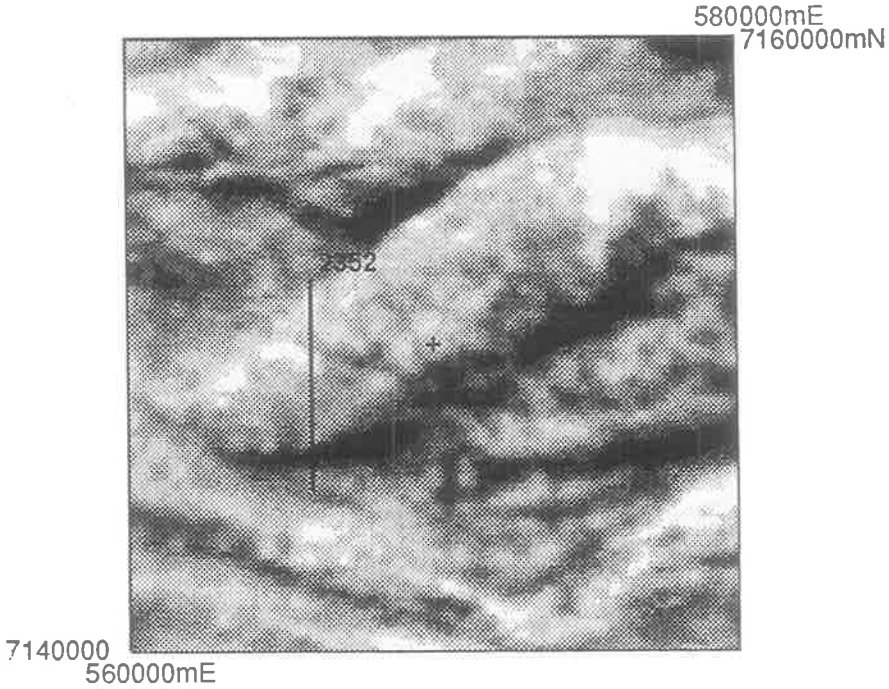

1:250 000

Body	Depth (m)	Strike	Suscep.(S.I.)	Dip	Depth Extent	Width
1	50	70	0.023	90	1000	4700

Body Specifications, Duffield 2352

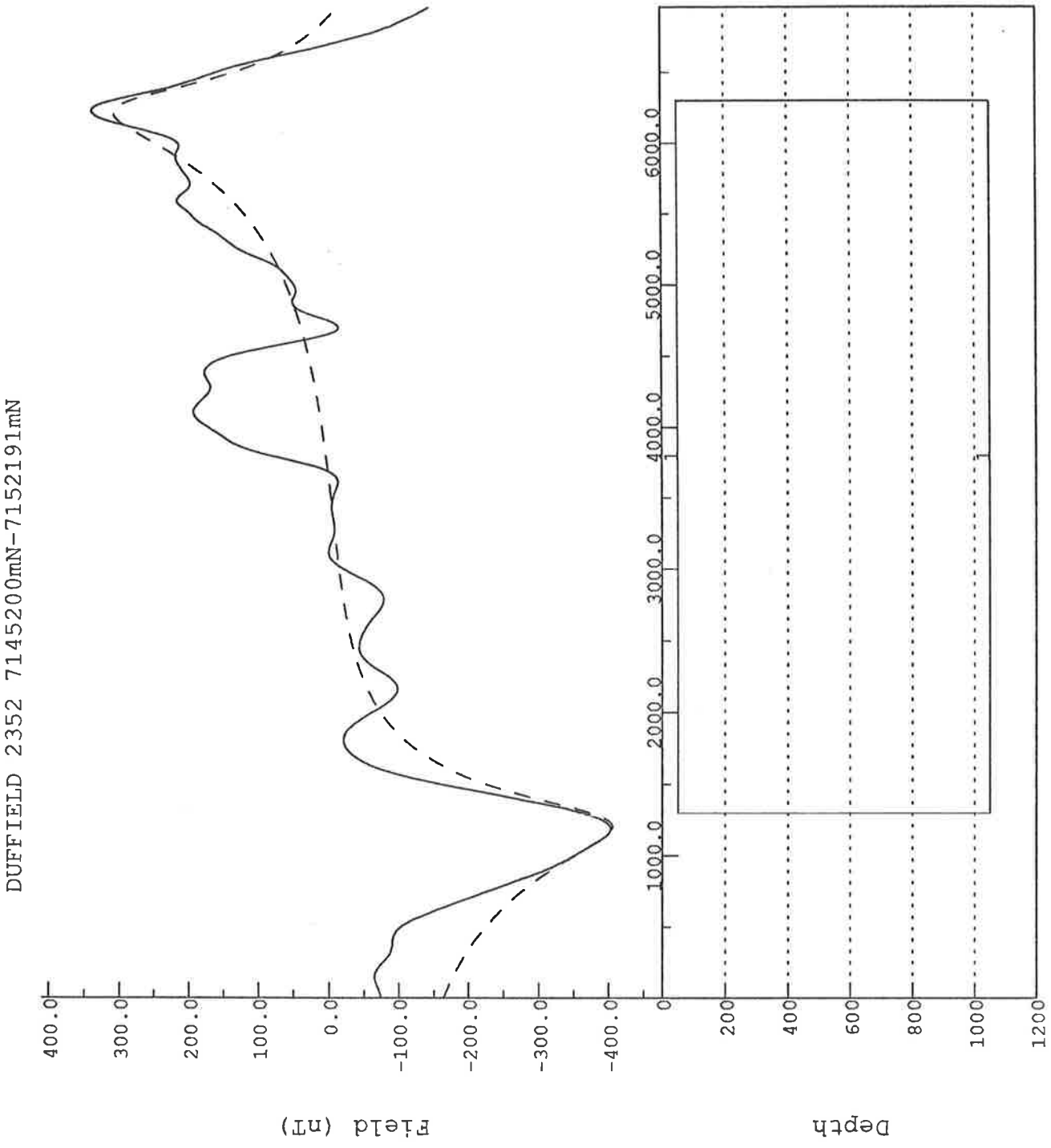

Figure 6.3: Modeled Section Line 2352 Through **SMu2** *Duffield* (dashed line is modeled profile, solid line observed data)

The strongly magnetic basement within **SMu1** is an elongate feature stretching the width of the study area. The southern boundary of the zone in the west of the study area is a prominent magnetic low suggesting that the zone is a normally magnetized block of higher magnetic susceptibility than the surrounding lithologies. Magnetic trends in the zone are generally east–west in the west and swinging around to southeast in the east of the area, parallel to the Domain boundary. There are numerous tightly folded horizons interpreted in the western section of the zone, all of which have an east–west axial trend, and they are considered to be of the same deformation event as the similar folds defined in **SMu2**.

6.4 Moderately Magnetic Basement Complex

Most of the Southern Domain is interpreted as moderately magnetic basement complex, lithomagnetic unit B2 on the interpretation maps, corresponding mainly with mottled textural zones. The moderately magnetic basement complex is considered as predominantly quartzofeldspathic lithologies which are reported to make up to 90% of the granulite terrain in South Australia (Collerson et al. (1972)). Quartzofeldspathic units generally have a low percentage of magnetic minerals and hence are expected to exhibit a lower magnetic activity than the mafic granulites.

SMo2 and **SMo4** make up the magnetic background for much of the Southern Domain. Outcrop within **SMo2** is scarce, but there is considerable Musgrave-Mann Metamorphics outcropping in **SMo4**. In some cases magnetic boundaries transgress outcrops which appear uniform in aerial photographs (southeastern *Cockburn*). The boundary between **SMo3** and **SMo4** in southern *Cockburn* is likely to be a fault related feature for at least part of its length, since it correlates with a very prominent airphoto lineament near Mt. Samuel (southern *Cockburn*). The area in southeastern *Cockburn* is one of the few places in the Southern Domain where a significant amount of outcrop would allow a detailed examination of the lithological expression of some of the interpreted magnetic boundaries.

Another large area of moderately magnetic basement complex occurs in zone **SMo3** in central *Cockburn*. This prominent zone in the Southern Domain crosses the western edge of the study area into Western Australia. Again, there is only very limited outcrop within the zone. Some rapakivi granites and granite gneisses outcropping in *SCOTT* in W.A. are likely to be within the western continuation of the zone. **SMo3** has a higher magnetic amplitude than the surrounding areas and magnetic trends are dominantly east–west. The zone thins rapidly to the east and is only several kilometres wide in *Duffield*, where it is truncated against **SG1**.

The geological significance of the zone is problematical and the limited outcrop which lies within the zone requires a more detailed examination than is presently available to enable a valid interpretation. Despite this inconclusive evidence the magnetic data still furnishes useful information on the large area, which is reasonably magnetically homogeneous and displays sharp boundaries around much of its border. A minor amount of extra geological information which could perhaps be gathered with limited access to the area would be of great assistance in the

interpretation.

A further area of moderately magnetic basement complex in **SMo1** is located in northern *Cockburn* and continues into southern *Pottoyu* along the Domain boundary. The zone has limited outcrop, with only some isolated photointerpreted Olia Gneiss. The magnetic activity in the southern section of the zone is low but increases to the north towards the Domain boundary where there are a number of well defined magnetic horizons which exhibit variable modeled dip directions. Some of these horizons are truncated against the eastern contact of the interpreted **NG2** granite. Deformation, in the form of faulting and folding, is clearly seen in the northeast corner of the zone, associated with the Woodroffe Thrust which defines the Domain boundary.

The southern boundary of the zone is a sharp contact but does not exhibit any strong magnetic anomalies; it is possibly related to a bounding fault or unconformity against the more magnetically active mafic unit in **SMu1**.

6.5 Weakly Magnetic Basement Complex

There are two areas which exhibit an uncharacteristic subdued magnetic response in the Southern Domain, zone **SG1** in southern *Duffield* and **SG2** in southern *Cockburn*.

SG1 is a granular zone containing only limited areas of mapped outcrop of granite and high grade metamorphics. In the lack of other evidence there are several potential explanations for its existence. One of these is that the area is covered by a shallow, possibly Cainozoic, basin with a generally thicker sequence of cover material than elsewhere in the Southern Domain. This would result in a subdued magnetic response over the otherwise strongly or moderately magnetic basement complex beneath the cover.

Another possibility is that the zone represents a re-entrant of the Woodroffe Thrust. It has been well established that the amphibolite facies gneiss and granite which are found beneath the Woodroffe Thrust in the Northern Domain are considerably lower in magnetic activity than the overlying granulite gneisses of the Southern Domain. It is possible that zone **SG1** is a window through the uppermost plate of the Thrust and the margins of the zone are the trace of the Woodroffe Thrust. A similar large scale re-entrant of the Thrust has been mapped on geological evidence to the east of the study area on *PETERMANN RANGES* and can be clearly seen in recently flown aeromagnetics over that area as a complex zone of decreased magnetic activity. The magnetic data on the sheets directly east of *Duffield* (primarily on *Butler Dome*) is very complex but several isolated zones of increased activity could be interpreted as klippen of the Woodroffe Thrust, one of which involves Dean Quartzite. If the latest movement on the Thrust is 540 my (Maboko et al., 1987) then it would be possible for the Dean Quartzite to be involved in the thrusting, since the quartzite is of upper Proterozoic age. If this is the case then some of the small granite outcrops mapped in **SG1** may be similar in composition to the Pottoyu Granite Complex.

A third interpretation of the zone, based on the B.M.R. Mann-Woodroffe aeromagnetic data,

has been made by Shelley and Downie (1971) who suggest that a large area of weakly magnetic granite may correlate with the subdued magnetic response of the zone.

The other weakly magnetic area is a granular textural zone, **SG2**, in southern *Cockburn*. **SG2** is interpreted to be a combination of an increasing thickness of cover and the Claude Hills member of the Giles Complex intrusions. The minor ultrabasic outcrops within the zone have been associated with the Claude Hills member of the Giles Complex by Forman (1972). Previous geophysical work over other members of the Giles Complex in S.A. has shown that most of the intrusions are characterized by a negative magnetic anomaly with a positive near the southern boundary, indicating strong reverse remanent magnetization (Smith, 1979; Shelley and Downie, 1971). **SG2** is a prominent negative magnetic anomaly but the southern boundary of the zone is not within the study area.

The size of the magnetic zone suggests that the Claude Hills Intrusion is considerably larger than the outcrop suggests. A detailed gravity survey over the area may be useful in better defining the extent and shape of the intrusive body, since other Giles Complex bodies have a significant positive density contrast (Smith, 1979).

6.6 Circular/Elliptical Features

Scattered throughout the Southern Domain are a number of circular and elliptical magnetic features which have been numbered on the interpretation maps for identification as C1–C12. They vary in both size and magnetic characteristics and can be divided into four main groups on the basis of their magnetic response. Most of the anomalies can be classified into one of these groups:

1. Magnetic Highs,
2. Magnetic Lows,
3. Normally Magnetically Polarized (highs in north, lows in south),
4. Reversely Magnetically Polarized (lows in north, highs in south).

C1 and C12 on *Cockburn* fall into the first class (magnetic highs) as does C5 in northern *Duffield*. C5 appears to have similar magnetic characteristics to the neighbouring strongly magnetic basement zone **SMu2**, and is likely to be an isolated section of the strongly magnetic basement complex within **SMu2**. Magnetic lows are represented by a very prominent low in southeastern *Cockburn* C9, and a more subdued feature, C7, in central *Cockburn*. An example of a normally polarized feature can be found in northwestern *Duffield*, C4 and in southwestern *Cockburn* C6 shows evidence of reverse magnetic polarization.

Several of the features are only subtle changes in magnetic character from their surrounding background and cannot be definitely placed in one of the above four classifications.

Without any geological control it is difficult to further categorize these anomalies. Several of the magnetic features correspond to isolated mapped outcrop, most of which is photointerpreted Olia Gneiss giving little help in the problem. The only feature wholly in good outcrop is the C9 low in southeastern *Cockburn* over mapped Musgrave-Mann Metamorphics. Examination of air photographs of the region revealed no apparent lithological variations in the area. The anomaly is also clearly visible in the earlier B.M.R. Mann-Woodroffe aeromagnetic survey which has a much broader flight line spacing than the Petermann survey. A distinct radiometric high is associated with C9 and is visible in the total count, potassium and thorium channels, which suggests that the anomaly has near surface expression and may be a pluton of acidic composition. Further ground follow up is required to confirm this interpretation.

The circular and elliptical anomalies throughout the Southern Domain are interpreted as igneous intrusions of unspecified composition, although C11 in southern *Duffield* is interpreted as a weakly magnetic granite on the basis of its subdued magnetic response. The features are distributed throughout the Domain, some within magnetic zones and some on the boundary between zones. Differences in the gross magnetic polarization of the individual bodies indicate that they have undergone different magnetic histories, related to differences in composition and their time of emplacement.

6.7 Folding within the Southern Domain

Several generations of folding have been recognized in the granulite gneisses of the Musgrave Block in South Australia. Goode (1970) identified three phases of folding in the gneisses surrounding the Kalka and Ewarara Giles Complex intrusions. The oldest has a northeast to north-northwest axial trend. This was followed by a second open to fairly tight folding event with an east–west trend. A third phase was recognised but structures were too poorly defined to characterize the style of folding. Moore (1970) recognized two folding events in the granulites around the Gosse Pile intrusion, both having east–west axial trends.

Folding interpreted from the aeromagnetic data from the Southern Domain is common, particularly in the areas of strongly magnetized basement complex. In **SMu2** open to tight east–west folding is evident at several localities. It is difficult to discern whether these folds represent two separate generations of folding, one tight folding and one with a more open style, or a single event with a variable fold style. Open northeasterly folds are also evident in the south of **SMu2**. Two generations of faulting are present in **SMu2** one trending northwest and another trending northeast. Some of the fold structures have been displaced by the later faulting. East–west folds have been delineated in **SMu1** and one particularly well defined folded horizon in central *Cockburn* has been recognized as an easterly plunging synform. It is considered that these structures were produced by the same deformation event as those folds recognised in **SMu2**.

There has been deformation of horizons associated with the circular/elliptical anomaly C3

within **SMu1** on northeastern *Cockburn*, suggesting that either the igneous body intruded and deformed the pre-existing magnetic horizons or rotation of the intrusion after emplacement caused deformation of the neighbouring magnetic horizons. A similar folded horizon is evident near the western edge of C1 on *Pottoyu/Cockburn.*

Folding is less common in the moderately magnetic basement complex. In **SMo4** in the vicinity of the boundary between *Duffield* and *Cockburn* two sets of folds are recognized one with an east–west axial trend and another trending north–south to northwest–southeast. One example of fold interference suggests that the east–west trending fold set has been refolded by the later north–south trending set. Well defined tight east–west folding is evident in northern **SMo3**. Southeasterly trending folds are interpreted in the vicinity of the Domain boundary in **SMo1** on southern *Petermann.*

It should be noted that since the survey flight lines run meridionally there is a bias towards magnetic features with a latitudinal trend in the geophysical data, and only rarely are north–south trending structures well defined.

6.8 Faulting within the Southern Domain

Faults are prominent in the Southern Domain. The largest is marked by zone **SBL** in southeastern *Cockburn.* This zone has a distinctive broad linear magnetic high at its centre and a surrounding area of increased magnetic activity. The whole zone is interpreted as the magnetic expression of the Mann Shear Zone.

The Mann Shear Zone has been mapped in South Australia as a steep southerly dipping mylonite zone and is associated with a distinctive linear magnetic anomaly (Smith, 1979) of 100–1000 nT (Shelley and Downie, 1971). The central anomaly in **SBL** adjoins the anomaly associated with the Mann Fault in South Australia, and is a positive magnetic feature of 400-900 nT. The section of the anomaly in the Northern Territory has been previously attributed to the magnetic expression of the Mann Fault by Smith (1979) on the basis of the Mann-Woodroffe aeromagnetic survey.

The central anomaly is interpreted to be the magnetic expression of the mylonite zone of the fault and has been modeled as dipping southerly at between 30–60 degrees, which is consistent with geological observations (Thomson, 1966). Lateral displacement of the order of one kilometre on the central mylonite zone are interpreted to be caused by three northeasterly strike-slip faults. A major dislocation of the central anomaly of the fault is evident in south central *Cockburn.* A left-lateral northeasterly cross cutting shear zone with about 5 kilometres of displacement and approximately 4 kilometres wide is interpreted as the cause of the offset. This later shearing event has the same trend as a similar feature mapped further south on *MANN.* It does not appear to have displaced the neighbouring zone boundaries, suggesting that both the Mann Shear Zone and the cross cutting shear are older than the development of the adjacent magnetic zones.

Interpreted faults within zone **SMo3** dominantly trend northwesterly, which is in contrast to the majority of faults interpreted further east on *Duffield*, which are mainly north to northeasterly, and probably indicates different periods of deformation affecting the strongly magnetic and moderately magnetic basement complexes. Cross cutting faults in unit B1 in northern **SMu2** imply that the northwesterly set are younger relative to the northeasterly trending set. The Domain boundary has been displaced at several locations on *Petermann* and *Duffield* by strike-slip faults of variable trend, obviously developed after the movement on the Woodroffe Thrust.

Several long northwesterly trending magnetic lineations cut across the Southern Domain and are quite clearly discernable in the directionally filtered magnetic images. Magnetic lineaments have not been marked on the interpretation maps since large numbers of such linear features can be interpreted and tend to result in an interpretation map which is difficult to use effectively. The northwesterly trending features are worthy of note for their exceptional length (60 kilometres). They may be the magnetic response of a northwest trending dyke swarm, similar trending dykes have been noted further south (Thomson and Major, 1968).

The structural evidence revealed from the aeromagnetic interpretation indicates that lithomagnetic units B1 and B2 have different deformational histories possibly related to differences in age and original crustal depth. The units have probably been juxtaposed into their present positions by extensive faulting and deformation during uplift of the Musgrave Block.

Chapter 7

Conclusions and Discussion

7.1 Introduction

The collection and interpretation of airborne magnetic and radiometric data over the Petermann Ranges area, which is characterized by lack of outcrop and access difficulties, is the first stage in a project to improve the geological understanding of the region. Additional processing and detailed interpretation of the geophysical data has led to a better understanding of the geology and structure in and around the study area, both in locations where the geology is known from outcrop and where no outcrop is available. The geophysical data have been used to subdivide the area into a number of magnetic textural zones and two larger magnetic domains, a Northern and a Southern Domain, which reflect broad scale geological structure.

This chapter presents an overview of the significant results which have come out of the interpretation of the geophysical data, in the form of a brief geological history of the area, developed from the geological literature and expanded using the information revealed from the interpretation.

7.2 Interpreted Geological History

The oldest rocks in the study area are the amphibolite facies gneisses, dated between 1525–1575 my by Maboko et al. (1987) and the granulite facies Musgrave-Mann Metamorphics. Most workers concur (Goode, 1970; Moore, 1970; Thomson, 1975) that these lithologies were laid down as a sedimentary sequence, with the metamorphic layering now visible in the rocks being related to the original sedimentary layering. The high grade metamorphics have undergone a complex multiphase deformation history. Goode (op. cit.) notes three phases of folding in the granulite around the Kalka and Ewarara members of the Giles Complex, Moore (1970) reports two phases of folding in the high grade rocks surrounding the Gosse Pile intrusion. Forman and Shaw (1973) note that there is evidence for at least two periods of metamorphism within the granulites of the southwest of the study area.

The geophysical data analysed in this study has defined a series of previously unrecognized

important structural and lithological boundaries which indicate a complex deformation history of the high grade basement rocks in the study area.

The granulite facies gneisses of the Southern Magnetic Domain, which have been previously mapped as a single unit, have been subdivided into two lithomagnetic units, a strongly magnetic mafic granulite and a moderately magnetic quartzofeldspathic granulite unit. The strongly magnetic basement complex in **SMu1** and **SMu2** is interpreted as a basement core in the Southern Magnetic Domain. The areas exhibit two and possibly three generations of folding delineated from the aeromagnetic data. A number of east–west trending folds with a style that varies from open to tight may represent two separate fold generations, a further event is represented by open northeasterly trending folds. The former set of folds have been displaced by a later series of faulting.

The moderately magnetic quartzofeldspathic granulites in the Southern Domain exhibit a different deformation history, with both east–west and north–south trending folding events. The quartzofeldspathic units possibly represent a younger cover sequence to the strongly magnetic basement complex, but they are unrelated to the lithologies of the Northern Magnetic Domain. The two different lithomagnetic units have been juxtaposed into their present positions by extensive uplift of the Musgrave Block and associated deformation and faulting along the magnetic zone boundaries.

Several of the circular/elliptical magnetic features in the Southern Domain are closely associated with magnetic zone boundaries (C2, C3, C4, C12) and are interpreted as igneous bodies which have intruded along crustal weaknesses developed by faulting along those boundaries.

Much of the amphibolite facies gneisses in the Northern Magnetic Domain are interpreted as original gneissic basement. The results of an early folding event in the gneiss are evident in zone **NMo4** where a thin well defined magnetic horizon is folded into a number of northwesterly trending folds.

The emplacement of the Giles Complex intrusions preceeded the major faulting which has been mapped south of the study area (Mann, Hinckley faults), (Goode, 1970). The Giles Complex is represented in the study area by a zone of subdued magnetic character associated with the Claude Hills intrusion in the Southern Magnetic Domain. One of the large scale faults, the Mann Fault Zone, is characterized in the area by a 400–900 nT magnetic high which adjoins a similar magnetic anomaly in South Australia. This central magnetic high is believed to be associated with the mylonite zone of the fault and modeled dips indicate that it is a steep southerly dipping feature. The other major fault in the area, the Woodroffe Thrust, may also have been initially active at this early stage.

Intrusion of much of the Pottoyu Granite Complex and other Kulgeran Granites within the Musgrave Block around 1100 my was possibly accompanied by the intrusion of some of the circular/elliptical magnetic features noted in the Southern Domain. This period of intrusion is interpreted as being followed by large scale basement shearing affecting the Olia Gneiss and Granites.

The area of linear magnetic texture in the Northern Domain which has been interpreted here as a basement shear zone is approximately 20 kilometres wide along most of its 100 kilometre length and trends east–west across the width of the study area. The shearing has overprinted the previously formed structures within the Olia Gneiss to form thin elongate magnetic horizons within the original basement Olia Gneiss and much of the Pottoyu Granite Complex. Individual southeasterly trending shear planes are discernable in the magnetic data, together with tight folding with a similar axial trend. Cross cutting short northeasterly faults are also interpreted in the zone. The shear zone may have been caused by a left-lateral strike-slip fault at depth, active before the main period of movement on the Woodroffe Thrust, although this interpretation lacks firm evidence.

Following the shearing event a further period of granitic emplacement prevailed. A large section of the Pottoyu Granite Complex in *Hull* and *Pottoyu* was emplaced, and the interpreted granitoid body on southwestern Pottoyu was probably intruded at the same time through the previously formed shear zone. The latter granitic body shows evidence for large scale fragments of the sheared material as xenoliths or roof pendants. Southeasterly trending dykes were emplaced in both these granites somewhat later. Another set of east–west dykes was emplaced along the eastern edge of the study area within the zone of shearing and one shows magnetic evidence for dipping to the south.

Following this period of igneous activity the volcanics of the younger basement were extruded in the north and to the west of the study area and this event was unconformably followed by a marine incursion and the deposition of the Dean Quartzite in a stable shelf environment (Forman, 1972) followed by the deposition of the evaporitic Pinyinna Beds, Inindia Beds and Winnall Beds.

The end of the Precambrian saw the development of the regional recumbent folding during the compressional Petermann Ranges Orogeny in the Northern Magnetic Domain and along much of the margin of the Amadeus Basin. This was probably accompanied by further uplift of the Musgrave Block and mobilization along the Woodroffe Thrust. Granitic bosses and plugs intruded the folded metasediments in the Northern Magnetic Domain, perhaps the result of localized melting and metamorphism of the younger basement lithologies. Mapped Olia Gneiss within the area of the fold nappe is also interpreted as the result of metamorphism and granitization of the younger basement, as suggested by Forman and Hancock (1964), and is differentiated from the basement Olia Gneiss which occurs further south. Regional scale open folding in **NMo2** also probably developed at this time. North–south trending strike-slip faults are considered to have developed after the regional folding in the sediments and younger basement, since they clearly cut across magnetic zones and the regional scale folding along the edge of the basin. Smaller scale faulting across magnetic zones and the Domain boundary also developed after the main structural events of the Petermann Ranges Orogeny and movement on the Woodroffe Thrust. Faulting within magnetic zones may have developed during the main deformation event.

Further uplift and erosion deposited the Mt. Currie Conglomerate towards the basin off the newly formed Petermann Ranges (Forman, 1972). Marine sedimentation took place in the Ordovician when thin outliers of the marine Stairway Sandstone developed in the study area (Cook, 1972).

The final significant geological event to be recorded in the magnetic data was the deposition of sediments of glacial origin (Daniels, 1974) in a shallow Permian basin on the northern edge of the granitoid body in western *Pottoyu* and stretching into Western Australia. Within the study area limited depth estimates in the basin indicate that it is of the order of 35 m deep, the deepest section being towards the east of the smooth magnetic zone **NS5**.

7.3 Conclusions

This study has shown that airborne magnetic and radiometric data are an essential tool for geological mapping in an area where ground based geological control is scarce and difficult to collect. Extensive processing and display of the data in various forms as digital greyscale images has proved invaluable as an interpretational aid, both to highlight broad scale structure and more detailed local features. The study has produced an improved understanding of the geology of the area, particularly in the central and southern sections where only limited geological information was available.

The geophysical data has been shown to fit the regional recumbent folding hypothesis proposed by Forman (Forman and Hancock, 1964) and has highlighted numerous other significant structural features in the Northern Domain, many previously unrecognized in the study area. Correlation between the aeromagnetic interpretation and the regional gravity field is also good.

A number of subdivisions have been made in the high grade basement of the Southern Magnetic Domain, including several circular and elliptical igneous intrusive bodies. The full geological significance of some of these divisions remains unclear and requires more detailed ground based work to gain a better understanding. Extensive faulting and folding have been delineated in both Magnetic Domains, and the location of both the Mann Fault Zone and the Woodroffe Thrust are well defined from the magnetic data.

The closer spaced flight lines (500 metres) of the Petermann survey data used in this interpretation have been a great advantage in defining important magnetic features which are not visible in the more broadly spaced (3200 metres) aeromagnetic data flown over the same area in the 1960's by the B.M.R.

The study area is a small section of the vast expanse of Precambrian and younger terrain in central Australia which has only been geologically mapped on a regional scale. This study has provided a further stepping stone in the slow process of compilation, interpretation and integration of geological and geophysical data which is necessary to gain a better understanding of a complex area.

Appendix A

Image Production and Processing

A.1 Introduction

The display of the geophysical data as digital images has been used extensively in the interpretation throughout this project. The system used displays the data on an Apple LaserWriter using the postscript graphics language and was developed in the Department of Geology and Geophysics by S. Rajagopalan. This appendix details the steps required to produce an image and the standard specifications used in the production of the images in this thesis. It also covers the processing techniques which have been applied to the geophysical data and found useful in the geological interpretation.

A.2 Mechanics of Producing an Image

The first step before either computer contouring or imaging of the data is to convert the geophysical data to a regular grid from a series of flight lines with closely spaced data points along the lines (15 to 20 metres) and a much larger distance between flight lines (500 metres). The choice of the grid cell size depends on several factors, including the flight line spacing, the application to which the resultant gridded data is to be used, and the amount of computer time and space available.

The gridding procedure used was developed by Dr. John Paine (Paine, 1987) and uses a method of iteratively calculating a grid of biquadratic spline coefficients. A grid cell size of 100 metres by 100 metres was chosen and all the magnetic and radiometric data were gridded onto this size. The coordinate system used were easting and northing metres from AMG zone 52. The process of gridding means that some of the high frequency data along flight lines is lost, and data is interpolated between flight lines. In general tie lines were not included in the gridded data sets because poor or absent leveling of the tie line data means they tend to show up as linear east–west trending features in the gridded data.

Each 1:100 000 sheet was subdivided into four areas of approximately the same size and with at least 2 kilometres (20 grid cells) of overlap into adjacent areas. These areas were gridded

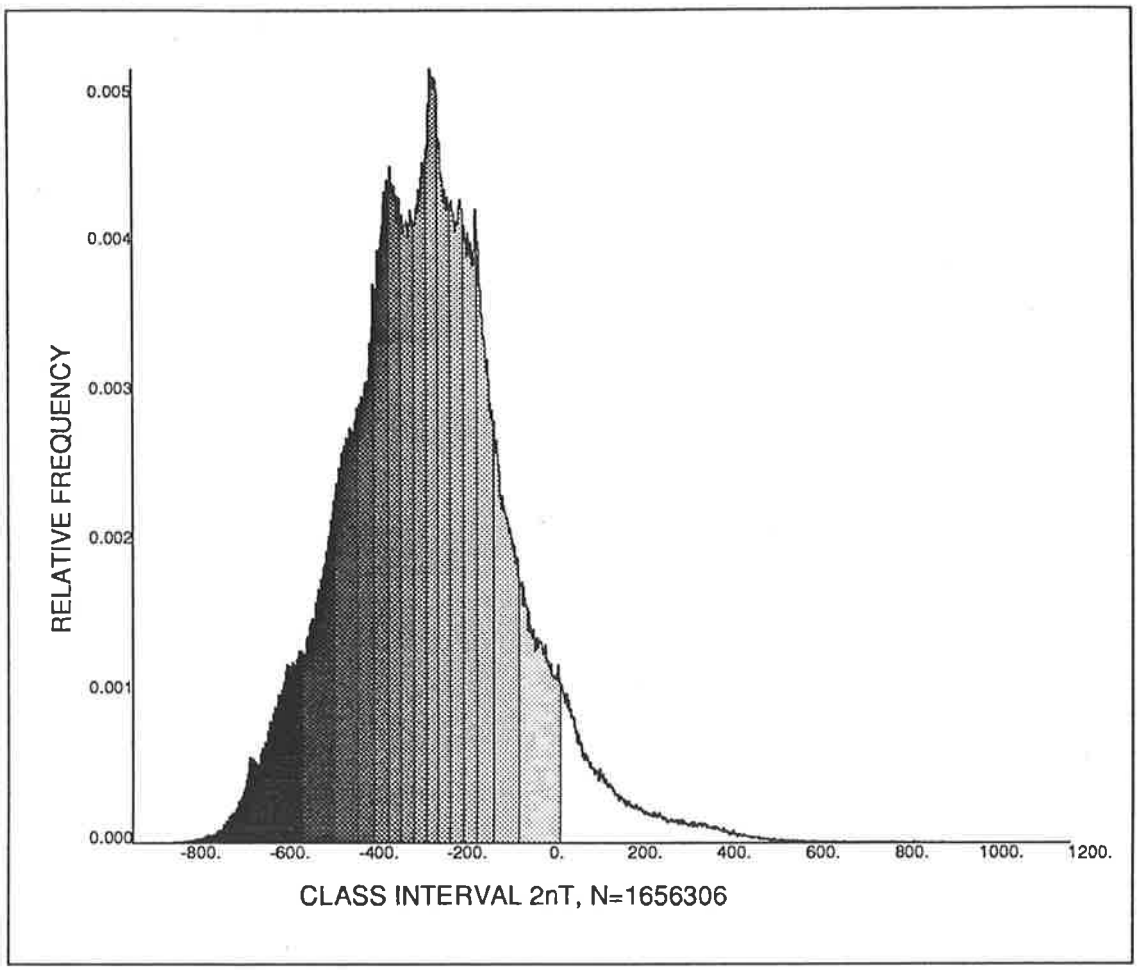

Figure A.1: Grey Level Distribution for Magnetic Data

separately and later reduced to the appropriate size, the overlap ensuring that the data would match at the edges. Thus by joining adjacent subareas the entire area can be reconstructed as a gridded data set suitable for computer contouring or imaging. The division of the sheets into the subareas had to be done because the gridding program has a limit to the size of output grid it can produce.

Once the data has been gridded a digital image or a contour map presentation can be calculated. If an image is to be produced the data must first be suitably stretched. Most output devices have a dynamic range of 256 grey shades, each shade represented by an integer value in that range. This means that the gridded data has to be rescaled or stretched to become integer values between 0 and 255. Obviously there are many ways in which this can be done and most of the standard stretches are well described in the literature (Drury, 1987; Castleman, 1979). The basic tool needed to decide how best to stretch the data is a histogram. The stretching technique used to display data in this thesis is an equal area stretch. The histogram of the data set is divided into N groups, where N is the number of grey levels desired in the image. The groups are chosen so that each has the same number of gridded data points within it, thus each

class contains the same number of pixels. Since a pixel represents a set area on the map (in this case 100 metres by 100 metres) this stretch implies that each greyscale colour has an equal area on the map. Figure A.1 illustrates the grey level distribution on a typical data histogram. The nature of the stretch means that grey levels representing data in the tails of the distributions have a much larger range than the grey levels representing data near the peak of the distribution.

The variable N, the number of grey levels, must also be chosen. Figure A.2 illustrates a small section of the *Pottoyu* sheet total field magnetics image with different numbers of grey levels (2, 4, 8, 16, 32 and 256). The figure illustrates that the difference in image quality between 16, 32 and 256 levels is minimal, but with less than 8 levels the images can be significantly lacking in detail. The number of grey levels used also influences the amount of computer time required to produce the image, so on the basis of image quality and time it was decided that 16 levels is the optimum number. The criterion of image quality is somewhat subjective and depends upon the detail required from the image and personal preference. All images presented in this thesis have been produced using 16 grey levels and an equal area stretch.

The scale of the images is the final variable that needs to be addressed. Digital images have an upper limit of scale beyond which individual pixels become too large and give the image a blocky effect. The upper limit of map scale with pixels of 100 metres was found to be 1:100 000. The images were produced at an original scale of 1:250 000 to avoid this blocky texture and because most other maps of the area (geology, topographic, gravity) are available at this scale. Unlike contour maps, in which small scales necessitate closely spaced contours being dropped and so producing a loss of detail, small scale pixel maps can still display all of the detail represented in a similar map of larger scale.

A.3 Image Processing

There are numerous types of images and processing techniques that can be employed, each enhancing certain aspects of the data which possibly do not show up in other processed version of the data. The images and processing techniques that have been used in this work and their attributes are discussed below.

Globally Stretched Images

Globally stretched images are the most common form of image and all but one pixel map discussed here is of the globally stretched type. Global images are produced by treating all the data as a single set, so the histogram and equal area stretch such as those in Figure A.1 are calculated using the entire data set. This results in a synoptic, uniformed view of the data.

Global images are particularly useful when working on the area as a whole. In comparing structures or magnetic intensities of areas separated by some distance one can be confident that the same grey shade represents the same range of magnetic field strengths. This is useful for

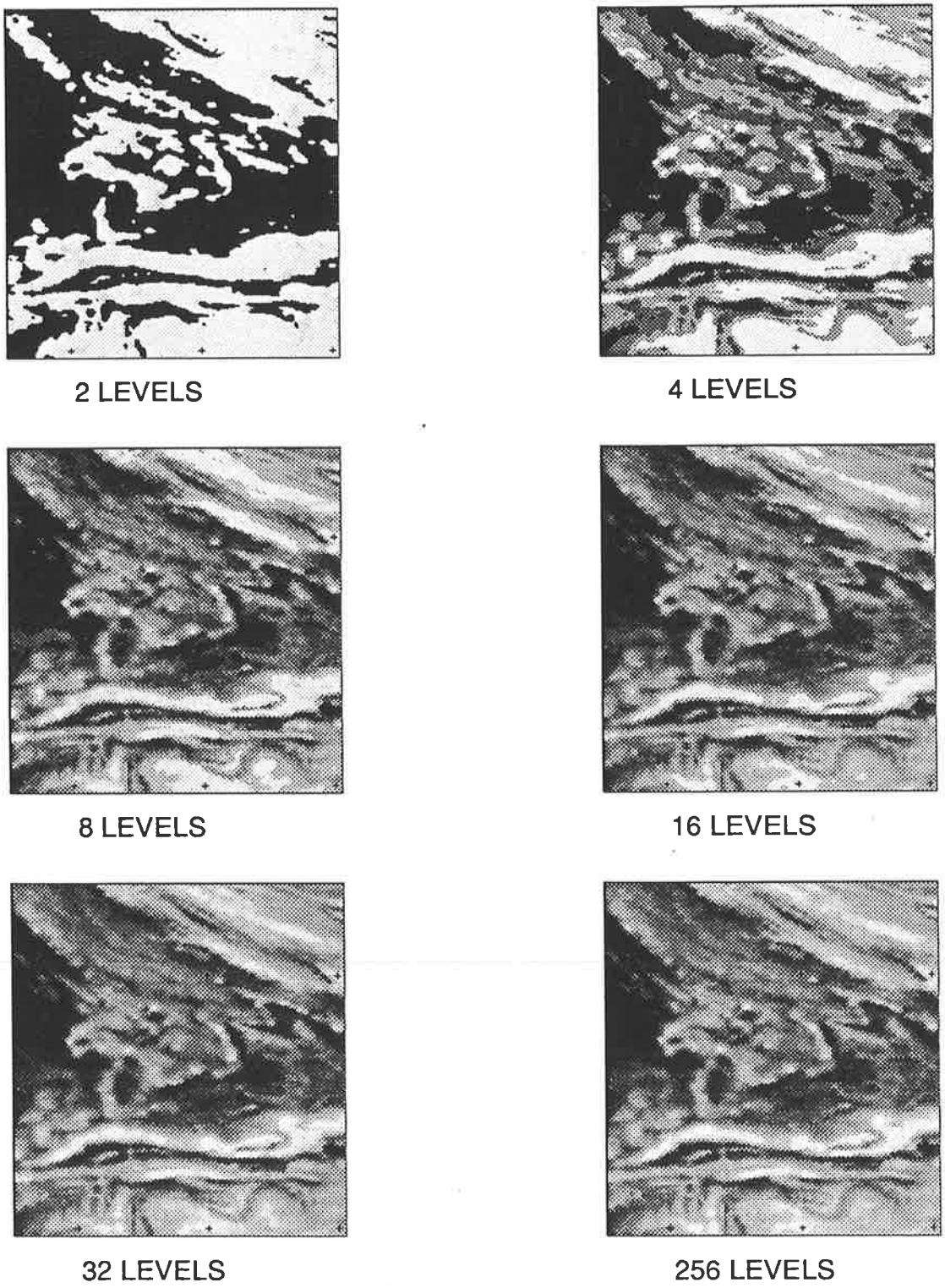

Figure A.2: Comparison of Various Numbers of Grey Levels

delineating zones of similar magnetic character and getting a general overview of the nature and quality of the data.

The major disadvantage of some globally stretched images is that quite large areas can be of the same greytone, appearing to be magnetically flat and showing no finer details. Such areas can be seen on the globally stretched total field magnetics (Figure A.3) in western *Pottoyu*, around 129°00, 25°15 where there is a large area of low magnetic intensity (black) with little detail discernable. This problem can be overcome by local contrast stretching, a simple processing technique discussed below.

Reverse Colour Images

Most examples of greyscaled aeromagnetic images (Kowalik and Glenn, 1987; Drury et al., 1987; Tucker et al., 1987) are produced with the highest levels of the magnetic field mapped as white and the areas of lowest magnetic intensity mapped as black. This convention has been also adopted in this work. The obvious alternative is to map high values as black and low values as white. This sort of negative image was produced using a global stretch and is represented at a scale of 1:1 000 000 in Figure A.4. The image shows the same amount of detail and the resultant good and bad points as discussed in the previous section but the different perspective given to the interpreter by the reversed colour sense is useful for revealing details not immediately obvious in images with the more conventional greytone scheme. The magnetic expression of the Mann Shear Zone, as a linear magnetic high several kilometres wide in the far southwest of the image is one example that is somewhat easier to pick in this style of image.

Locally Stretched Images

The problem of globally stretched images having quite large areas of the same greytone can be overcome by local contrast stretching. Kowalik and Glenn (1987) suggest a transformation of the data using a moving box car window which will accentuate subtle features. It was found that a simpler and more effective method of local contrast stretching could be applied to the data used in this work with very satisfactory results. This technique involves breaking the entire data set down into smaller subareas of manageable size. Each subarea is treated as an individual image by calculating an individual equal area stretch which maps local high values to whites and local low values to black. Figure A.5 shows the results of this process on the total field magnetics. The areas that where noted as lacking in detail in the previous images show up considerably more interesting and significant detail in the locally stretched image.

The process of local contrast stretching gives the overall image a patchwork appearance, with each of the subareas chosen being quite obvious. This means that it is difficult to use the locally stretched image to define zones of similar magnetic characteristics and compare different areas separated by significant distances.

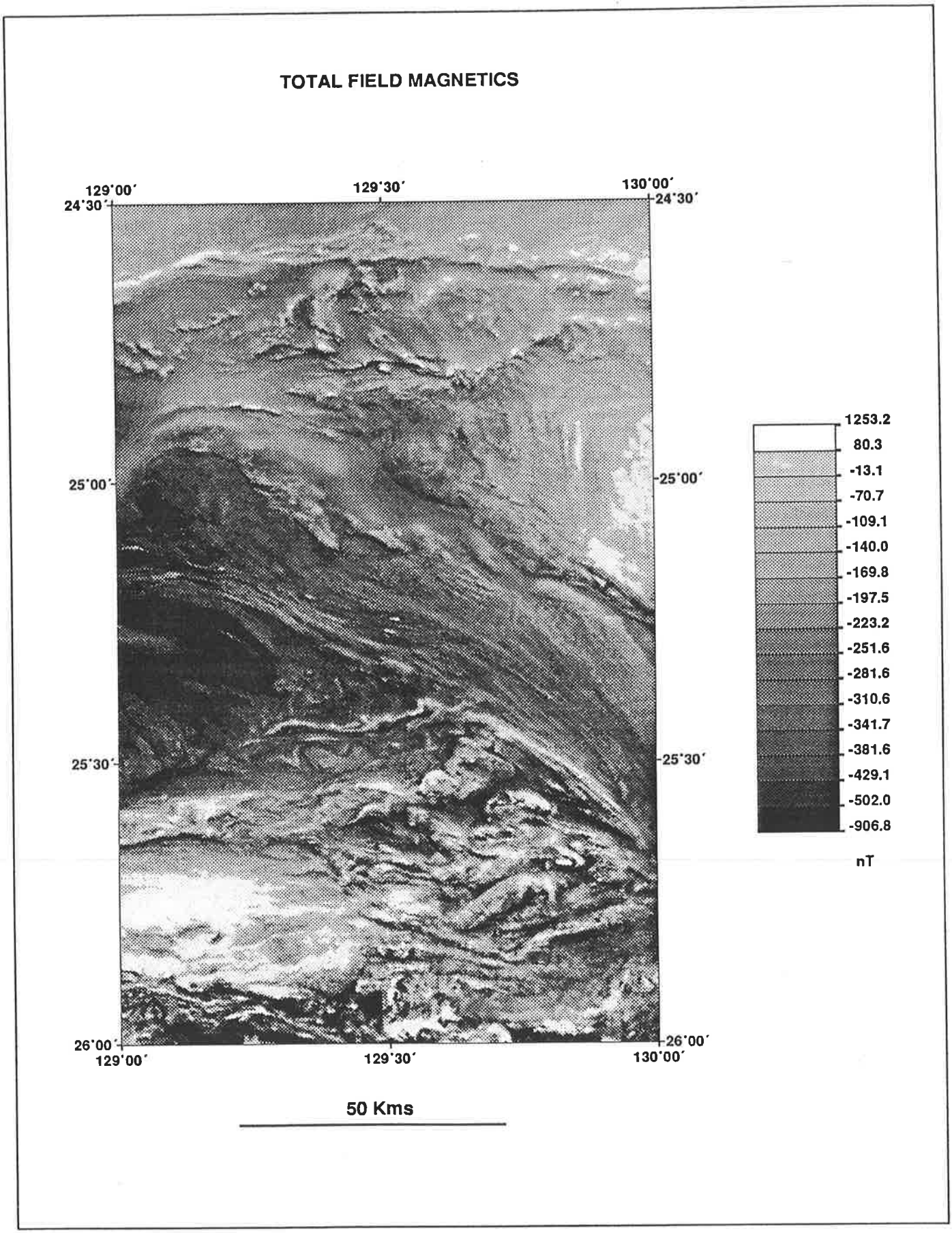

Figure A.3: Total Field Magnetics Greyscale Digital Image

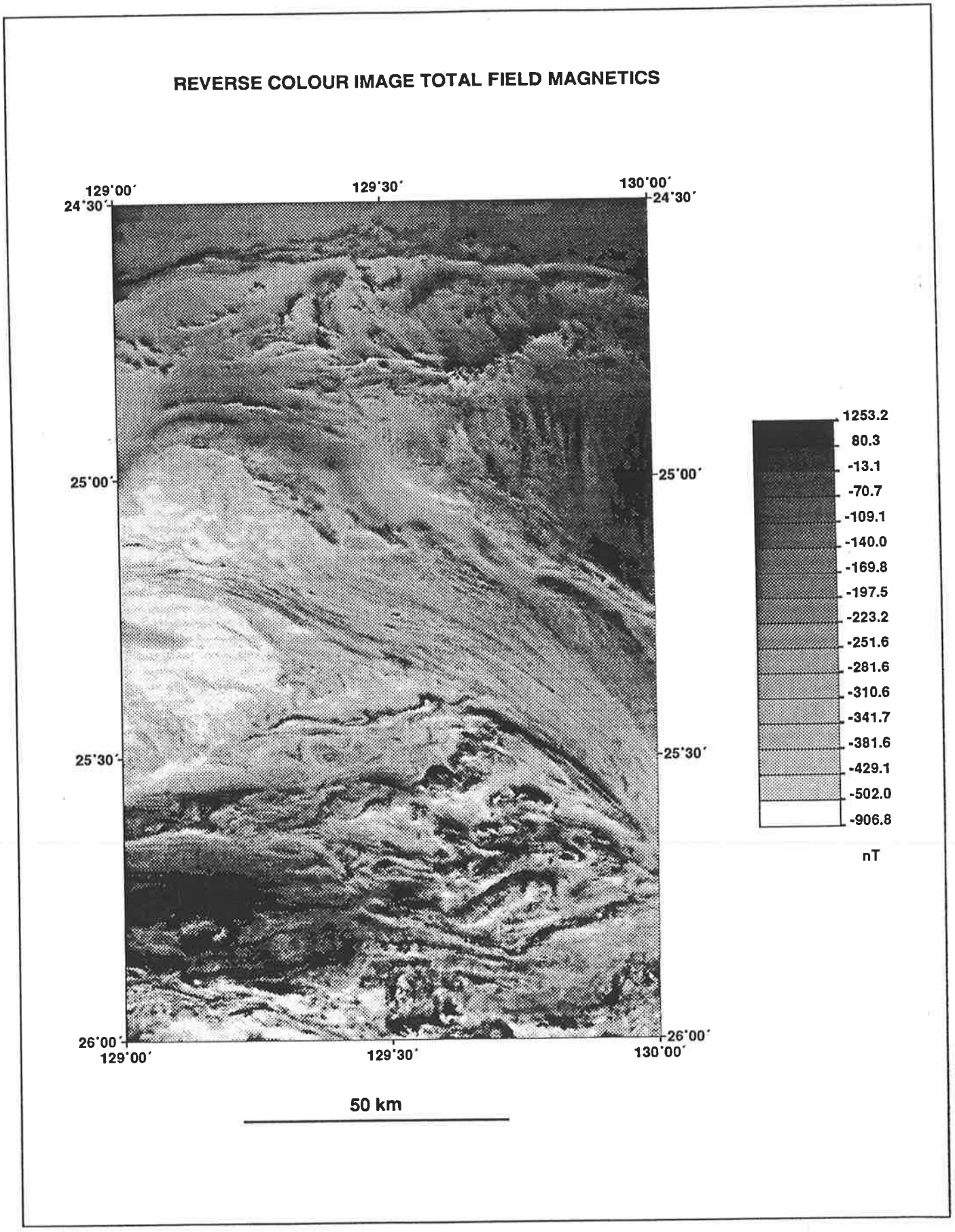

Figure A.4: Reverse Colour Total Field Magnetics

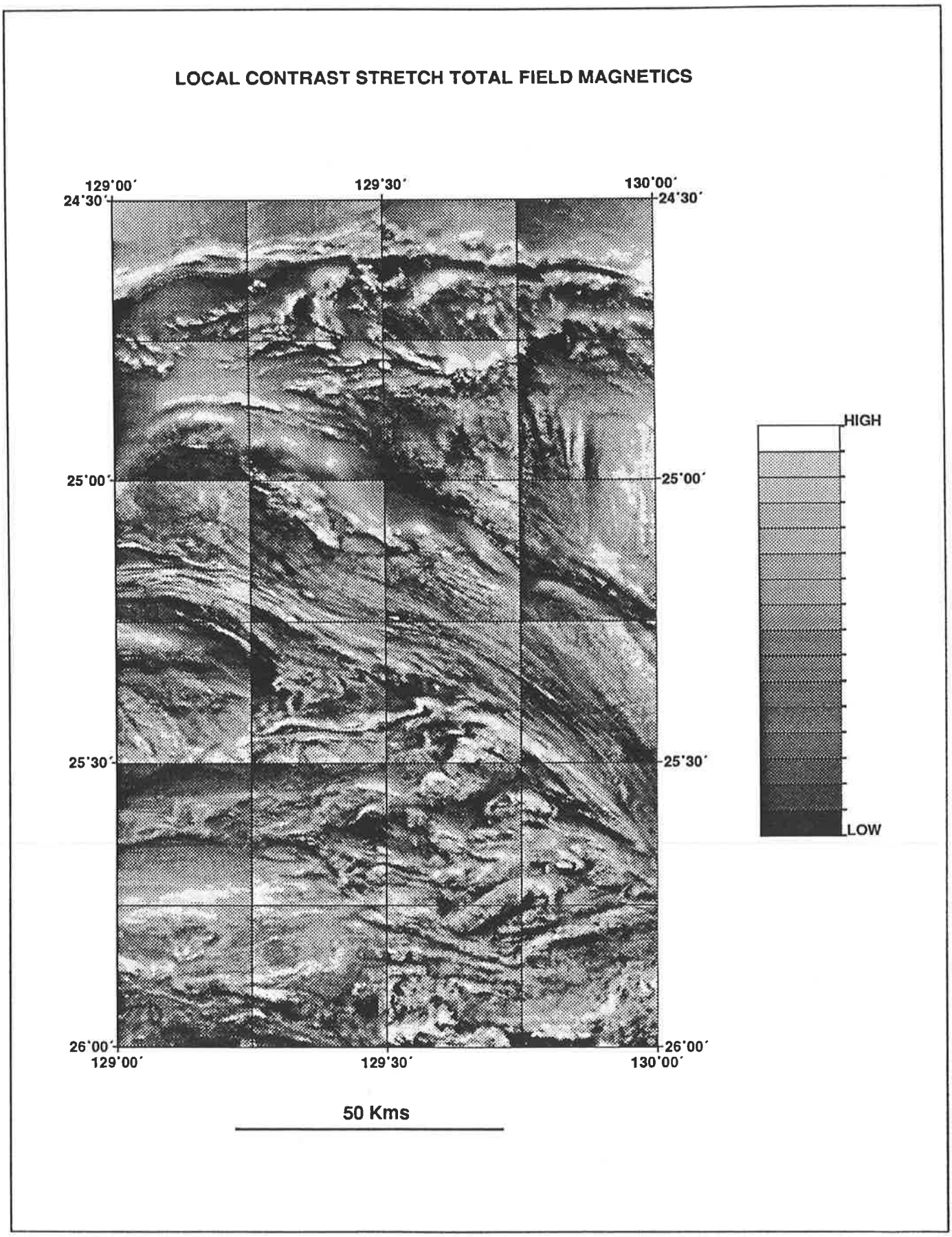

Figure A.5: Locally Stretched Total Magnetic Field

Directional Filtering

Application of digital filtering techniques mean that a whole new series of images can be produced from the original gridded data. One effective filtering method is directional filtering. This is achieved by calculating an approximation to the horizontal gradient of the data in a specified direction using a convolution of two 3 × 3 or larger matrices with the data set. This has the result of enhancing features that trend in the chosen direction and subduing features normal to the chosen direction. The convolution matrices used here were 3 × 3 of the form:

$$\cos\alpha \begin{pmatrix} 1 & 1 & 1 \\ 0 & 0 & 0 \\ -1 & -1 & -1 \end{pmatrix} + \sin\alpha \begin{pmatrix} 1 & 0 & -1 \\ 1 & 0 & -1 \\ 1 & 0 & -1 \end{pmatrix}$$

where α is the azimuth of the direction in which to enhance features (Kowalik and Glenn, 1987). Any direction can be chosen, but the best direction is perpendicular to the flight lines, the main reasons being:

1. The flight line direction is chosen to run perpendicular to the general geological strike of the area, and hence the general trend of magnetic features.
2. Filtering in directions other than perpendicular to the flight lines tends to accentuate ridging along the flight line direction due to poor leveling of the data.

Figure A.6 is an example the total magnetic field filtered perpendicular to the flight lines ($\alpha = 90°$). This type of processing gives the data the illusion of surface texture which is very useful for delineating textural zones. The map also brings out subtle linear features within the data and accentuates the higher frequency components.

Vertical Gradient

Another form of digital filtering is the calculation of the vertical derivative, or vertical gradient of the magnetic data. It is well known that the vertical gradient is very effective in producing higher resolution in potential field data, accentuating anomalies caused by near surface sources.

A 177 point filter operator was applied to the gridded data (McGrath, 1975) using the optimal programming method suggested by Holroyd (1975). The resulting image is shown in Figure A.7. The figure shows that the technique accentuates continuous horizons and more subtle features not visible in the unfiltered images. It also brings out areas of slowly varying smooth magnetic field attributable to nonmagnetic sediments. One feature highlighted by this processing technique is the east–west trending tie lines which were inadvertently included in the gridded data in part of the *Hull* sheet, in the far northwest corner of the map area.

The vertical gradient image, although effective in accentuating higher frequency detail, tends to break down in areas of high magnetic relief, such as the southern section of the study area, where it is difficult to follow individual horizons.

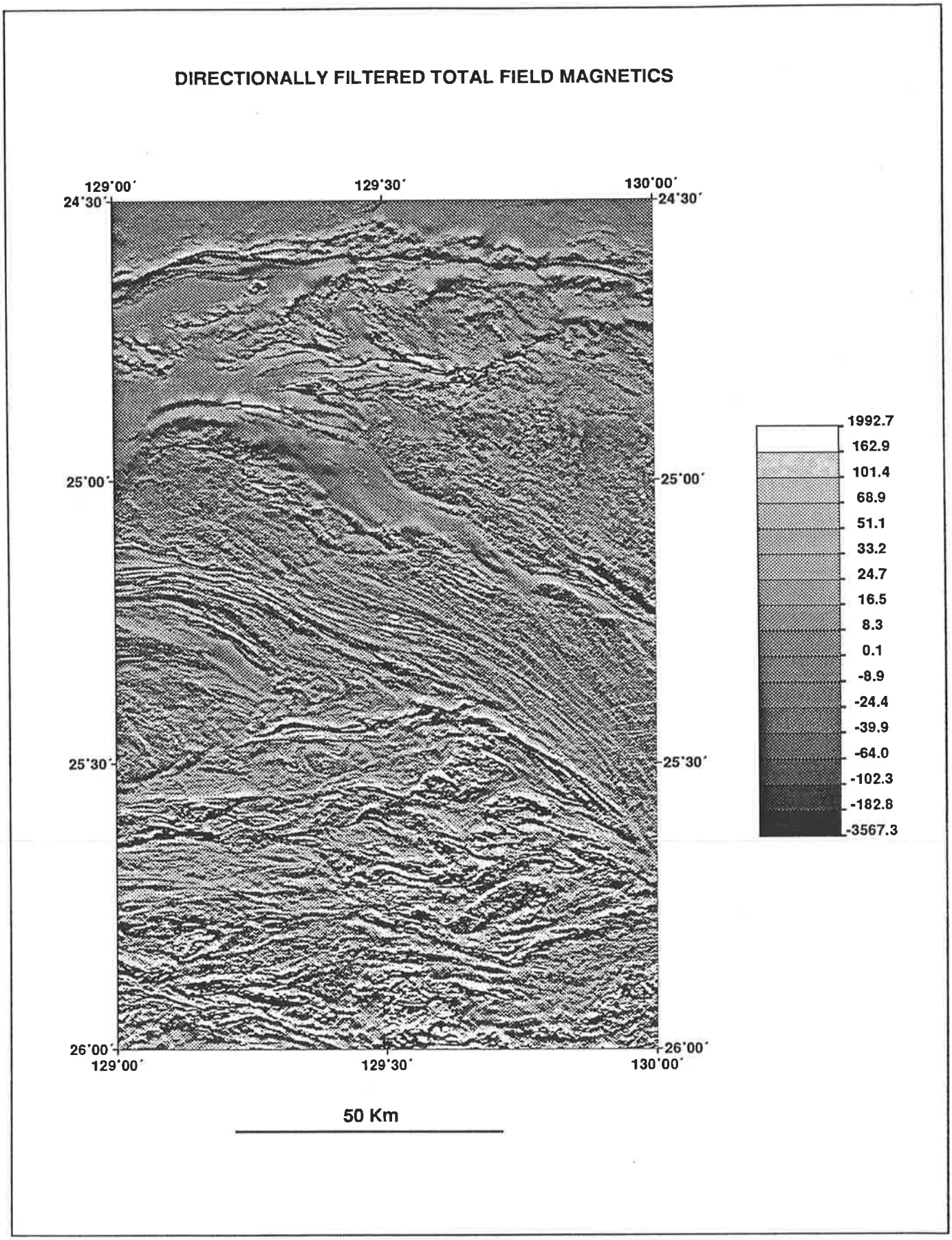

Figure A.6: East–West Directionally Filtered Magnetics

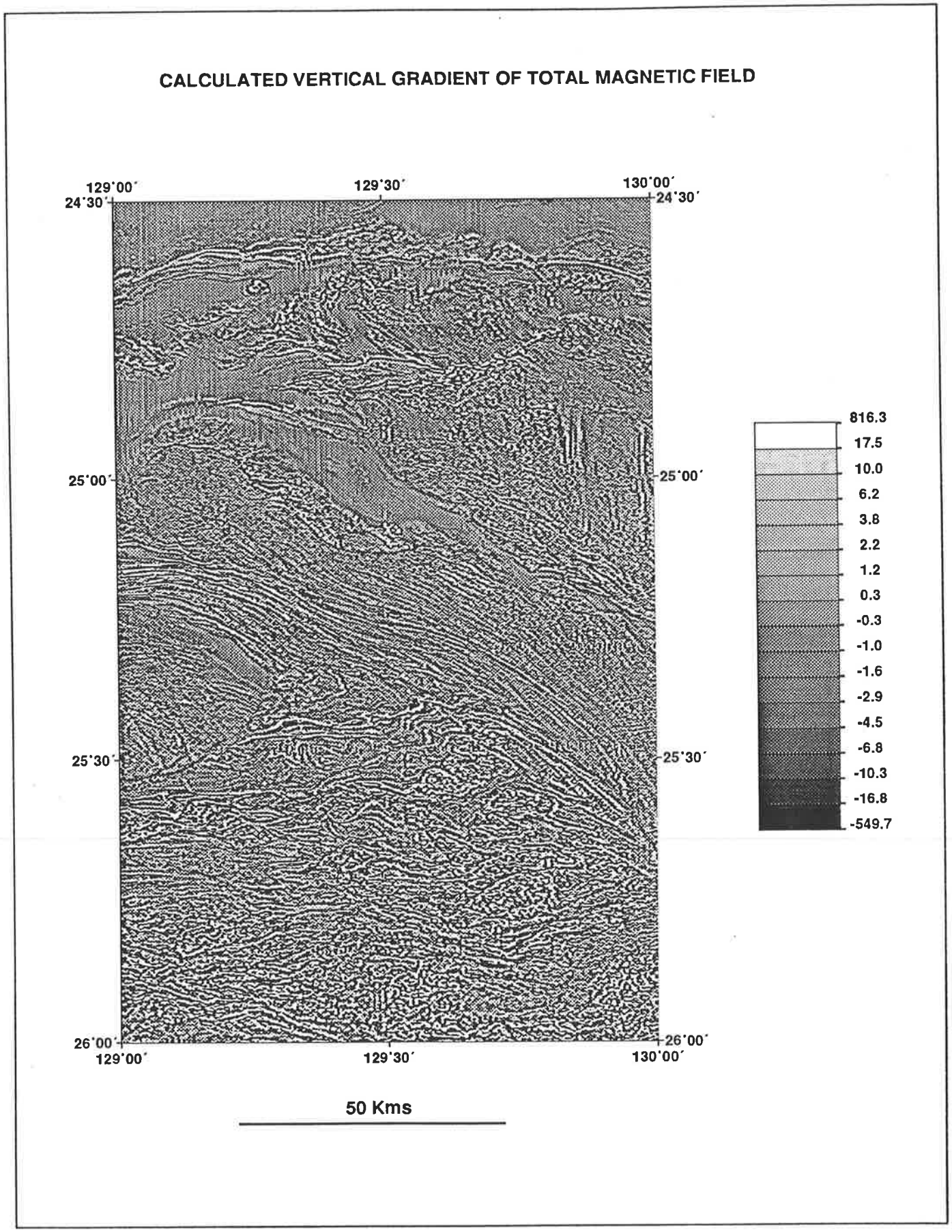

Figure A.7: Calculated Vertical Gradient of the Total Magnetic Field

Radiometrics

All of the above processing techniques have been discussed with reference to the magnetic data, but images of the radiometric data can also be produced, and indeed, are often the best way to display such data. The higher statistical noise in radiometric data sets means that some of the digital filtering techniques cannot be applied with as much success as on the magnetic data.

A.4 Discussion

There are many other processing options available, some of which were investigated in this project but not used extensively. The possible variations are limited only by time. However no one image will optimally present all the desired features of the data set. Each processing technique will highlight a certain aspect or several aspects of the data which will not show up in another type of image. Thus it is important to produce several different versions of the data using processing techniques as described here to get different perspectives. The work undertaken during this project suggests that a core group of three basic images be produced for the magnetic data, a globally stretched image, a locally stretched image and a directionally filtered image which enhances features perpendicular to the flight line direction of the survey. These three images were found to be the most useful in the geological interpretation of the magnetic data. Further processing techniques can then be applied to help with the interpretation of difficult areas or to enhance particular aspects of the data which the three images mentioned above do not adequately cover.

Appendix B

Survey Specifications

B.1 Introduction

The airborne magnetic and radiometric data used in this thesis were collected as a single survey by Austirex International, under contract to the Northern Territory Department of Mines and Energy. The survey was flown between 20 September and 28 October 1985 and comprised approximately 38000 line kilometres over an area of 18000 square kilometres. The specifications of the survey and preliminary processing of the data are set out below (Part C in Simons, 1986).

B.2 Survey Specifications

The Petermann airborne survey was flown in an Aerocommander 500s (VH-FGS) with north–south flight lines at a nominal spacing of 500 metres. East–west tie lines were flown every 5000 metres. The nominal mean terrain clearance was 100 metres. Navigation was doppler assisted visual navigation using black and white photographs. Terrain clearance was recorded by a Collins ALT-50 radio-altimeter with a sensitivity of 0.1 metres on an operating range of 0 to 610 metres.

A base station Geometrics G826A proton precession magnetometer with a sensitivity of 0.25 nT and a sampling interval of 10 seconds was used to monitor the diurnal variation of the Earth's magnetic field. The base station was situated at Yulara, near Ayers Rock, approximately 100 kilometres east of the survey area.

The airborne magnetometer was a Scintrex VIW 2321-H6 of the alkali vapour type with a resolution of 0.005 nT mounted in a tail stinger. The magnetic field was recorded with a sensitivity of 0.1 nT at a constant time interval of 0.25 seconds, which represents approximately 15 to 20 metres on the ground.

The spectrometer system used was a Geometrics GR800/900D with a total volume of thallium activated sodium iodide crystals of 33.56 litres (2048 cubic inches). The system had 256 channels and a spectral range between 0.3–6.0 million electronvolts. The energy windows and channels used are set out in Table B.1

Channel Name	Channels	Energy Window (MeV)
Total Count	2–254	0.321–2.995
Potassium	101–120	1.368–1.579
Uranium	128–147	1.653–1.864
Thorium	198–236	2.393–2.805
Cosmic	255–255	2.995–6.000

Table B.1: Spectrometer Specifications

B.3 Data Processing

Some preliminary processing and corrections were applied to the magnetic field data before it was recorded onto the located data tapes. The magnetic data was diurnally corrected, offset (parallax) corrected and the Australian Geomagnetic Reference Field (AGRF) was removed.

The radiometric data on the located tapes were uncorrected except for a dead time correction (which is discussed further in Appendix C). Further corrections applied to the radiometric data prior to use are also described in Appendix C.

Appendix C

Radiometric Corrections

C.1 Introduction

The radiometric data on the located tapes supplied by the Northern Territory Department of Mines and Energy were in the form of five uncorrected channels, total count, potassium, uranium, thorium and cosmic count all recorded in counts per second. Prior to using the data for gridding and interpretation they required several standard corrections (Wilkes, 1988; Darnely, 1983) which are outlined here. The relevant coefficients for the various corrections were obtained from Part C of Simons (1986) and through personal communications with Mr. P. Robinson of Austirex International.

C.2 Background and Cosmic

Initially the background and cosmic count rates need to be removed from the data. These are determined by flying a series of high altitude stacks over water so that the contribution of radioactive atmospheric radon gas and radiation due to ground based sources is negligibly small. These tests were done over the water southwest of Perth. A plot of count rate for the four channels (total count, potassium, uranium, thorium) versus the cosmic count rate is constructed from the data from the altitude stacks and a regression line fitted to the plotted points. Thus the aircraft background for each channel is determined by the intercept value of the regression line when the cosmic count rate is zero, and the cosmic contribution to each channel is determined by the slope of the regression line. The goodness of fit of the regression line is quantified in the correlation coefficient which is reported in Table C.1. Both these corrections are subtracted from each of the four raw channel count rates using an equation of the form of C.1.

$$N_{bc} = N_{raw} - N_{bg} - \theta N_{cosmic} \tag{C.1}$$

Where N_{bc} is the background and cosmic corrected count rate, N_{raw} is the raw count rates (deadtime corrected only), N_{bg} is the background count rate for the channel from Table C.1, θ is

the cosmic correction factor for the channel from Table C.1 and N_{cosmic} is the measured cosmic count rate.

Channel	Background Counts/Sec	Cosmic θ	Correlation Coefficient
Total Count	222.51	2.482	0.996
Potassium	17.86	0.130	0.968
Uranium	7.57	0.121	0.977
Thorium	3.85	0.138	0.995

Table C.1: Background and Cosmic Correction Factors

C.3 Stripping

A stripping, or spectral interaction, correction is required for the potassium, uranium and thorium channels to calculate the contribution of potassium (K^{40}), uranium (Bi^{214}), and thorium (Tl^{208}) to their respective channels. The correction minimizes the effects of interactions (Compton scattering) of gamma rays on their path between the ground and the recorder in the aircraft. The uranium channel requires correcting for scattering from the thorium channel and the potassium channel requires correcting for scattering from both the thorium and uranium channels. A small correction is required for gamma rays originating in the uranium decay series being measured in the thorium channel.

The stripping correction coefficients are determined by experiment for each individual gamma ray spectrometer system and take the form A/B (counts in channel B per counts in channel A). The factors appropriate to the system used in the Petermann survey are shown in Table C.2.

Thorium/Uranium	α	0.251
Thorium/Potassium	β	0.448
Uranium/Potassium	γ	0.834
Uranium/Thorium	ε	0.050

Table C.2: Stripping Correction Coefficients

The stripping corrections were applied using equations C.2 –C.4 after the background and cosmic corrections had been applied.

$$N_{th}^{s} = \frac{C_4 - \varepsilon C_3}{(1 - \varepsilon\alpha)} \tag{C.2}$$

$$N_{u}^{s} = \frac{C_3 - \alpha C_4}{(1 - \varepsilon\alpha)} \tag{C.3}$$

$$N_k^s = C_2 - C_3\frac{(\alpha - \beta\varepsilon)}{(1-\varepsilon\alpha)} - C_4\frac{(\beta - \alpha\gamma)}{(1-\varepsilon\alpha)} \tag{C.4}$$

Where the superscript ^{s} means the stripping corrected count rates for each of the channels defined by the subscript. C_2, C_3, C_4 refer to the count rates measured in channels 2 (potassium), 3 (uranium) and 4 (thorium) after the deadtime, background and cosmic corrections have been applied. The constants are those taken from Table C.2.

C.4 Altitude

The measured count rates are very dependant upon the distance from the source, so an altitude correction is required to level the data to a constant nominal altitude of the survey which was 100 metres. The altitude correction is closely approximated by the exponential form of equation C.5

$$N_h = N_n e^{-\mu\Delta h} \tag{C.5}$$

Where N_h is the count rate at height h above the ground, N_n is the desired count rate at the nominal altitude, μ is the altitude attenuation coefficient applicable to the particular channel shown in Table C.3 and Δh is the difference between the true altitude of the reading and the nominal altitude in metres.

Channel	Attenuation Coefficient μ
Total Count	0.005407
Potassium	0.007884
Uranium	0.002545
Thorium	0.006560

Table C.3: Altitude Attenuation Factors

C.5 Radon and Deadtime

Two further corrections which can be applied to radiometric data are the atmospheric radon correction which compensates for varying amounts of the radioactive gas radon found in the atmosphere, and the deadtime correction.

The radon correction is applied rarely when the locality of the survey permits easy daily test flights over large bodies of water to measure the abundance of radon without the interference of ground based radioactive sources. As there was no such body of water available close to the Petermann survey area the correction could not be made and this is a major reason why there is some obvious striping along the flight line direction in the radiometric images. Variations in the

amount of atmospheric radon tend to affect the uranium channel more than the other channels (Green, 1987).

The deadtime correction is needed to take account of the time during which the system cannot register another gamma ray interaction after it has received one previously. This correction is applied by multiplying the measured count rates by the factor shown in C.6, where t is the deadtime per interaction, which is 8 microseconds per total count for the system used, and N is the measured count rate.

$$\frac{1}{(1 - Nt)} \tag{C.6}$$

As mentioned previously the deadtime correction had been applied to the data before it was written to the located tapes.

C.6 Equivalent Ground Concentrations

Once the series of corrections described above have been made to the data the corrected count rates can then be converted to equivalent ground concentrations by dividing by an appropriate constant derived from carefully calibrating the spectrometer system over an area of known elemental ground concentrations. Such a calibration test was run over the Dalgety test range in New South Wales and the calculated coefficients are set out in Table C.4. To convert the corrected count rates to equivalent ground concentrations the count rates are simply divided by the constant which applies to that particular channel.

The units of equivalent ground concentrations are measured in equivalent parts per million (eppm) for the uranium and thorium channels, equivalent percent (%) for the potassium channel and radioelement concentration units (Ur) for the total count channel, where 1 Ur produces the same instrumental response as an identical source containing 1 ppm of uranium in radioactive equilibrium (Darnely, 1982).

Channel	Concentration Coeff.
Total Count	250.0
Potassium	100.0
Uranium	34.8
Thorium	7.5

Table C.4: Elemental Conversion Factors

The conversion of count rates to equivalent concentrations not only gives an estimate of the radioelement concentrations in the near surface but it also means that data of different vintages and recorded using different instruments can be quantitatively compared. Simple corrected

count rate data from different surveys cannot be compared, since the measured count rates are dependent upon the measuring system, crystal size, recording time and other system parameters.

A fortran program was written to apply all the above corrections to the raw data. The corrected count rates were gridded as counts per second, not as equivalent ground concentrations, and the gridded data was then converted to equivalent ground concentration units.

Appendix D

Abbreviations

	General
A.G.R.F.	Australian Geomagnetic Reference Field
A.M.G.	Australian Map Grid
B.M.R.	Bureau of Mineral Resources (Australia)
E	east
eppm	equivalent parts per million
$g\,cm^{-3}$	grams per cubic centimetre
K	potassium
km	kilometres
m	metres
MeV	million electron volts (unit of particle energy)
mGal	milligal (unit of gravitational acceleration)
my	million years before the present
N	north
nT	nanoteslas (unit of magnetic flux density)
N.T.	Northern Territory
N.T.D.M.E.	Northern Territory Department of Mines and Energy
N.T.G.S.	Northern Territory Geological Survey
Pb	lead
ppm	parts per million
Rb	rubidium
S	south
S.A.	South Australia
S.I.	International System of metric units
Sr	strontium
Th	thorium
U	uranium

Ur	radioelement concentration units
vg	vertical gradient of total magnetic field
W	west
W.A.	Western Australia

Magnetic Textural Zones (see Chapter 3)

BL	broad linear
G	granular
L	linear
Mo	mottled
Mu	muricate
S	smooth

Lithomagnetic Units (see interpretation maps)

AB	basement gneiss
AM	metamorphosed, granitized gneiss
B1	strongly magnetic basement complex
B2	weakly magnetic basement complex
F	fault related magnetic anomalies
G1	magnetic granites
G2	nonmagnetic granites
P	magnetic porphyry
V1	magnetic metavolcanics
V2	nonmagnetic metavolcanics

Bibliography

ADOBE SYSTEMS INC., 1985, Postscript Language Reference Manual: *Addison-Wesley Publishing Company*

ADOBE SYTEMS INC., 1985, Postscript Language, Tutorial and Cookbook: *Addison-Wesley Publishing Company*

ANFILOFF, V. & LUYENDYK, A., 1986, Production of Pixel Maps of Airborne Magnetic Data for Australia, with Examples for the Roper River 1:1 000 000 Sheet: *Exploration Geophysics Vol.17* pp. 113–117

ANFILOFF, V. & SHAW, R.D., 1973, The Gravity Effects of Three Large Uplifted Blocks in Separate Australian Shield Areas: *Proc. Symp. on Earth's Gravitational Field and Secular Variation in Position* pp. 273–289

ARRIENS, P.A. & LAMBERT, I.B., 1969, On the Age and Strontium Isotopic Geochemistry of Granulite Facies Rocks from Fraser Range, W.A. and the Musgrave Ranges, Central Australia: *Geol. Soc. Aust. Spec. Publ. 2* pp. 377–388

ASWATHANARAYANA, U., 1985, Principles of Nuclear Geology: *A.A. Balkema Rotterdam, Publishers* pp. 103–150

BARNETT, C.T., 1976, Theoretical Modeling of the Magnetic and Gravitational Fields of an Arbitrarily Shaped Three Dimensional Body: *Geophysics Vol.41 No.6* pp. 1353–1364

BATES, R.G., 1966, Airborne Radioactive Surveys, an Aid to Geological Mapping: *Mining Geophysics Vol.1* pp. 67–76

BARKER, C.J. & MARLIN, C.D. et al., 1987, The Ludwig Users Guide Version 4.0 April 1987: *University of Adelaide, University Computing Services.*

BELL, T.H., 1974, Mylonitic Development in the Woodroffe Thrust North of Amata, Musgrave Ranges, Central Australia: *Unpublished Ph.D. Thesis, University of Adelaide*

BIRCH, F., 1954, Heat from Radioactivity: *In Faul, H. (ed.) Nuclear Geology, John Wiley and Sons New York* pp. 148–166

Blackader, R.G., & Dumych, H. & Griffin, P.J., 1979, Guide for Preparation of Geological Maps and Reports: *Geol. Surv. Canada Miscellaneuos Reports 29*

BRADSHAW, J.D. & EVANS, P.R., 1988, Palaeozoic Tectonics, Amadeus Basin Central Australia: *A.P.E.A. Journal 1988* pp. 267–282

BROOKFIELD, M., 1970, Dune Trends and Wind Regime in Central Australia: *Zeitschrift Für Geomorphologie Supplementband 10*

BOYD, D.M., 1967, The Contribution of Airborne Magnetic Surveys to Geological Mapping: *In Morley, L.W. (ed.) Mining and Ground Water Geophysics 1967. Geological Survey of Canada Economic Geology Report 26* pp. 213–227

BUBNER, G.J., 1977, A Detailed Gravity and Magnetic Investigation of Southern Iron Duke, South Middleback Ranges: *Unpublished Honours Thesis, University of Adelaide*

CADY, J.W., 1980, Calculation of Gravity and Magnetic Anomalies of Finite Length Right Polygonal Prisms: *Geophysics Vol.45 No.10* pp. 1507–1512

CADY, J.W., 1981, Erratum to Paper "Calculation of Gravity and Magnetic Anomalies of Finite Length Right Polygonal Prisms": *Geophysics Vol.46* pp. 958–958

CAMERON, E.M. (ed.), 1983, Uranium Exploration in Athabasca Basin, Saskatchewan, Canada: *Geological Survey of Canada Paper 82-11*

CASTLEMAN, K.R., 1979, Digital Image Processing: *Prentice-Hall Inc. Publishers*

CHARBONNEAU, B.W., 1982, Radiometric Study of Three Radioactive Granites in the Canadian Shield: Elliot Lake Ontario; Fort Smith and Fury and Hecla, N.W.T.: *In Maurice, Y.T. (ed.) Uranium in Granites: Geological Survey of Canada Paper 81-23* pp. 91–99

CLARK, D.A., 1983, Comments on Magnetic Petrophysics: *Aust. Soc. Explor. Geophys. Bulletin Vol.14* pp. 49–62

COOK, P.J., 1972, Sedimentological Studies on the Stairway Sandstone of Central Australia: *Aust. Bur. Min. Res. Geol. and Geophys. Bulletin 95*

COOKSON, G.G., 1987, Magnetic Tape Operations Users Guide for VAX/VMS, Version 1.0.: *The University of Adelaide, University Computing Services.*

CORDELL, L. & KNEPPER, D.H., 1987, Aeromagnetic Images: Fresh Insights to the Buried Basement, Rolla Quadrangle, southeast Missouri: *Geophysics Vol.52 No.2* pp. 218–231

COLLERSON, K.D., 1972, High Grade Metamorphic and Structural Relationships Near Amata, Musgrave Ranges, Central Australia: *Unpublished Ph.D. Thesis University of Adelaide*

COLLERSON, K.D. & OLIVER, R.L. & RUTLAND, R.W.R., 1972, An Example of Structural and Metamorphic Relationships in the Musgrave Orogenic Belt, Central Australia: *Journal of the Geological Society of Australia Vol.18 No.4* pp. 379–393

COX, K.G. & BELL, J.D. & PANKHURST, R.J., 1979, Interpretation of Igneous Rocks: *George Allen and Unwin*

D'ADDARIO, G.W. & TUCKER, D.H., 1986, Magnetic Domain Map -A New Minerals Exploration Tool: *Cartography Vol.15 No.2* pp. 116–119

DANIELS, J.L., 1974, The Geology of the Blackstone Region Western Australia: *Geological Survey of Western Australia Bulletin 123*

DANIELS, J.L., 1972, Scott Sheet 1:250 000 Geological Series–Explanatory Notes: *Australian Government Publishing Service Canberra*

DANIELS, J.L. & HIERN, M.N. & FRUZZETTE, D., 1975, Musgrave Block–Sundry Mineralization: *In Knight, G.L. (ed.) Economic Geology of Australia and Papua New Guinea Vol.1 Metals* pp. 445–459

DARNLEY, A.G., 1972, Airborne Gamma-Ray Survey Techniques, Present and Future: *In Watson, K and Regan, R.D.(eds.) Remote Sensing : Society of Exploration Geophysics Geophysical Reprint Series No.3* pp. 493–534

DARNLEY, A.G., 1982, Hot Granites: Some General Remarks: *In Maurice, Y.T. (ed.) Uranium in Granites: Geological Survey of Canada Paper 81-23* pp. 1–10

DING, P. & JAMES, P.R., 1985, Structural Evolution of the Harts Range Area and Its Implications for the Development of the Arunta Block, Central Australia: *Precambrian Research Vol.27* pp. 251–276

DOMZALSKI, W., 1957, Some Problems of the Aeromagnetic Surveys: *Geophysical Prospecting Vol.5 No.4* pp. 469–479

DRURY, S.A., 1987, Image Interpretation in Geology: *Allen and Unwin London Publishers*

DRURY, S.A. & WALKER, A.S.D., 1987, Display and Enhancement of Gridded Aeromagnetic Data of the Solway Basin: *International Journal of Remote Sensing Vol.8 No.10* pp. 1433–1444

DUFF, B.A. & LANGWORTHY, A.P., 1974, Orogenic Zones in Central Australia: Intraplate Tectonics?: *Nature Vol.249* pp. 645–646

DUVAL, J.S., 1976, Statistical Interpretation of Airborne Gamma-Ray Spectrometer Data Using Factor Analysis: *In Exploration for Uranium Deposits Proc. Series I.A.E.A. Vienna* pp. 71–80

DUVAL, J.S., 1977, High Sensitivity Gamma-Ray Spectrometry–State of the Art and Trial Application of Factor Analysis: *Geophysics Vol.42 No.3* pp. 549–559

DUVAL, J.S. & COOK, B.K. & ADAMS, J.A.S., 1971, A Study of the Circle of Investigation of an Airborne Gamma-Ray Spectrometer: *Journal of Geophysical Research Vol.76* pp. 8466–8470

ELLIS, H.A., 1937, Report on Some Observations Made on a Journey from Alice Springs N.T.

to the Country North of the Rawlinson Range in W.A.: *W.A. Dept. Mines. Annual Report, 1936* pp. 62–77

EMERSON, D.W., 1973, A Geophysical Study of Part of the Eastern Margin of the Yilgarn Block Western Australia: *Unpublished Ph.D. Thesis University of Sydney*

EMERSON, D.W. (ed.), 1979, Proceedings from Applied Magnetic Interpretation Symposium: *Bull. Aust. Soc. Expl. Geophys. Vol.10 No.1* pp. 3–5

FACER, R.A., 1971, Magnetic Properties of Rocks from the Giles Complex, Central Australia: *J. Proc. Roy. Soc. NSW Vol.104* pp. 45–61

FAHRIG, W.F. & EADE, K.E. & ADAMS, J.A.S., 1967, Abundance of Radioactive Elements in Crystalline Shield Rocks: *Nature Vol.214* pp. 1002–1003

FARBRIDGE, R.A., 1967, Drilling for Water in the Cobb Depression North of Wingellina: *Geol. Surv. West. Aust. Ann. Report for 1967* pp. 59–60

FINLAYSON, D.M., 1973, Isomagnetic Maps of the Australian Region for the Epoch 1970.0: *Aust. Bur. Min. Res. Geol. and Geophys. Report 159*

FORMAN, D.J. & HANCOCK, P.M., 1964, Regional Geology of the Southern Margin of the Amadeus Basin, Rawlinson Range to Mulga Park Station: *Aust. Bur. Min. Res. Geol. and Geophys. Unpublished Record 1964/41*

FORMAN, D.J., 1965, Rawlinson Sheet 1:250 000 Geological Series–Explanatory Notes: *Aust. Bur. Min. Res. Geol. and Geophys. Canberra A.C.T.*

FORMAN, D.J., 1966, The Geology of the Southwestern Margin of the Amadeus Basin, Central Australia: *Aust. Bur. Min. Res. Geol. and Geophys. Report No.87*

FORMAN, D.J., 1966a, Bloods Range Sheet 1:250 000 Geological Series–Explanatory Notes: *Aust. Bur. Min. Res. Geol. and Geophys. Canberrs A.C.T.*

FORMAN, D.J., 1971, The Arltunga Nappe Complex, McDonnell Ranges Northern Territory Australia: *Geol. Soc. Australia Jour. Vol.18* pp. 173–182

FORMAN, D.J., 1972, Petermann Ranges Sheet 1:250 000 Geological Series–Explanatory Notes: *Aust. Bur. Min. Res. Geol. and Geophys. Canberra A.C.T.*

FORMAN, D.J. & SHAW, R.D., 1973, Deformation of the Crust and Upper Mantle in Central Australia: *Aust. Bur. Min. Res. Geol. and Geophys. Bulletin 144*

FRASER, A.R., 1976, Gravity Provinces and Their Nomenclature: *B.M.R. Jour. of Aust. Geol. and Geophys. Vol.1 No.4* pp. 350–352

FROELICH, A.J. & KRIEG, E.A., 1969, Geophysical-Geological Study of the Northern Amadeus Trough, Australia: *Bull Am. Ass. Petrol. Geol. Vol.53* pp. 1978–2004

GRANT, F.S., 1985, Aeromagnetics, Geology and Ore Environments 1. Magnetite in Igneous,

Sedimentary and Metamorphic Rocks, an Overview: *Geoexploration Vol.23* pp. 303–333

GRANT, F.S., 1985, Aeromagnetics, Geology and Ore Environments 2. Magnetite and Ore Environments: *Geoexploration Vol.23* pp. 335–362

GRAY, C.M., 1979, Geochronology of Granulite Facies Gneisses in the Western Musgrave Block, Central Australia: *Geol. Soc. Aust. Jour. Vol.25* pp. 403–414

GRASTY, R.L., 1975, Uranium Measurements By Airborne Gamma-Ray Spectrometry: *In Watson, K. & Regan, R.(eds.) Remote Sensing : Society of Exploration Geophysics Geophysical Reprint Series No.3* pp. 535–551

GREEN, A.A., 1987, Leveling Airborne Radiometric Data Using Between Channel Correlation Information: *Geophysics Vol.52 No.11* pp. 1557–1562

GREGORY, A.F., 1960, Geological Interpretation of Aeroradioactivity Data: *Geol. Surv. Canada Bulletin 66*

GREGORY, A.F., 1983, Interpretative Geological Mapping as an Aid to Exploration in the NEA/IAEA Athabasca Test Area: *In Cameron, E.M. (ed.) Geol. Surv. Canada Paper 82-11* pp. 171–178

GOODE, A.D.T., 1970, The Petrology and Structure of the Kalka and Ewarara Layered Basic Intrusions, Giles Complex, Central Australia: *Unpublished Ph.D. Thesis University of Adelaide*

GUILLOU, R.B. & SCHMIDT, R.G., 1960, Correlation of Aeroradioactivity Data and Areal Geology: *U.S.G.S. Prof. Paper 400–B* pp. B119–B121

HAGGERTY, S.E., 1979, The Aeromagnetic Mineralogy of Igneous Rocks: *Can. Jour. Earth Sci. Vol.16* pp. 1281–1293

HARALICK, R.M., 1984, Digital Step Edges from Zero Crossing of Second Directional Derivatives: *IEEE Transactions on Pattern Analysis and Machine Intelligence Vol.PAMI 6* pp. 58–68

HEIER, K.S. & ADAMS, J.A.S., 1965, Concentration of Radioactive Elements in Deep Crustal Material: *Geochim. Cosmochim. ACTA Vol.29* pp. 53–61

HENKEL, H. & GUZMAN, M., 1977, Magnetic Features of Fracture Zones: *Geoexploration Vol.15* pp. 173–181

HOLROYD, M.T., 1975, The Extension of ADAM (Aeromagnetic Data Automatic Mapping) System to Include the Application of Two Dimensional Digital Filters to Gridded Data: *Geol. Surv. Canada Report of Activities Part a 75–1a* pp. 109–110

HOOD, P.J. & McGRATH, P.H. & KORNIK, L.J., 1975, Evaluation of Derived Vertical Gradient Results in the Timmins Area, Ontario: *Geol. Surv. Canada Paper 75–1 Part A* pp. 111–115

HORWITZ, R.C. & DANIELS, J.L., 1967, A Late Precambrian Belt of Vulcanicity in Central Australia: *Geol. Surv. W. Aust. Ann. Rep. 1966* pp. 94–97

HORWITZ, R.C. & DANIELS, J.L. & KRIEWALDT, M.J.P., 1966, Structural Layering in the Precambrian of the Musgrave Block, Western Australia: *W.A. Dept. of Mines Ann. Rep. 1966* pp. 100–102

HOSSFIELD, P.S., 1954, Stratigraphy and Structure of the Northern Territory: *Trans. Roy. Soc. S. Aust. Vol.77* pp. 103–161

HUNTER, D.R. (ed.), 1981, Precambrian of the Southern Hemisphere: *Elsevier Scientific Publishing Company*

IAEA, 1979, Gamma Ray Surveys in Uranium Exploration, Tecnichal Report Series No 186: *IAEA Vienna, 1979*

ISLES, D.J., 1983, A Regional Geophysical Study of the Broken Hill Block, N.S.W.: *Unpublished Ph.D. Thesis University of Adelaide*

JAIN, S. & SCHUUR, W. & CURTIS, C.E., 1974, Source Parameter Map-A New Aid to Aeromagnetic Data Interpretation: *Jour. Can. Soc. Explor. Geophys. Vol.10 No.1* pp. 39–51

JAMES, P.R. & DING, P., 1988, Caterpillar Tectonics in the Harts Range Area: a Kinship Between Two Sequential Proterozoic Extension -Collision Orogenic Belts Within the Eastern Arunta Inlier of Central Australia: *Precambrian Research Vol.40* pp. 199–216

JOKLIK, G.F., 1952, Geological Reconnaissance of the Southwestern Portion of the Northern Territory: *Aust. Bur. Min. Res. Geol. and Geophys. Report No.10*

JORGENSON, J.T., 1966, Photogeological Evaluation of Project 'A' Southwest Northern Territory P.A. Nos. 1435 and 1546 By Geophoto Resources Consultants: *N.T.D.M.E. Open File Company Report for Planet Mining Co. Pty. Ltd*

KENNETH McMAHON & PARTNERS PTY LTD, 1968, Geochemical Survey of the Petermann Ranges, Southwest Northern Territory: *N.T.D.M.E. Open File Company Report for Planet Mining Co. Pty. Ltd*

KHAN, D.M., 1979, Radiometric Studies in the Lower Proterozoic Willyama Complex Broken Hill District: *Unpublished M.Sc. Thesis University of Adelaide*

KIEK, T. & JONES, C.R., 1986, Zeta Plotting Users Guide: Version 3.0 Dec. 1986: *University of Adelaide, University Computing Services*

KILLEEN, P.G. & HUNTER, J.A. & CARSON, J.M., 1971, Some Effects of Altitude and Sampling Rate in Airborne Gamma-Ray Spectrometric Surveying: *Geoexploration Vol.9 No.4* pp. 231–234

KILLEEN, P.G., 1976, Discussion of Paper By Duval (1976): *In Exploration for Uranium Ore Deposits, Proc Series IAEA Vienna* pp. 80–81

KILLEEN, P.G., 1979, Gamma Ray Spectrometric Methods in Uranium Exploration–Application and Interpretation: *In Hood, P.J (ed.) Geophysics and Geochemistry in the Search*

for Metallic Ores Geol. Surv. Canada. Econ. Geol. Rep. 31 pp. 163–229

KIRSCHVINK, J.L., 1978, The Precambrian–Cambrian Boundary Problem: Magnetostratigraphy of the Amadeus Basin, Central Australia: *Geol. Mag. Vol.115* pp. 139–150

KORSCH, R.J. & LINDSAY, J.F., 1989, Relationship Between Deformation and Basin Evolution in the Intracratonic Amadeus Basin, Central Australia: *Tectonophysics Vol.158* pp. 5–22

KOWALIK, W.S. & GLENN, W.E., 1987, Image Processing of Aeromagnetic Data and Integration With Landsat Images For Improved Structural Interpretation: *Geophysics Vol.52 No.7* pp. 875–884

KRÖNER, A. & GREILING, R. (eds.), 1984, Precambrian Tectonics Illustrated: *Internat. Union of Geol. Sci. Commission on Tectonics, Subcommission on Precambrian structural Type Regions Final Report*

KRUTIKHOVSKAYA, Z.A. & PASHKEVICH, I.K. & SIMONENKO, T.N., 1973, Magnetic Anomalies of Precambrian Shields and Some Problems of the Geological Interpretation: *Canadian Journal of Earth Sciences Vol.10* pp. 629–636

KUZNETSOV, A.A., 1987, The Origin of the Granulite Layer of the Earths Crust (as Exemplified By the Anabar Shield): *International Geology Review Vol.29* pp. 383–394

LAMBECK, K., 1983, Structure and Evolution of the Intercratonic Basins of Central Australia: *Geophys. Jour. Roy. Astron. Soc. Vol.74* pp. 843–886

LAMBECK, K., 1984, Structure and Evolution of the Amadeus, Officer and Ngalia Basins of Central Australia: *Aust. Jour. of Earth Sci. Vol.31* pp. 25–48

LAMBERT, I.B. & HEIER, K.S., 1968, The Vertical Distribution of Uranium Thorium and Potassium in the Continental Crust: *Geochim Cosmochim ACTA Vol.31* pp. 377–390

LAMPORT, L., 1986, LaTeX, A Document Preparation System: *Addison-Wesley Publishing Company*

LETROS, S. & STRANGWAY, D.W. & TASILLO HIRT, A.M. & GEISSMAN, J.W. & JENSON, L.S., 1983, Aeromagnetic Interpretation of the Kirkland Lake–Larder Lake Portion of the Abitibi Greenstone Belt, Ontario: *Can. Jour. of Earth Sci. Vol.20* pp. 548–560

LLOYD, J.W. & JACOBSON, G., 1987, The Hydrogeology of the Amadeus Basin, Central Australia: *Journal of Hydrology Vol.93* pp. 1–24

LONSDALE, G.F. & FLAVELLE, A.J., 1968, Amadeus and South Canning Basin Gravity Survey, Northern Territory and Western Australia, 1962: *Aust. Bur. Min. Res. Geol. and Geophys. Report 133*

LØVBORG, L. & MOSE, E., 1987, Counting Statistics in Radioelement Assaying With a Portable Spectrometer: *Geophysics Vol.52 No.4* pp. 555–563

MABOKO, M. & McDOUGALL, I. & ZIETHER, P. & WILLIAMS, I., 1987, Thermal History

of High Grade Terranes in the Musgrave Ranges Central Australia: *A.N.U. Research School of Earth Sciences Annual Report 1987*

MAJOR, R.B., 1970, Woodroffe Thrust Zone in the Musgrave Ranges: *Quart. Notes. Geol. Surv. S. Aust. Vol.35* pp. 9–11

MATHUR, S.P., 1976, Relation of Bouguer Anomalies to Crustal Structure in Southwestern and Central Australia: *Jour. Aust. Bur. Min. Res. Geol. and Geophys. Vol.1* pp. 277–286

MAURICE, Y.T. (ed.), 1980, Uranium in Granites, Proceedings of a Workshop Held in Ottawa Ontario 25–26 Nov. 1980: *Canadian Geol. Surv. Paper 81-23*

McGRATH, P.H. & HOLROYD, M.T. & HOOD, P.J., 1974, An Experimental High Resolution Aeromagnetic Survey in the Kamloops Area, British Columbia: *Canadian Geol. Surv. Paper 74-1 Part B* pp. 103–106

McGRATH, P.H., 1975, A Two Dimensional Vertical Derivative Operator: *Canadian Geol. Surv. Paper 75-1 Part A* pp. 107–108

McGRATH, P.H. & KORNIK, L.J. & DODS, S.D., 1976, A Method for the Compilation of High Quality Calculated First Vertical Derivative Aeromagnetic Maps: *Canadian Geol. Surv. Paper 76 Part C* pp. 7–17

McINTYRE, J.I., 1981, Accurate Display of Fine Detail in Aeromagnetic Data: *Bull. Aust. Soc. Explor. Geophys. Vol.12 No.4* pp. 82–88

McELHINNY, M.W. & EMBLETON, B.J.J., 1976, Precambrian and Early Palaeozoic Palaeomagnetism in Australia: *Philos. Trans. R. Soc. London A280* pp. 417–431

McSHARRY, P.J., 1973, Reducing Errors in Airborne Gamma–Ray Spectrometry: *Bull. Aust. Soc. Explor. Geophys. Vol.4 No.1* pp. 31–41

MENDELSOHN, F., 1973, Mobile Belts: *Spec. Public. Geol. Soc. S. Africa* pp. 507–508

MILLER, R.C. & ROWAN, I.S., 1968, Nickel Exploration–Claude Hills Extension, Northern Territory: *S. Aust. Min. Review. Vol.125*

MILTON, B.E. & PARKER, A.J., 1973, An Interpretation of Geophysical Observations on the Northern Margin of the Eastern Officer Basin: *Quart. Notes. Geol. Surv. S. Aust. Vol.46* pp. 10–14

MIRAMS, R.C., 1964, The Geology of the Mann 4-Mile Sheet: *Dept. Mines. S. Aust. Rep. of Investigations. Vol.25* pp. 1–30

MOORE, A.C., 1970, The Geology of the Gosse Pile Ultramafic Intrusion and of the Surrounding Granulites, Tomkinson Range, Central Australia: *Unpublished Ph.D. Thesis, University of Adelaide.*

MOORE, A.C. & GOODE, A.D.T., 1978, Petrography and Origin of the Granulite Facies Rocks on the Western Musgrave Block Central Australia: *Jour. Geol. Soc. of Aust. Vol.25 Part 6*

pp. 341–358

MORSE, J.G.(ed.), 1977, Nuclear Methods in Mineral Exploration and Production: *Elsevier Scientific Publishing Co.*

MUTTON, A. & SHAW, R.D., 1979, Physical Property Measurements as an Aid to Magnetic Interpretation in Basement Terrains: *Bull. Aust. Soc. Explor. Geophys. Vol.10* pp. 79–91

MOXHAM, R.M., 1960, Airborne Radioactivity Surveys in Geologic Exploration: *Geophysics Vol.25* pp. 408–432

NESBITT, R.W. & GOODE, A.D.T. & MOORE, A.C. & HOPWOOD, T.P., 1970, The Giles Complex, Central Australia: A Stratified Sequence of Mafic and Ultramafic Intrusions: *Geol. Surv. S. Africa Spec. Public. No.1*

NEWTON, A.R. & SLANEY, V.R., 1978, Geological Interpretation of an Airborne Gamma-Ray Spectrometer Survey of the Hearne Lake Area, Northwest Territories: *Canadian Geol. Surv. Paper 77-32*

N.T.D.M.E., 1986, Annual Report Geological Survey Division: *Northern Territory Department of Mines and Energy Annual Report 1985-86* pp. 38–47

N.T.D.M.E., 1987, Annual Report Geological Survey Division: *Northern Territory Department of Mines and Energy Annual Report 1986-87* pp. 44–54

PAINE, J.W., 1987, VAX Routines for Gridding and Contouring: *Unpublished Internal Report, Department of Geology and Geophysics, University of Adelaide*

PAINE, J.W., 1987, Gamma Users Guide: *Unpublished Internal Report, Department of Geology and Geophysics, University of Adelaide*

PARKER GAY, S., 1972, Aeromagnetic Lineaments, Their Geological Significance and Their Significance Geology: *American Stereo Map Company, Salt Lake City , Utah*

PARKER GAY, S., 1973, Pervasive Orthogonal Fracturing in Earth's Continental Crust, (a Closer Look At The New Basement Tectonics): *American Stereo Map Company, Salt Lake City, Utah*

PATERSON, N.R., 1974, Canadian Mining Geophysics, 1974: *Jour. Can. Soc. Explor. Geophys. Vol.10 No.1* pp. 9–22

PATERSON, N.R. & REEVES, C.V., 1985, Applications of Gravity and Magnetic Surveys: The State of the Art in 1985: *Geophysics Vol.50 No.12* pp. 2558–2594

PETERS, L.J., 1949, The Direct Approach to Magnetic Interpretation and Its Practical Application: *Geophysics Vol.14* pp. 290–319

PITKIN, J.A., 1968, Airborne Measurement of Terrestrial Radioactivity as an Aid to Geological Mapping: *U.S.G.S. Prof Paper 516-F*

PLUMB, K.A., 1985, Subdivision and Correlation of Late Precambrian Sequences in Australia: *Precambrian Research Vol.29* pp. 303–329

POTTS, M.J., 1976, Computer Methods for Geologic Analysis of Radiometric Data: *In Exploration for Uranium Ore Deposits, Proc. Series I.A.E.A. Vienna* pp. 149–156

PRAKASA RAO, T.K.S. & SUBRAHMANYAM, M., 1988, Characteristic Curves for the Inversion of Magnetic Anomalies of Spherical Ore Bodies: *Pure and Applied Geophysics Vol.126 No.1* pp. 69–83

PREISS, W.V. & FORBES, B.G., 1981, Stratigraphy, Correlation and Sedimentary History of Adelaidean (Late Proterozoic) Basins in Australia: *Precambrian Research Vol.15* pp. 255–304

RAM BABU, M.V. & VIJAYAKUMAR, V. & ATCHUTA RAO, D., 1986, A Simple Method for the Analysis of Magnetic Anomalies Over Dyke-like Bodies: *Geophysics Vol.51 No.5* pp. 1119–1126

REFORD, M.S., 1980, Magnetic Method: *Geophysics Vol.45 No.11* pp. 1640–1658

REFORD, M.S. & SUMNER, J.S., 1964, Aeromagnetics: *Geophysics Vol.29 No.4* pp. 482–516

RICHARDSON, K.A., 1983, Airborne Gamma-Ray Spectrometric Survey of the NEA/IAEA Athabasca Test Survey Area: *In Cameron, E.M. (ed.) Geol. Surv. Canada Paper 82-11* pp. 167–170

RICHARDSON, K.A. & KILLEEN, P.G., 1980, Regional Radiogenic Heat Production Mapping By Airborne Gamma Ray Spectrometry: *Geol. Surv. Canada Current Research Paper 80-1B*

ROY, R.F. & BLACKWELL, D.D. & BIRCH, F., 1968, Heat Generation of Plutonic Rocks and Continental Heat Flow Provinces: *Earth and Planetary Sci. Letters Vol.5* pp. 1–12

ROWAN, I.S., 1967, Regional Gravity Survey of Mann and Woodroffe 1:250 000 Sheet Areas: *S.A.Dept. Mines and Energy Unpublished Report RB 64/33*

SAKAKURA, A.W., 1957, Scattered Gamma Rays from Thick Uranium Sources: *U.S.G.S. Bulletin 1052-A*

SALOMAN, K.B., 1978, An Efficient Point-in-Polygon Algorithm: *Computers and Geoscience Vol.4* pp. 173–178

SAUNDERS, D.F. & POTTS, M.J., 1976, Interpretation and Application of High Sensitivity Airborne Gamma-Ray Spectrometer Data: *In Exploration for Uranium Ore Deposits, I.A.E.A. Vienna 1976*

SCHRODER, R.J. & GORTER, J.D., 1984, A Review of Recent Exploration and Hydrocarbon Potential of the Amadeus Basin, Northern Territory: *Jour. Aust. Petrol. Ass. Vol.24* pp. 19–41

SHARMA, P.V., 1987, Magnetic Method Applied to Mineral Exploration: *Ore Geology Review Vol.2* pp. 323–357

SHAW, R.D. & STEWART, A.J. & BLACK, L.P., 1984, The Arunta Inlier: A Complex Ensialic Mobile Belt in Central Australia: Part 2 Tectonic History: *Aust. Jour. of Earth Sci. Vol.31* pp. 457–484

SHELLEY, E.P. & DOWNIE, D.N., 1971, Mann-Woodroffe Aeromagnetic Survey, South Australia 1969: *Aust. Bur. Min. Resour. Geol. and Geophys. Record 1971/19 (unpubl..)*

SHERGOLD, J.H. & JAGO, J.B. & COOPER, R.A. & LAURIE, J.R., 1985, The Cambrian System in Australia, Antarctica and New Zealand: *International Union of Geological Science Publication No.19*

SIMONS, B.A., 1986, Report on the Petermann Airborne Geophysical Survey: *Northern Territory Geological Survey Technical Report GS 86/8 A-C 1986*

SMITH, M.R. & JENSON, M.L., 1974, A Theory of Intracontinental Tectonic Adjustment: *Geol. Soc. Amer. Abstracts With Program, Vol.6 No.3* pp. 255–255

SMITH, R.J., 1979, An Interpretation of Magnetic and Gravity Data in the Musgrave Block in South Australia: *South. Aust. Depart. Mines and Energy Report 79/103 (unpubl.)*

SMITHSON, S.B. & HEIER, K.S., 1971, K, U, TH Distribution Between Normal and Charnockitic Facies of a Deep Granitic Intrusion: *Earth and Plan . Sci. Letters Vol.12* pp. 325–326

SPRIGG, R.C., 1958, The North-West Province: *Jour. Geol. Soc. Aust. Vol.5 No.2* pp. 80–87

SPRIGG, R.C. & WILSON, R.B., 1959, The Musgrave Mountain Belt in South Australia: *Geol. Rdsch. Vol.47* pp. 531–542

STEWART, I.C.F. & BOYD, D.M., 1983, Enhancement of Aeromagnetic Trends from Broken Hill, Using the Second Derivative: *Bull. Aust. Soc. of Explor. Geophys. Vol.14 No.1* pp. 11–21

STOKES, E., 1986, Lasseter's Gold: *Australian Geographic Vol.1 No.1* pp. 35–51

STRANGWAY, D.W., 1966, Rock Magnetism and Geological Correlation: *Mining Geophysics Vol.1* pp. 54–66

STRANGWAY, D.W., 1966, Magnetic Characteristics of Rocks: *Mining Geophysics Vol.2* pp. 454–473

SUTTON, D.J. & MUMME, W.G., 1957, The Effect of Remanent Magnetization in Aeromagnetic Interpretation: *Aust. Jour. of Physics Vol.10* pp. 547–557

SUTTON, J. & WATSON, J.V., 1974, Tectonic Evolution of Continents in Early Proterozoic Times: *Nature Vol.247* pp. 433–435

TAKESHI UEMURA & SHINJIRO MIZUTANI (eds.), 1979, Geological Structures: *John Wiley and Sons*

TAMMANMAA, J.K. & GRASTY, R.L. & PELTONIEMA, M., 1976, The Reduction of Statistical Noise in Airborne Radiometric Data: *Can. Jour. Earth. Sci. Vol.13 No.10* pp. 1351–1357

THOMSON, B.P., 1966, Report on Rifts and Major Shear Fault, South Australia: *South Aust. Dept. Mines and Energy Report 62/93 (unpubl.)*

THOMSON, B.P., 1969, Precambrian Crystalline Basement: *In Parkin, L.W. (ed.) Handbook of South Australian Geology.*

THOMSON, B.P., 1970, A Review of the Precambrian and Lower Palaeozoic Tectonics of South Australia: *Trans. Roy. Soc. S. Aust. Vol.94* pp. 193–221

THOMSON, B.P., 1975, Musgrave Block-Regional Geology: *In Knight, C.L. (ed.) Economic Geology of Australia and Papua New Guinea Vol.1 Metals.* pp. 451–454

THOMSON, B.P. & MAJOR, R.B., 1968, Outline of Geology of Western Musgrave Block. S.A.–Pre-aeromagnetic Survey Report: *South Aust. Dept. Mines and Energy Report 66/124 (unpubl.)*

TREVORROW, A., 1986, Local Guide to LaTeX Under VAX/VMS: *University Computing Services, University of Adelaide*

TREVORROW, A., 1987, PSPRINT Users Guide, Version 1.1 for VAX/VMS: *University Computing Services, University of Adelaide*

TSEO, G., 1986, Longitudinal Dunes: Their Genesis and Ordering: *Unpublished Ph.D. Thesis University of Adelaide*

TUCKER, D.H. & D'ADDARIO, G.W.,1986, Albany 1:1 000 000 Map Sheet, Magnetic Domains. Interpretation of Aeromagnetic Anomaly Pixel Map Series: *Aust. Bur. Min. Resour.*

TUCKER, D.H. & D'ADDARIO, G.W., 1986a, Roper River 1:1 000 000 Map Sheet, Magnetic Domains. Interpretation of Aeromagnetic Anomaly Pixel Map Series: *Aust. Bur. Min. Resour.*

TUCKER, D.H. & D'ADDARIO, G.W., 1987, A Systematic Visual Approach to Interpretation of Aeromagnetic Total Intensity Anomaly Pixel Maps At 1:1 000 000 Scale: *Bull. Aust. Soc. Explor. Geophys. Vol.18* pp. 212–215

TWIDALE, R. & WOPFNER, H., 1981, Aeolian Landforms of Central Australia: *Zeitschrift Für Geomorphologie Vol.25* pp. 353–358

UKAIGWE, N.F., 1985, Interpretation of Aeromagnetic Data of the Olary Province and the Development of Interpretation Methods: *Unpublished Ph.D. Thesis University of Adelaide*

VEEVERS, J.J. & JONES, J.G. & POWELL, C, McA., 1988, Tectonic Framework of Australia's Sedimentary Basins: *A.P.E.A. Journal Vol.22 Part 1* pp. 283–300

WATSON, J.V., 1973, Effects of Reworking on High Grade Gneiss Complexes: *Phil. Trans.*

Roy. Soc. Lond. Vol.A273 pp. 443–456

WELLS, A.T., 1968, Evolution of Salt Anticlines and Salt Domes in the Amadeus Basin, Central Australia: *Geol. Soc. Amer. Spec. Paper 88* pp. 229–247

WELLS, A.T. & FORMAN, D.J. & RANFORD, L.C. & COOK, P.J., 1969, Geology of the Amadeus Basin, Central Australia: *Aust. Bur. Min. Resour. Geol. and Geophys. Bulletin 100*

WELLS, A.T. & STEWART, A.J. & SKWARKO, S.K., 1966, Geology of the Southeastern Part of the Amadeus Basin, Northern Territory: *Aust. Bur. Min. Resour. Geol. and Geophys. Report 88*

WINDLEY, B.F., 1977, The Evolving Continents: *John Wiley and Sons*

WHITING, T.H., 1983, Interpretation Methods: *Unpublished Internal Report, Department of Geology and Geophysics, University of Adelaide*

WHITING, T.H., 1986, Aeromagnetics as an Aid to Geological Mapping -A Case History from the Arunta Inlier, Northern Territory: *Aust. Jour. Earth Sci. Vol.33* pp. 271–286

WHITING, T.H., 1987, A Study of the Lithology and Structure of the Eastern Arunta Inlier Based on Aeromagnetic Interpretation: *Unpublished Ph.D. Thesis University of Adelaide*

WILKES, P.G., 1988, Computer Processing of Airborne Gamma Ray Spectrometer Data: *A.S.E.G. Conference Adelaide 1988 Airborne Geophysics Short Course*

WILCOX, R.E. & HARDING, T.P. & SEELY, D.R., 1973, Basic Wrench Tectonics: *Amer. Assoc. Petrol. Geol. Bull. Vol.57 No.1* pp. 74–96

WILSON, A.F., 1946, The Charnokitic and Ancient Pyroxene Gneisses of the Musgrave Ranges Northwest of South Australia: *Unpublished M.Sc. Thesis University of Western Australia*

WILSON, A.F., 1947, The Charnokitic and Associated Rocks of Northwestern South Australia Part 1 The Musgrave Ranges an Introductory Account: *Trans. Roy. Soc. S. Aust. Vol.71 No.2* pp. 195–211

WILSON, A.F., 1948, The Charnokitic and Associated Rocks of Northwestern South Australia Part 2 Dolerites from the Musgrave and Everard Ranges: *Trans. Roy. Soc. S. Aust. Vol.72* pp. 178–200

WILSON, A.F., 1953, The Significance of Lineation in Central Australia: *Aust. Jour. of Sci. Vol.16* pp. 47–50

WILSON, A.F., 1954, Studies on Australian Charnokitic Rocks and Related Problem: *Unpublished D.Sc. Thesis, University of Western Australia*

WILSON, A.F., 1960, The Charnokitic Granites and Associated Granites of Central Australia: *Trans. Roy. Soc. S. Aust. Vol.83* pp. 37–76

WILSON, A.F., 1966, A Geological Report on the Mineral Prospects in the Vicinity of the Petermann Ranges, N.T. Consultant Geologists Report for Planet Mining Company Pty. Ltd: *N.T.D.M.E. Open File Company Report, (unpubl.) CR66/22*

WILSON, A.F., 1969, The Mineral Potential of Granulite Terranes: *Proc. Australas. Inst. Min. Metall. Vol.231* pp. 41–46

WILSON, A.F., 1969a, Problems of Exploration of Metals in Granulite Terranes With Particular Reference to Australian Localities.: *Geol. Soc. Aust. Spec. Pub. 2* pp. 375–376

WILSON, A.F. & COMPSTON, W. & JEFFREY, P.M. & RILEY, G.H., 1960, Radioactive Ages from the Precambrian Rocks in Australia: *Jour. Geol. Soc. Australia Vol.6 No.2* pp. 179–196

WOYZBUN, P., 1968, Report on the Airborne Magnetic Survey in the Petermann Ranges Northern Territory Report By Geophys. Resour. Development Co. to Planet Mining Co. Pty. Ltd: *N.T.D.M.E. Open File Company Report (unpubl.) CR68/44*

WYATT, B.W., 1983, Application of High Resolution Aeromagnetics to Petroleum Search in the Southern Amadeus Basin: *Exploration Geophys. Vol.14 No.3/4* pp. 183–185

YOUNG, G.A., 1977, Geological Interpretation of Geophysical Results, Glenormiston Special Airborne Survey, Queensland 1977: *Aust. Bur. Min. Resour. Geol. and Geophys. Report 253*

YOUNG, G.A. & SHELLEY, E.P., 1977, Amadeus Basin Airborne Magnetic and Radiometric Survey, Northern Territory 1969: *Aust. Bur. Min. Resour. Geol. and Geophys. Report 187*